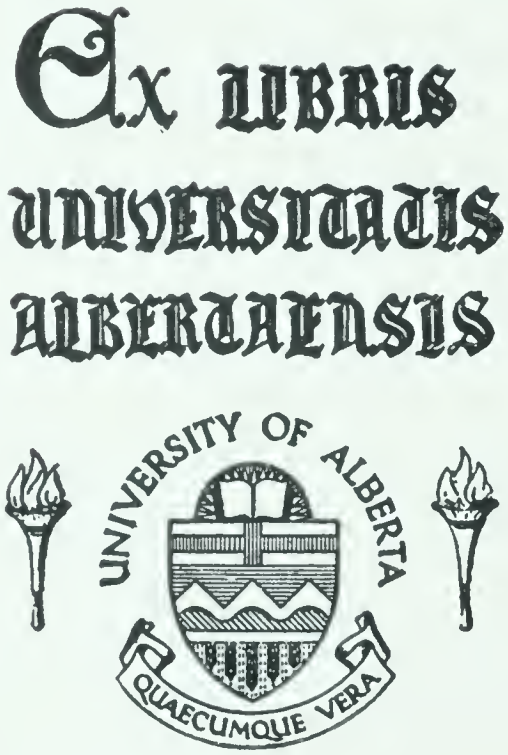

University of Alberta
Printing Department

THE UNIVERSITY OF ALBERTA

PETROLOGY OF THE CARBONATE ROCKS OF THE SIYEH FORMATION, SOUTHWESTERN ALBERTA

A THESIS

SUBMITTED TO THE FACULTY OF GRADUATE STUDIES

IN PARTIAL FULFILMENT OF THE REQUIREMENTS FOR THE

DEGREE OF MASTER OF SCIENCE

DEPARTMENT OF GEOLOGY

by

JOHN DOUGLAS ADSHEAD, B.Sc.

EDMONTON, ALBERTA

APRIL, 1963

ABSTRACT

Precambrian carbonate rocks of the Siyeh formation are described from a section located near the north boundary of Waterton Park, southwestern Alberta.

Mottling is common in the Siyeh carbonates and is related to several types of sedimentary structures, all of which are diagenetic in origin and are attributed to processes of soft sediment slumping and fracture development in addition to authigenic cementation.

The Siyeh sediments were derived from a low-lying source area southeast of the site of deposition. The source rocks were fine-grained, low-grade metamorphic schists and phyllites composed largely of quartz and fine-grained micaceous minerals. Some granites may have been present.

Deposition of the clastic constituents was followed by extensive diagenetic calcitization, which the present study indicates may have been responsible for most if not all of the calcite in the Siyeh rocks. Late diagenetic dolomitization, affecting all beds to some degree, represents the last major phase of mineralization in the Siyeh sediments.

The presence of algae, oolites, and graded bedding indicates that the Siyeh sediments accumulated in a shallow sea, similar to the Recent Shark Bay marine lagoon of Western Australia.

ACKNOWLEDGMENTS

The writer is indebted to all members of the Department of Geology, and particularly to Dr. J.F. Lerbekmo, who guided the thesis research and critically read the manuscript, offering many helpful suggestions. Dr. F.A. Campbell helped with the section on mineral composition, and Dr. R.A. Burwash critically read the manuscript. Dr. S. Pawluk of the Department of Soil Science, University of Alberta, kindly supervised the CO_2 analyses. Mr. M.A. Carrigy of the Research Council of Alberta programmed the cross-bed results.

Special thanks are due Dr. G.B. Mellon of the Research Council of Alberta, who suggested the thesis problem and supervised the field work. His constructive criticism and helpful suggestions are gratefully acknowledged. The writer is also indebted to the Research Council of Alberta for providing the equipment and funds for the field study as well as the chemical analyses and thin sections.

Figures were draughted by Mr. F. Copeland. Mr. F. Dimitrov photographed the hand specimens.

TABLE OF CONTENTS

ILLUSTRATIONS

INTRODUCTION

PROBLEM AND OBJECTIVE

The antiquity and generally unfossiliferous nature of Precambrian sedimentary rocks has led many geologists to the conclusion that conditions of deposition in Precambrian times were considerably different from those existing during the deposition of younger sediments and at the present time. However, Pettijohn (1943), from a study of the petrographic properties and sedimentary structures of early Precambrian detrital rocks from the Timiskaming system of the Canadian Shield, concluded that the similarity between Precambrian and post-Precambrian detrital sediments "is so striking that little doubt remains that both the Archean and the younger deposits were formed in an identical manner." Little detailed petrographic information is available on Precambrian carbonate rocks, although information on younger carbonate deposits is rapidly being made available from the study of recent carbonate sedimentation. Access to this information greatly aids in the interpretation of the genesis of ancient carbonate rocks.

The objective of the present investigation is to describe the composition, texture, and sedimentary structures of the carbonate rocks of the Precambrian Siyeh formation in southwestern Alberta, in order to determine the factors governing the deposition of these rocks. In contrast to most Precambrian sedimentary assemblages, rocks of the Lewis (Belt) series* of southwestern Alberta are essentially unmetamorphosed and are

---

* The term "Belt" was first used by Dr. A.C. Peale (1893) to describe the "Belt formation", in which he included all sediments lying unconformably above Archaean metamorphic rocks, and overlain (unconformably) by fossiliferous Cambrian sediments, near Three Forks (Belt Mountains area) Montana. According to present usage by the United States Geological Survey, the "Belt series" refers to all strata of Proterozoic age in the Montana area. In the Lewis and Clark Ranges in Canada the term "Lewis series" (Daly, 1912) is commonly used by Canadian geologists in reference to the same assemblage; the strata are comparable in age to rocks of the Purcell System in the Western Cordillera (Douglas, 1952).

thus particularly amenable to detailed petrographic study of their depositional fabric.

PREVIOUS WORK

Many geologists have contributed to the understanding of the structure and stratigraphy of the Precambrian sedimentary rocks of the Eastern Cordillera, and in particular the Lewis series, with which the present study is specifically concerned. G.M. Dawson (1875) was among the first to examine the Proterozoic strata in the Front Ranges. Walcott (1899) drew attention to "fossils"* in the "Greyson shales" of the "Belt terrane" in the Little Belt and Big Belt mountains of west-central Montana. He also identified and classified some of the Belt algal forms (Walcott, 1914). Willis (1902) presented the first detailed account of the structure and stratigraphy of the Belt rocks in the Glacier area of Montana. He recognized and described for the first time the Lewis overthrust and related structural features; he also described and named the various formations of the Belt series in that area. Daly (1912) published an excellent account of the structure, stratigraphy, and petrography of the Proterozoic rocks exposed along the International Boundary in Alberta, British Columbia, and Montana.

Some time later, Fenton and Fenton (1931, 1933, 1937) classified the various algal forms and described in detail the sedimentary structures and stratigraphic subdivisions of the Belt series. Rezak (1957) reclassified the Belt stromatolites. Ross (1959) published a comprehensive report on the structure and stratigraphy of the Glacier-Flathead area, northwestern Montana. Hunt (1961) contributed to the understanding of the igneous rocks associated with the Belt sediments in south-

---

* Fragments of "crustaceans" and "worm trails".

western Alberta and southeastern British Columbia. Officers of the Geological Survey of Canada have mapped much of the area underlain by Belt strata in Canada, and the information gained from the works of Hage (1943), Douglas (1952), Norris (1959), and Price (1959) was of great assistance in the present study.

GENERAL GEOLOGY

STRUCTURE AND PHYSIOGRAPHY

Strata of late Precambrian (Proterozoic) age form the Eastern Ranges of the Rocky Mountains in southwestern Alberta, having been thrust more than 40 miles to the northeast over Upper Cretaceous rocks in early Tertiary time (Ross, 1959). An area of about 360 square miles in the southwest corner of the province is underlain by these Proterozoic rocks (Figure 1). The Lewis thrust fault, along which this movement took place, dips at low angles to the southwest under the eastern front of the Rocky Mountains. The Proterozoic strata lying above the fault have been folded into a broad northwest trending syncline, forming a mountainous belt 95 miles long, which extends from latitude 49 degrees 22 minutes in British Columbia to the Roosevelt Pass in Montana at latitude 48 degrees 20 minutes. The strata are bounded on the east by the northwest trending trace of the Lewis fault. At Prairie Bluff, 24 miles north of the International Boundary, the fault trace swings abruptly to the west, and 40 miles south of the border in the vicinity of Roosevelt Pass it makes an equally abrupt turn to the southwest, delimiting the Lewis thrust sheet to the north and south, respectively. The Flathead normal fault, dipping steeply to the southwest, bounds the Lewis thrust sheet on the west and roughly parallels the trend of the Lewis thrust plane; to the north the Flathead fault dies out around latitude 49 degrees 30 minutes (Price, 1959). North of Waterton Lakes National Park, between the Lewis thrust and the diminishing Flathead fault, Proterozoic strata dip under a succession of Cambrian, Devonian, and Mississippian rocks. These Paleozoic strata are the lowest beds exposed above the Lewis fault trace as it continues northward along the margin of the Flathead Range.

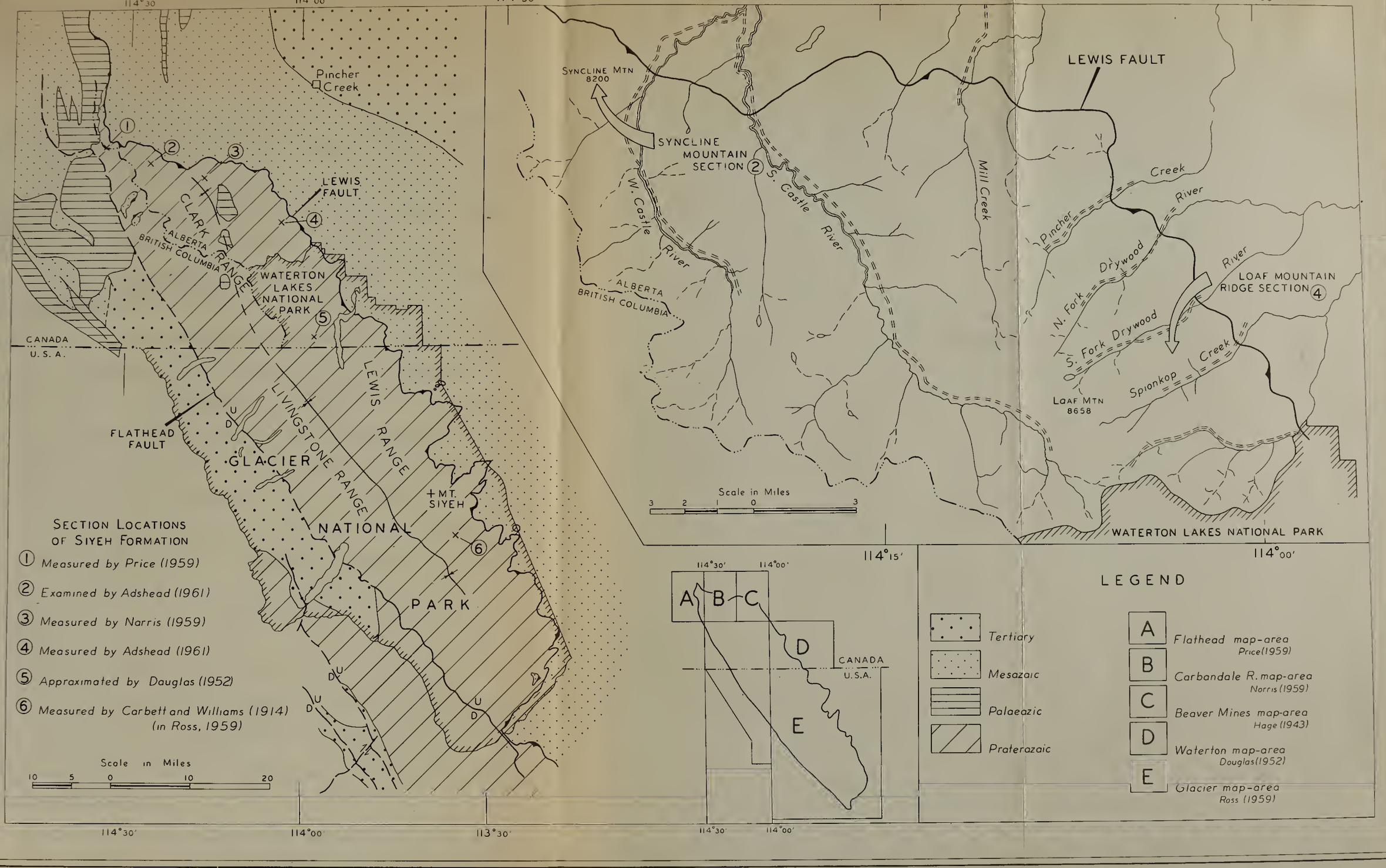

Figure 1. Index Map

This gently deformed sheet of Precambrian strata straddling the International Boundary has been divided into the Lewis and Livingstone Ranges in Montana by Willis (1902), and the Lewis and Clark Ranges in Canada by Daly (1912). The present physiography of the Lewis and Clark Ranges results largely from glacial erosion, as shown by the outstanding development of U-shaped valleys, cirques, knife ridges, and pyramidal peaks. Although there is some evidence for pre-Wisconsin glaciation on the plains to the east, none has been found in the mountains to date (Daly, 1912, p. 578; Ross, 1959, p. 73). The drainage pattern is irregular in the Clark Range, stream courses being determined largely by glacial erosion. North of Waterton Park, the Clark Range (east of the Continental Divide) drains through the Castle and Oldman rivers; in Waterton Park it drains through the Waterton, Belly, Oldman, and South Saskatchewan rivers eventually to Hudson Bay. The Clark Range west of the Continental Divide drains through the Flathead River eventually to the Columbia River system. Average relief in the Clark Range is 3000 to 3500 feet with a maximum of over 4000 feet near Mount Blakiston (Waterton Park), one of the highest peaks, with a summit altitude of 9047 feet above sea level. Most summits range in altitude between 7500 and 8500 feet.

STRATIGRAPHY OF THE BELT ROCKS

The Lewis series as defined by Daly (1912) in the Lewis and Clark Ranges comprises eight formations with a total thickness of 11,100 feet, and constitutes a conformable sequence of shallow water deposits composed largely of fine-grained detrital material and dolomites.

The formations of the Lewis series as described by Douglas (1957) are shown in Table 1.

Table 1. Lewis series in the Lewis and Clark Ranges, Canada

Formation	Thickness (feet)	Lithology
Kintla	2,900	red and green argillite
Sheppard	600	dolomite, argillite
Purcell lava	200	amygdaloidal basalt flow
Siyeh	3,000	limestone, dolomite, green and grey argillite
Grinnell	1,000	red argillite, quartzite, conglomerate
Appekunny	1,100-1,625	green and red argillite, quartzite
Altyn	1,000	laminated dolomite, sandy dolomite, algal beds, black argillite
Waterton	617 (base not exposed)	varicoloured dolomite, banded limestone and dolomite, argillite

The uppermost Kintla beds are overlain by Middle Cambrian trilobite-bearing strata. However, structural evidence for an unconformity is lacking, and Ross (1959, p. 75) concludes that if pre-Paleozoic diastrophism did in fact occur, its effects were very slight and must have been operative over a wide area, possibly representing a continuation of activity which began at the close of Siyeh deposition.

The nature and thickness of the rocks which originally underlay the Lewis series are unknown, as borehole penetrations of the Lewis thrust sheet pass into Upper Cretaceous shales (Daly, 1912; Clark, 1954). To the west Norris (1959)

reported that 1500 feet of strata belonging to the basal Waterton formation are found lying in faulted contact over severely contorted Upper Cretaceous (Wapiabi and basal Belly River) strata in the Gate Creek and Haig Brook fensters in the Clark Range of British Columbia. The base of the Belt sediments is not exposed in that area of Montana underlain by the Lewis thrust sheet, and no exposures of basal Waterton strata have been found to date (Ross, 1959, p. 19). However, the contact between Proterozoic sediments and Archaean metamorphic rocks is exposed in the Belt Mountains in the west-central part of the state.

SIYEH FORMATION

Definition

The Siyeh formation was named by Willis (1902) for a dominantly carbonate sequence exposed on Mount Siyeh about 18.5 miles south of the International Boundary and 3.5 miles west of the Lewis fault trace. At that time he correctly concluded that the Siyeh formation was of Algonkian age and not Devonian and Carboniferous as previously supposed by G.M. Dawson (1885).

The underlying red shales and quartzites of the Grinnell formation grade upward into the basal Siyeh beds, and the base of the Siyeh formation is placed at the point where the lithologic assemblage changes from red shale and thick-bedded white quartzite, containing scattered red and green shale pebbles, to predominantly light green shale with thin quartzite lenses and bands. The lower part of the Siyeh formation consists mainly of carbonates and is about 1900 feet thick. Dolomites, mottled limestones, and shales (calcareous and dolomitic) constitute the major lithologies. The upper Siyeh is largely a clastic assemblage of red and green shales with minor dolomitic beds and is about 500 feet in thickness.

The upper limit of the Siyeh formation is herein considered to be the base of the Purcell lava. This upper limit which has been chosen by Canadian geologists is an excellent marker horizon throughout the Clark Range. However, Fenton and Fenton (1937), and Ross (1959) exclude the upper argillaceous rocks from the "Siyeh limestone," including them with similarly arenaceous and argillaceous strata of the overlying Sheppard and Kintla formations.

Subdivisions of the Siyeh

Although Daly (1912) was the first to distinguish subdivisions within the Siyeh formation, his thickness values are considerably in excess of thicknesses measured by recent workers. Fenton and Fenton (1937) modified Daly's four divisions, recognizing two as algal zones and raising the other two units to member status (Figure 2).

The Siyeh formation was measured and sampled by the writer on Loaf Mountain ridge (Figure 1) where it can be divided into nine major lithological units (Table 2) with a total thickness of 2407 feet. The boundaries between units are based on the appearance or disappearance of characteristic rock types, some of which persist through two or more units.

Figure 2. Comparison of gross lithology of the Siyeh formation at: (A) International Boundary, showing the five major subdivisions of Daly (1912); (B) Glacier Park, Montana, showing the four divisions of the "Siyeh formation" (a-d) and the Spokane formation (e) of Fenton and Fenton (1937); and (C) Loaf Mountain ridge, southwestern Alberta, showing the nine units distinguished in the present study.

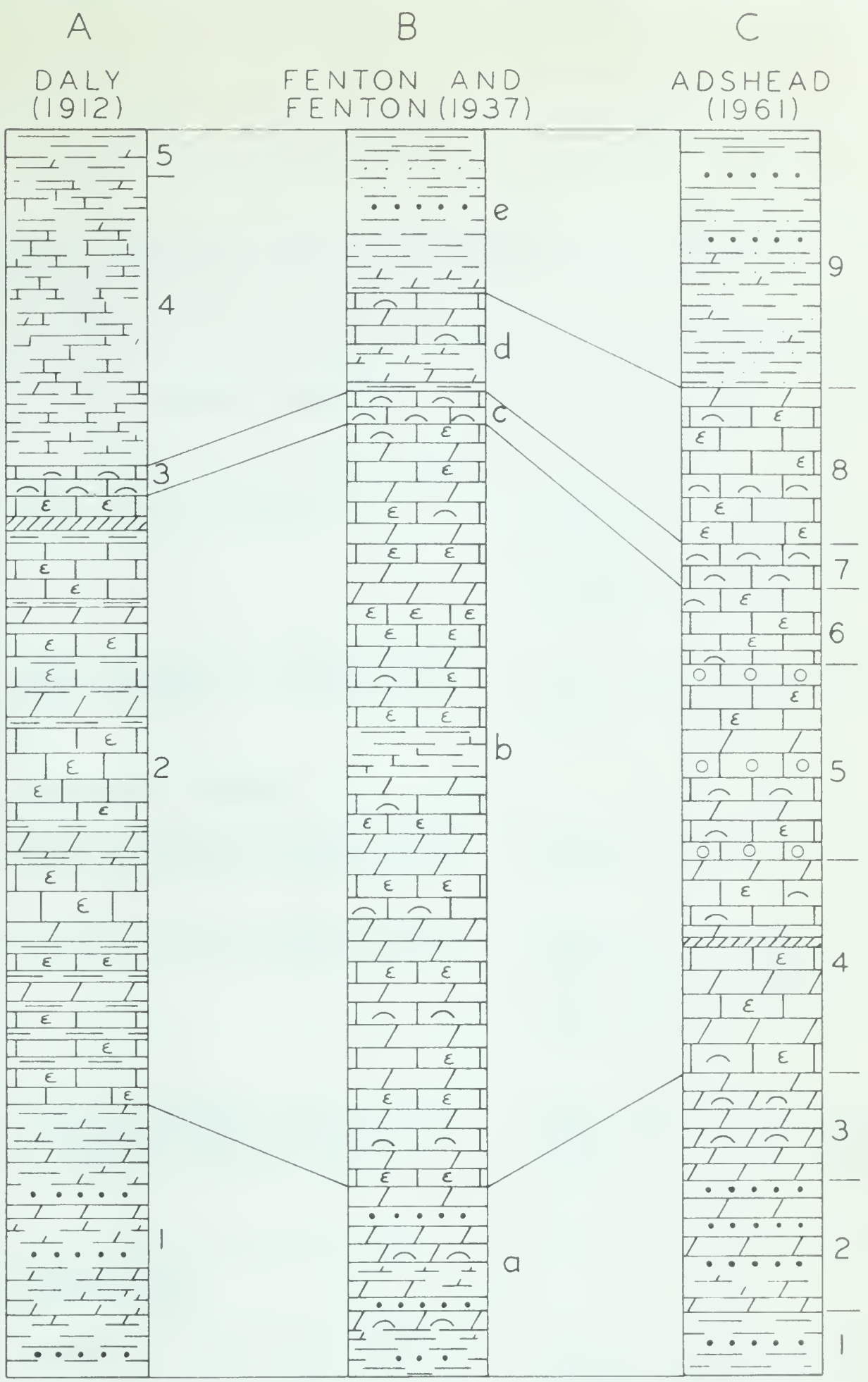

LEGEND

Calc. sh
Dol. sh
Silty sh
Quartzite
Dolomite
Algal dol
Algal ls
Oolitic ls
Mottled ls
Diabase sill

a *Collenia symmetrica* zone
b Goathaunt member
c *Collenia frequens* zone
d Granite Park member
e Spokane formation

Figure 2.

Table 2. Lithologic subdivisions of Siyeh formation at Loaf Mountain ridge. (Characteristic lithologies are underlined.)

Unit Thickness (feet)	Dominant Lithology	Minor Lithology
(9) 503	shale, silty green and red	siltstone, green and red; dolomite, silty; quartzite; algal dolomite; shale pebble conglomerate, dolomitic.
(8) 303	mottled limestone; calcareous shale; algal limestone.	mottle conglomerate; dolomite, silty; shale pebble conglomerate, calcareous.
(7) 87	algal reef, calcareous.	
(6) 144	mottled limestone; calcareous shale	mottle conglomerate; algal limestone.
(5) 380	mottled limestone; dolomitic shale	dolomite; silty; oolites, calcareous; calcareous shale; algal limestone; mottle conglomerate; shale pebble conglomerate.
151 (4) 404 18 253	mottled limestone; dolomite, silty. Thickness of diabase sill (18 feet) excluded from total thickness.	algal limestone; mottle conglomerate; calcareous shale; dolomitic shale; shale pebble conglomerate; quartzose bands.
(3) 208	algal dolomite; dolomitic shale; dolomite, silty	quartzose bands; quartzite.
(2) 251	dolomite, silty; dolomitic shale	shale pebble conglomerate, dolomitic; algal dolomite; quartzose bands; oolites.
(1) 127	shale, silty, light green.	quartzite.
2,407	Total thickness	

Lateral variation in the thickness of the Siyeh formation in the Lewis thrust sheet is shown in Table 3. Section localities are shown on Figure 1. From available information the Siyeh appears to thin to the northwest, although more data are needed to confirm this trend.

Table 3. Lateral thickness variation of Siyeh formation in Lewis thrust sheet (thicknesses in feet).

1. Price (1959)	2. Adshead (1961)	3. Norris (1959)	4. Adshead (1961)	5. Douglas (1952)	6. Corbett and Williams (1914)
			Unit 9 (detritals) 503	600	
100	190				
	30	335	Unit 8 (carbonates) 303		680
	70	65	Unit 7 (algal reef) 87		78
			Units 4, 5, and 6. (carbonates) 928	900	
1000			Units 2 and 3 (carbonates and detritals) 459		
30		1250	Unit 1 (detritals) 127	500	1520
1130(C)	290(I)	1650(C)	2407(C)	2000-3000(E)	2278(i)

(C) Complete section
(I) Incomplete section
(E) Thickness estimated

SAMPLING PROCEDURE AND ANALYTICAL TECHNIQUES

SAMPLING PROCEDURE

The Siyeh formation was measured and sampled in detail on a ridge extending to the northeast from Loaf Mountain, and lying between the South Fork of Drywood Creek and Spionkop Creek (Figure 1). The section, which is herein referred to as the Loaf Mountain ridge section, is located about four miles north of Waterton National Park in Secs. 22 and 27, Tp. 3, R. 1, W. 5th Mer.; it is readily accessible by road, being about 25 miles southwest of Pincher Creek, Alberta. At this locality systematic samples were obtained at the base of each measured 10-foot interval, and additional samples were taken wherever special features warranted it.

The second Siyeh section is located in Sec. 2, Tp. 5, R. 4, W. 5th Mer. and was measured on the east face of Syncline Mountain (Figure 1) by means of a pocket altimeter. The lower part of the section is cut by numerous minor faults and only a few selected samples were obtained here.

A total of 339 systematic samples, and 143 special samples was collected during the course of the field work, 258 of the former and 123 of the latter being obtained from the Siyeh formation on Loaf Mountain ridge.

ANALYTICAL TECHNIQUES

In the field, a lithologic classification (p. 16) was adopted and each systematic sample collected was classed as one of the rock types defined. Composite samples of each of eight major rock types were chemically analyzed. Normative compositions were determined from the analyzed samples, which were subsequently

used as standards for the determination of calcite and dolomite content in 48 systematic samples, using X-ray diffraction techniques.

The mineral composition of 42 systematic samples was determined by point-counts of thin sections. Textural properties were also measured and described, and fabric detail of various sedimentary structures was obtained. However, the nature of the sedimentary structures of the rocks was determined largely from binocular examination of about 80 rock slices etched with dilute hydrochloric acid. The thicknesses of graded beds in 35 systematic samples were also determined from polished rock slices.

FIELD CLASSIFICATION

Rocks of the Siyeh formation vary widely both in composition and texture. Diversified internal, bedding plane, and diagenetic chemical structures add to the complexity of the lithologic varieties. In the field, a classification of rock types was devised (Table 4). As this basic breakdown proved valid even after detailed petrographic and X-ray investigation, most of the nomenclature remains unaltered. (Where minor modifications have been made, they are so indicated.)

Certain rock types deserve special mention, among which are the mottled limestones and pseudoconglomerates. Various structures (to be discussed) contribute to mottling in the Siyeh rocks, and as it is often difficult to determine in outcrop the true nature of the mottling, the term pseudoconglomerate was used in the field to embrace those rocks in which the mottles are not obviously related to fracturing.

The carbonate sequence (units 2 to 8) of the Siyeh formation includes many thin bands, one-half inch to two inches thick, of intraformational conglomerate and breccia. The breccias consist of very small fragments (most less than one millimeter in length) of calcite and laminated sediment embedded in a silty argillaceous matrix, and appear in some cases to have formed as a result of intrastratal slippage rather than surface brecciation. The conglomerates contain moderately to well-rounded pebbles, in many instances of very small size, and frequently show imbricate structure. Phenoclasts are of three types: laminated dolomitic silt, laminated calcareous silt, and nearly pure calcite. In the third case the phenoclasts are fragments of the calcitic infillings of shrinkage fractures, and conglomerates in which the majority of pebbles are of this type are designated "mottle conglomerates", as the phenoclasts were originally veinlets of calcite acting as mottles in a silty host sediment. The mottle conglomerates which show imbricate structure or evidence of discrete pheno-

TABLE 4 FIELD CLASSIFICATION OF THE SIYEH ROCKS

Rock type	Composition	Texture	Structures*	Weathering habit	Fracture colour	Weathered colour
1. Aphanite with calcite fracture segregations	Calcareous, silty	Very fine-grained to microgranular	Calcitic segregations related to fracturing; graded bedding	Massive to platy; characteristic mottled appearance	Medium-to-dark grey with light grey (silty) bands	Dark grey calcitic segregations in buff host rock
2. Pseudoconglomerate	As above	As above	Calcitic "blotches" and pinching and swelling bands parallel to bedding, graded bedding; irregular lumps and stringers of silt in fine-grained matrix.	Massive to platy	As above	Dark grey calcitic and brown silty areas in buff host rock
Aphanite 3.	As above	As above	No mottle structure; graded bedding	Massive to platy	As above	Buff
Shale	Calcareous, with silty laminae			Fissile	Medium-to-dark grey	Light grey
Dolomite	Noncalcareous, silty	Very fine-grained to microgranular	Graded bedding	Massive to platy	Dark-to-light grey	Buff
Shale	Dolomitic, with silty laminae			Fissile	Medium-to-dark grey	Light grey
Algal limestone and Algal dolomite	Predominantly calcitic or predominantly dolomitic; silty	Very fine-grained	Finely laminated	Resistant beds	Light grey	Light grey to buff
Colite	Predominantly calcareous	Oolitic, medium-to-fine grained	In some instances associated shale pebble phenoclasts	Resistant beds	Light grey	Light grey
Quartzite	Dolomitic	Very coarse-to-medium grained		Massive	Whitish-to-very light grey	Buff
Shale 4.	Noncalcareous with silty laminae			Fissile	Medium-to-light green	Light greenish grey
Flat pebble and edgewise intraformational conglomerates.	Predominantly silty dolomite pebbles in dolomitic silt matrix, or, predominantly silty limestone pebbles or almost pure calcite pebbles in calcareous silt matrix.	Phenoclasts up to 2 inches long, most under one inch.	Imbricate structure common	Thin bands with more resistant phenoclasts weathering in relief	Light grey	Buff
5. Fine pseudoconglomerate	Phenoclasts of pure calcite predominate over rock fragments	Most phenoclasts under one-half inch long		Calcitic phenoclasts weather preferentially in resistant silty matrix	Light-to-dark grey	Dark grey-to-black phenoclasts in buff matrix

Notes:

1. Classified under mottled limestones in the petrographic analysis. Includes rocks containing shrinkage fractures, slump fractures, and slump fractures superimposed on shrinkage fractures. When possible, the various types were distinguished in the field.
2. Classified under mottled limestones in the petrographic analysis. Rocks exhibiting irregular bedding due to soft sediment slumping are grouped with authigenic calcite growth structures under pseudoconglomerate.
3. Renamed limestone.
4. X-ray diffraction results indicate the near absence of carbonate.
5. Includes slump breccia and fine mottle conglomerate.

* With the exception of the algae, all rocks show evidence of cross-lamination.

clasts enclosed in matrix material were classed with the dolomitic and calcareous shale-pebble conglomerates under flat-pebble or edgewise intraformational conglomerates (Table 4). In the field, as it was often impossible to distinguish individual pebbles in many thin, dense, fine "conglomeratic" bands, the term "fine pseudoconglomerate" was used to describe such rocks, which in the laboratory proved to be breccias or fine mottle conglomerates.

CHEMICAL AND MINERAL COMPOSITION

CHEMICAL COMPOSITION

The chemical composition of the Siyeh rocks is known only from analyses of a few spot samples (Daly, 1912, p 75; Ross, 1959, p. 55). However, the rocks are so variable in composition, that such analyses are almost certainly not representative of the average chemcial composition of the formation. For the present study, 258 samples collected at 10 foot intervals throughout the formation on Loaf Mountain ridge, were grouped into 12 rock types. One gram fractions from each of eight of the most frequently occurring lithologic types were combined to give eight composite samples for chemical and X-ray analysis, corresponding to the eight major rock types (Table 5).

Table 5. Distribution of rock types comprising eight composite samples of the Siyeh formation

Sample	Rock type	Total systematic samples per composite
Siy-1	shale	22
Siy-2	quartzite	4
Siy-3	dolomitic shale	37[1]
Siy-4	dolomite	46[2]
Siy-5	calcareous shale	26
Siy-6	limestone	43[3]
Siy-7	algal limestone	17
Siy-8	upper clastics	40[4]

(1) includes seven samples from unit 9
(2) includes three samples from unit 9
(3) predominantly mottled but includes five "non-mottled" samples.
(4) all shale and quartzite from unit 9 above major carbonate sequence.

Table 6. Wet chemical analyses of eight composite samples of the Siyeh formation

Sample	Siy-1 Shale	Siy-2 Qtzite	Siy-3 Dol. sh.	Siy-4 Dol.	Siy-5 Calc. sh.	Siy-6 Mott. ls.	Siy-7 Algal ls.	Siy-8 U.clast.
SiO_2	57.40%	73.26%	51.23%	38.41%	46.35%	40.02%	20.08%	68.34%
Al_2O_3	11.29	3.28	9.45	4.56	8.42	6.09	1.90	11.27
Total iron as Fe_2O_3	3.62	1.47	2.79	2.34	2.41	2.17	1.24	4.41
Total iron as FeO	3.25	1.33	2.51	2.11	2.17	1.96	1.12	3.96
TiO_2	0.38	0.07	0.33	0.17	0.32	0.13	0.09	0.47
P_2O_5	0.13	0.09	0.11	0.08	0.09	0.10	0.04	0.08
CaO	5.22	5.83	9.31	16.62	16.83	22.62	39.97	3.12
MgO	7.41	4.81	8.60	12.67	6.10	5.66	2.85	2.99
Na_2O	0.36	0.27	0.62	0.33	0.65	0.45	0.24	1.12
K_2O	3.72	1.24	2.72	1.24	2.16	1.50	0.59	3.56
CO_2	7.15	8.43	12.28	23.15	14.82	18.57	32.25	2.75
H_2O	3.15	0.62	2.82	1.78	2.70	3.38	1.19	2.13
Total (excluding FeO)	99.83	99.37	100.26	101.35	100.85	100.69	100.44	100.24
Per cent soluble in dilute HCl	17.0	18.8	27.9	50.0	34.2	45.3	73.6	7.7

Analyses by H. Wagenbauer, Research Council of Alberta
CO_2 analyses by S. Pawluk, Department of Soil Science

The carbonates are low in CO_2 and rich in SiO_2, with the exception of the algal limestones, indicating the relative impurity of these rocks. The high K_2O/Na_2O ratio possibly indicates an excess of potash-bearing minerals over plagioclase, which if present, constitutes only a small proportion of the rocks.

MINERAL COMPOSITION

The major mineral constituents in the Siyeh formation were identified by optical and X-ray techniques. Quantitative estimates of the average mineral composition are based on normative analyses of the chemical data in Table 6, using the results of optical and X-ray examination as a guide. In addition, the percentages of calcite and dolomite in 48 systematic samples were determined by X-ray diffraction techniques.

Mineral identification

Thin section examination

Examination of numerous thin sections showed that the following minerals or mineral constituents were present: dolomite; calcite; quartz; microcline; untwinned feldspar; soda plagioclase ($An_{10}Ab_{90}$)*; mica, coarse and fine-grained varieties; and chlorite. Minor amounts of hematite and sphene were observed in most thin sections. Trace amounts of pyrite, and extremely rare zircon, hornblende, and tourmaline were present.

X-ray diffraction patterns

The major mineral constituents were also determined from X-ray diffraction powder patterns of 12 samples representing the main lithologic types, and from patterns

---

* Determination by Michael Levy method (Kerr, 1959, p. 258)

of the 8 composite powders of the chemically analyzed samples (Table 5). Smear mounts of samples were analyzed using a North American Phillips X-ray diffractometer with nickel filtered copper X-radiation.

The following minerals were identified: dolomite, calcite, quartz, microcline, soda plagioclase, muscovite-illite, chlorite, and in some samples indications of pyrite and orthoclase.

Because of the relatively high proportion of fine-grained "clayey" minerals in the rocks, an attempt was made to determine the composition of this material more accurately by examining the finer details of the X-ray patterns. All patterns show the presence of the following peaks: 7Å (002 chlorite, 001 kaolinite), 10Å [001 "mica" (illite, muscovite, montmorillonite)], and 14Å (001 chlorite). Although the kaolinite 001 reflection overlaps the 002 chlorite reflection, the absence of a peak in the range 1.48 to 1.49Å corresponding to the kaolinite 060 peak indicates the absence of that mineral (Warshaw and Roy, 1961, p. 1479).

Examination of several glycolated samples shows no shift in the 10Å peak, confirming the absence of montmorillonite and associated mixed layer clays.

Two forms of mica are present in thin sections: finely crystalline clay-size in the matrix of the rocks and large detrital shreds of muscovite. The former is most abundant.

X-ray diffraction powder patterns of various samples yield a moderately sharp symmetrical 10Å "mica" peak. Examination of the 2θ interval corresponding to the 060 "mica" reflection reveals the presence of two peaks: 1.503 to 1.505Å, and 1.515 to 1.523Å. Although peak intensities are similar in some instances, the peak height of the 1.503 to 1.505Å 060 is generally greater. Both appear to represent dioctahedral varieties [060 = 1.50 to 1.52Å (Warshaw and Roy, 1961, p. 1480)],

as does the presence of a medium--rather than weak--5Å second order reflection (MacEwen, 1950). The 1.503 to 1.505Å peak is probably the 060 reflection for illite, which, according to Warshaw and Roy, should have a spacing of about 1.50Å. This appears to be the fine-grained "matrix" mica observed in thin sections. The other dioctahedral reflection may be that of the coarser shreds of muscovite seen in thin section.

For the purpose of calculating the norms of the eight composite samples, the 10Å micaceous minerals have been assigned the same composition as ideal muscovites (Table 7).

Most of the chlorite observed in thin sections is present as clay-sized particles intimately mixed with illite of similar size, the combined clays constituting the major portion of the "matrix". Because of this, it is impossible to determine chlorite composition by conventional optical techniques. However, using the procedure outlined by Shirozo (1958), the approximate chlorite composition may be determined from X-ray diffraction powder patterns. Shirozu showed that the "b" cell dimension [d(010)] is systematically related to the (octahedral) Fe^{+2} content, and the "c" dimension [d(001)] related to the amount of (tetrahedral) Al^{+3} as determined from numerous chemical analyses and X-ray diffraction powder studies of a number of chlorites. In order to obtain the "b" and "c" dimensions the 2θ positions of the 001 and the 020 reflections were determined from powder patterns of 13 samples by slow scanning (1/8° per minute) over the appropriate peak positions. The mean cell dimensions so derived are shown below.

d(001)	d(010)
14.345Å	9.232Å

Using the d(001) and the d(010) from the Siyeh chlorite, the derived content values (from Shirozu's graphs), expressed as (n)Al^{+3} and (n)Fe^{+2} are substituted in the

ideal chlorite formula* to derive the composition of the chlorite. The $(n)Al^{+3}$ and $(n)Fe^{+2}$ were found to be 0.79 and 0.60 respectively. The results of the X-ray determination (Table 7) indicate a high-magnesium chlorite (Mg^{+2}/Fe^{+2} = 7.68).

Normative analyses

Formulae used to calculate the normative mineral composition of the eight Siyeh rock types are shown in Table 7, the composition of chlorite and albite having been derived by means of X-ray and optical techniques. Eight of the minerals are present in all of the rock types, but the presence of apatite and rutile is inferred only from chemical analyses.

Table 7. Normative minerals of Siyeh rocks

Mineral	Formula		Gram Molecular Weight
Quartz	SiO_2		60.0
K-feldspar	$K_2O \cdot Al_2O_3 \cdot 6SiO_2$		556.0
Albite	90%$Na_2O \cdot Al_2O_3 \cdot 6SiO_2$	471.6	
	10%$CaO \cdot Al_2O_3 \cdot 2SiO_2$	27.8	499.4
Calcite	$CaO \cdot CO_2$		100.0
Dolomite	$CaO \cdot MgO \cdot 2CO_2$		184.3
Muscovite	$K_2O \cdot 3Al_2O_3 \cdot 6SiO_2 \cdot 2H_2O$		796.0
Chlorite	$4.61MgO \cdot O.6FeO.0.79Al_2O_3 \cdot 3.21SiO_2 \cdot 4H_2O$		572.5
Pyrite	FeS_2		120.0
Apatite	$3CaO \cdot P_2O_5$		310.0
Rutile	TiO_2		80.0

* $[(Mg, Fe^{+2})_{6-(n)Fe}(Fe^{+3}, Al)_{(n)Al}]\ [Al_{(n)Al}Si_{4-(n)Al}]\ O_{10}(OH)_8$

As the assemblage and composition of minerals is assumed to be the same for each chemically analyzed composite sample (rock type), oxide percentages may be converted to mole fractions,* and subsequently distributed among each of the normative minerals according to the procedure outlined in Table 8. Mineral percentages are calculated from the mole fractions of assigned oxides (calcite example, Table 8). The normative mineral compositions of the eight composite rock types are shown in Table 8.

The relationship between chemical and mineral composition for each composite sample is shown on Figure 3. The classification scheme used is based on mineral composition and takes into account the relative importance of the following mineral groups: carbonate, clay, and quartz-feldspar. In cases where combined carbonate minerals exceed clay or quartz content, the rocks are classed as carbonates and named after the dominant carbonate constituent.

Calcite-dolomite percentages

The percentages of calcite and dolomite in 48 systematic samples taken at 40 foot intervals throughout the Siyeh carbonate sequence (units 2 to 8) at the Loaf Mountain ridge locality were determined by X-ray diffraction techniques.

Eight chemically analyzed composite samples, for which the normative percentages of calcite and dolomite had been calculated, were used as standards. Although the norm-calculated percentage values for most of the minerals are approximate, the total carbonate percentages are only as accurate as the values of CO_2 from the chemical analyses. The data for the acid soluble portion (largely carbonate) of the eight composite samples corroborates the total carbonate values (calcite plus dolomite) derived by normative calculation.

---

* Wt. per cent oxide/GMW oxide.

Table 8. Procedure for calculation of normative composition of eight Siyeh rock types.

step	1	2	3	4	5	6	7	8	9	10	11
"normative mineral	Rutile	Apatite	Ab_{90}	Ab_{10}	$CaO \cdot CO_2$	$MgO \cdot CO_2$	Chlorite	Muscovite	K-feldspar	Quartz	Pyrite
assigned mole fraction	(A) TiO_2	(A) P_2O_5	(A) Na_2O	(E)* CaO	(R) CaO	(R) CO_2	(R) MgO	(R) H_2O	(R) K_2O	(R) SiO_2	(R) FeO
		(E) CaO	(E) Al_2O_3	(E) Al_2O_3	(E) CO_2	(E) MgO	(E) FeO	(E) K_2O	(E) Al_2O_3		
			(E) SiO_2	(E) SiO_2			(E) H_2O	(E) Al_2O_3	(E) SiO_2		
							(E) Al_2O_3	(E) SiO_2			
							(E) SiO_2				

(A) all
(R) remaining
(E) equivalent mole fraction
MF mole fraction
GMW gram molecular weight
* 1/9 amount of MF Na_2O of CaO

Mineral weight per cent is calculated from mole fraction of mineralogic grouping, for example:
Wt. per cent calcite = (MF CaO-MF MgO) (GMW calcite)

Table 9. Normative composition of eight Siyeh rock types.

SAMPLE	ROCK TYPE	NORMATIVE MINERALS*									
		QUARTZ-FELDSPAR			CARBONATES		CLAYS		OTHERS		
		Quartz	Albite	K-feldspar	Calcite	Dolomite	Chlorite	Muscovite	Pyrite	Apatite	Rutile
Siy-1	SHALE	35.05	2.97	0.27	1.64	12.88	13.37	29.62	3.53	0.30	0.37
Siy-2	QUARTZITE	65.56	2.45	5.06	1.06	16.67	3.69	3.42	1.75	0.28	0.06
Siy-3	DOLOMITIC SHALE	31.77	5.46	--	4.38	20.87	11.80	22.52	2.57	0.30	0.33
Siy-4	DOLOMITE	27.06	2.85	0.48	5.97	41.27	10.22	9.62	2.13	0.24	0.16
Siy-5	CALCAREOUS SHALE	28.77	5.68	--	24.92	7.22	13.51	17.48	1.82	0.27	0.33
Siy-6	MOTTLED LIMESTONE	26.95	3.86	--	37.39	4.09	13.04	12.62	1.61	0.31	0.13
Siy-7	ALGAL LIMESTONE	14.21	2.06	--	67.92	3.82	6.12	4.61	1.07	0.12	0.07
Siy-8	UPPER CLASTICS	43.46	9.67	3.15	3.79	2.10	7.52	24.23	5.40	0.24	0.44

* Two decimal places shown as values recalculated to 100 per cent.

Chemical Symbols

Ca = CaO
Co = CO_2
M = MgO
S = SiO_2
Ot others

Mineral Symbols

Ct = calcite
Cm = chlorite-muscovite
D = dolomite
F = feldspor
Q = quortz
Ot = others

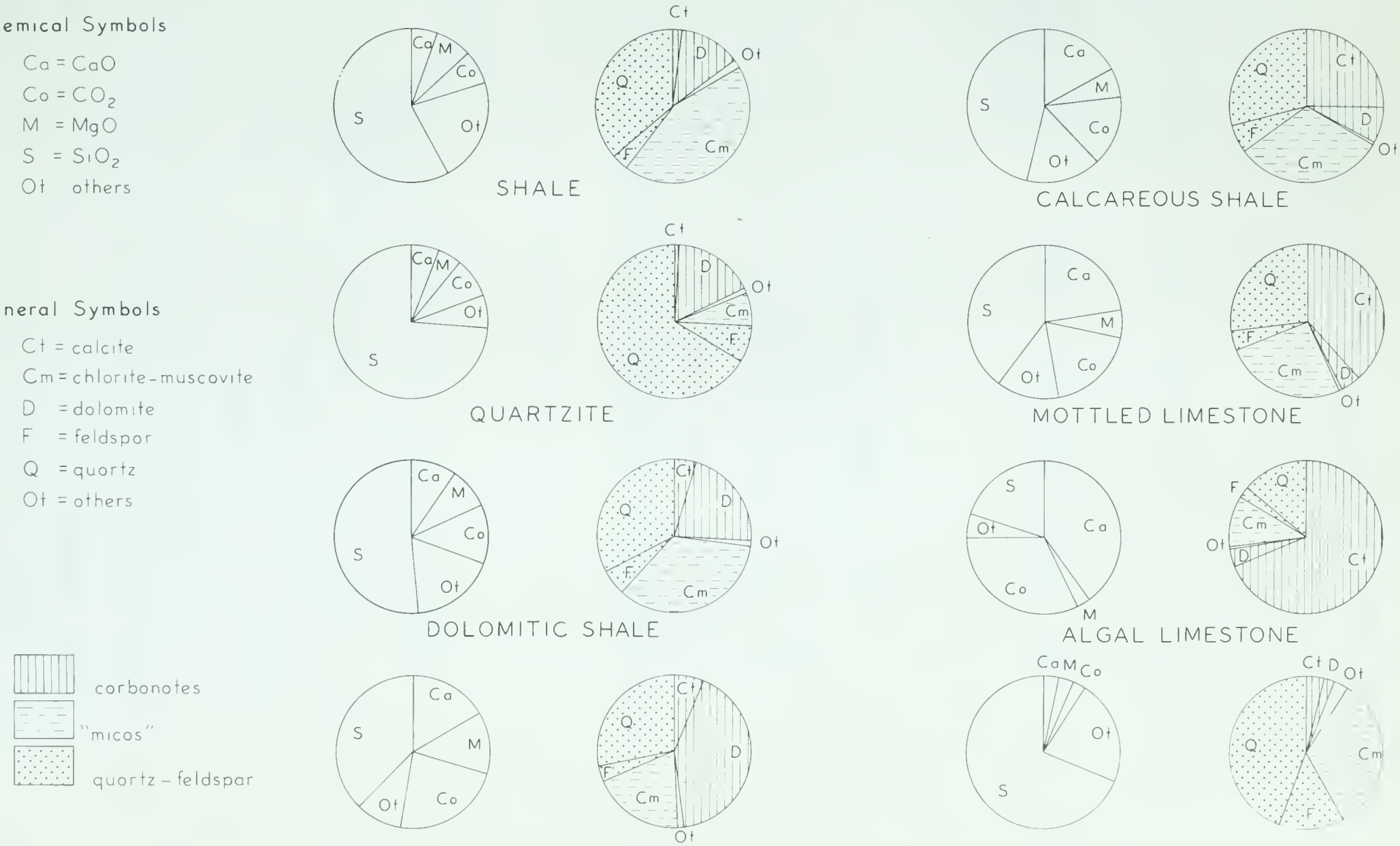

Figure 3. Chemical and mineral composition of eight composite samples from the Siyeh formation.

Table 10. Relationship between sample fraction soluble in dilute HCl and normative carbonate (calcite plus dolomite)

Composite sample	Siy-1	-2	-3	-4	-5	-6	-7	-8
Weight per cent soluble in dilute HCl	17.0	18.8	27.9	50.0	34.2	45.3	73.6	7.7
Weight per cent carbonate from normative calculations	14.5	17.7	25.3	47.2	32.1	41.5	71.7	5.9

As the total carbonate percentages for each rock type are fairly accurate, and as most of the CaO in the Siyeh rocks is used in the carbonates (calcite, $CaO \cdot CO_2$ accounts for more than 96 per cent of the total CaO in seven out of eight of the composite samples), the normative percentages of calcite and dolomite depend largely on the CaO values from the chemical analyses, and are thus accurate to within several per cent.

Technique

Representative portions (20 to 35 grams) of the 48 samples were reduced by hand mortar to fragments of sand size. About three grams of well-mixed "sand" were withdrawn from each of the 48 samples and ground in acetone in a mechanical mortar for one hour. From one-half to one gram of the resulting fine silt to clay size powder was mixed with a viscous mixture of three drops of "Duco" cement and five milliliters of acetone. A dropper was used to transfer the suspension from the mixing beaker to glass slides, two or three of which had been placed on a large glass plate. When each slide was completely covered with the fluid, the plate was gently tilted in all directions, shifting the settling grains uniformly over the slide surfaces during the evaporation of the acetone.

In this manner, five slides were prepared from each of the 8 chemically analyzed composite samples and two slides from each of the 48 systematic samples, giving a total of 136 sedimented X-ray powder mounts.

The powder mounts were analyzed using a North American Phillips X-ray diffractometer with nickel filtered copper X-radiation. A fixed-count method was employed (Tennant and Berger, 1957, pp. 24-25), whereby the counting device was operated at three successive 2θ positions (background, calcite 3.03Å line, and dolomite 2.88Å line). The time elapsed at each position was recorded for a fixed number of counts, giving a series of relative intensities for each of the three positions. Peak positions were approached from one direction in order to reduce the effect of "slap" in the goniometer mechanism.

The 2θ positions of the strongest calcite and dolomite reflections were determined by averaging the peak positions from a number of X-ray powder diffraction patterns, run at 1/8° per minute over the 2θ interval 28° to 30°. The selected background location is sufficiently removed from the positions of reflections of other minerals that interference effects are minimized. The 2θ positions used are shown below:

Background	Calcite: 3.03Å	Dolomite: 2.88Å
28.50°	29.37°	30.84°

As longer time intervals yield more precise intensities, the 6400-count setting was used. The time required for five consecutive 6400-count sequences was recorded for each of the three 2θ positions on the 40 "standard" sample slides; two consecutive 6400-count sequences were recorded (at the 2θ positions) for the 96 systematic sample slides. Calcite, dolomite, and background time-intensity readings were converted to counts per second values, and a correction was made for

background to give the relative calcite-dolomite intensities for each slide (Appendix A).

Standard curves for calcite and dolomite

Mean diffraction X-radiation intensity values of calcite and dolomite for each composite sample, representing the average of the results of five slides per sample, are shown in Table 11 with the corresponding normative percentage values derived from the chemical analyses. Due to a minor correction in the calcite and dolomite norms after the X-ray work was completed, percentages of calcite and dolomite used in the derivation of the standard curves are slightly higher than the corrected values shown in Table 9. However, as all values of calcite and dolomite are less than 0.71 per cent higher in the initial norm calculations (Table 11), the regression equations derived from the initial data remain unchanged.

Table 11. Per cent calcite and dolomite with corresponding X-radiation intensity values for eight composite samples.

Composite sample	Norm-calculated weight per cent calcite	Calcite intensity in counts per second	Norm-calculated weight per cent dolomite	Dolomite intensity in counts per second
Siy-1	1.69	1.97	13.23	154.37
Siy-2	1.07	3.92	16.86	183.95
Siy-3	4.49	13.24	21.30	218.69
Siy-4	6.08	8.41	41.98	338.92
Siy-5	25.38	177.99	7.36	64.67
Siy-6	38.00	226.73	4.16	71.25
Siy-7	68.57	426.80	3.86	31.63
Siy-8	3.91	41.41	2.17	26.06

The relationship between weight per cent calcite and diffraction X-radiation intensity (Figure 4) for the eight composite samples in Table 9 is given by the regression equation:

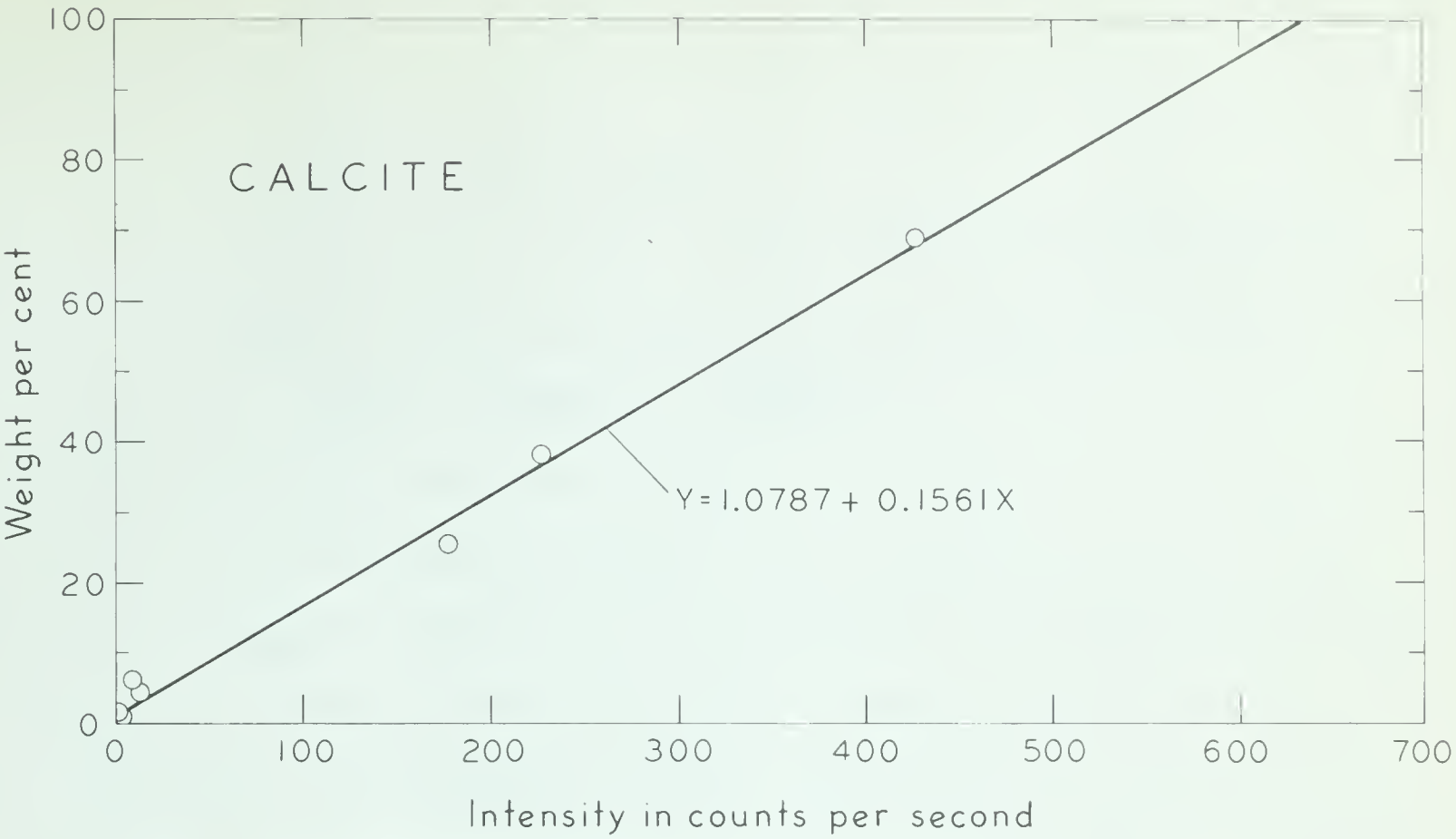

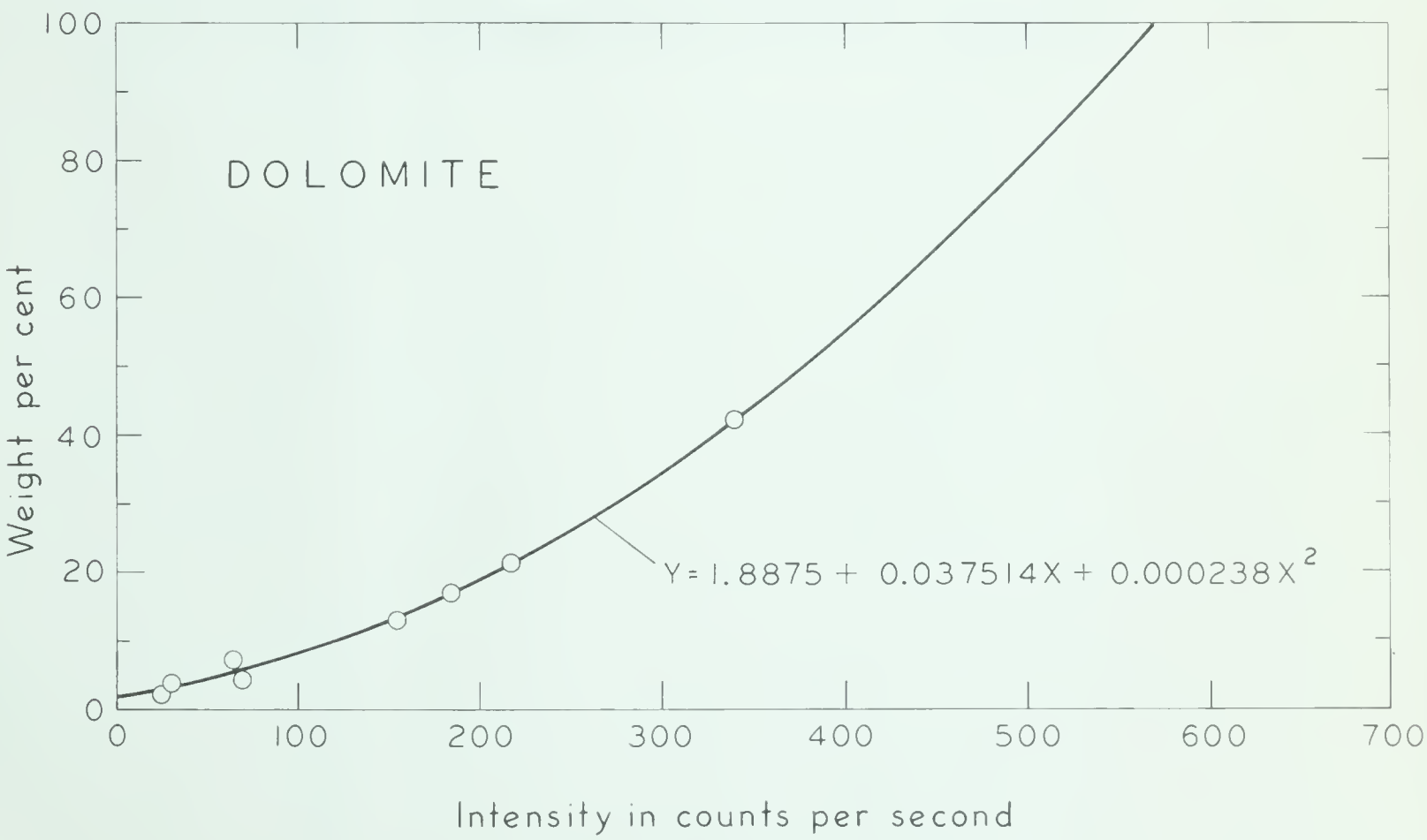

Figure 4. Standard curves for calcite and dolomite.

$Y = 1.0787 + 0.1561\ X$

Y = per cent calcite by weight

X = the intensity of diffraction CuK_{α} radiation in counts per second

Similarly, the dolomite regression equation (Figure 4) is as follows:

$Y = 1.8875 + 0.037514\ X + 0.000238\ X^2$

Y = per cent dolomite by weight

X = the intensity of diffraction CuK_{α} radiation in counts per second.

Regression equations were calculated by the "least squares method" (Arkin and Colton, 1959, pp. 50-66), as applied to linear (calcite) and non-linear (dolomite) trends. Mean X-radiation intensity values (two slides per sample) of the 48 systematic samples were substituted in the above equations to determine weight percentages of calcite and dolomite. The stratigraphic distribution of the carbonate minerals is shown on Figure 4; percentage values are listed in Appendix A.

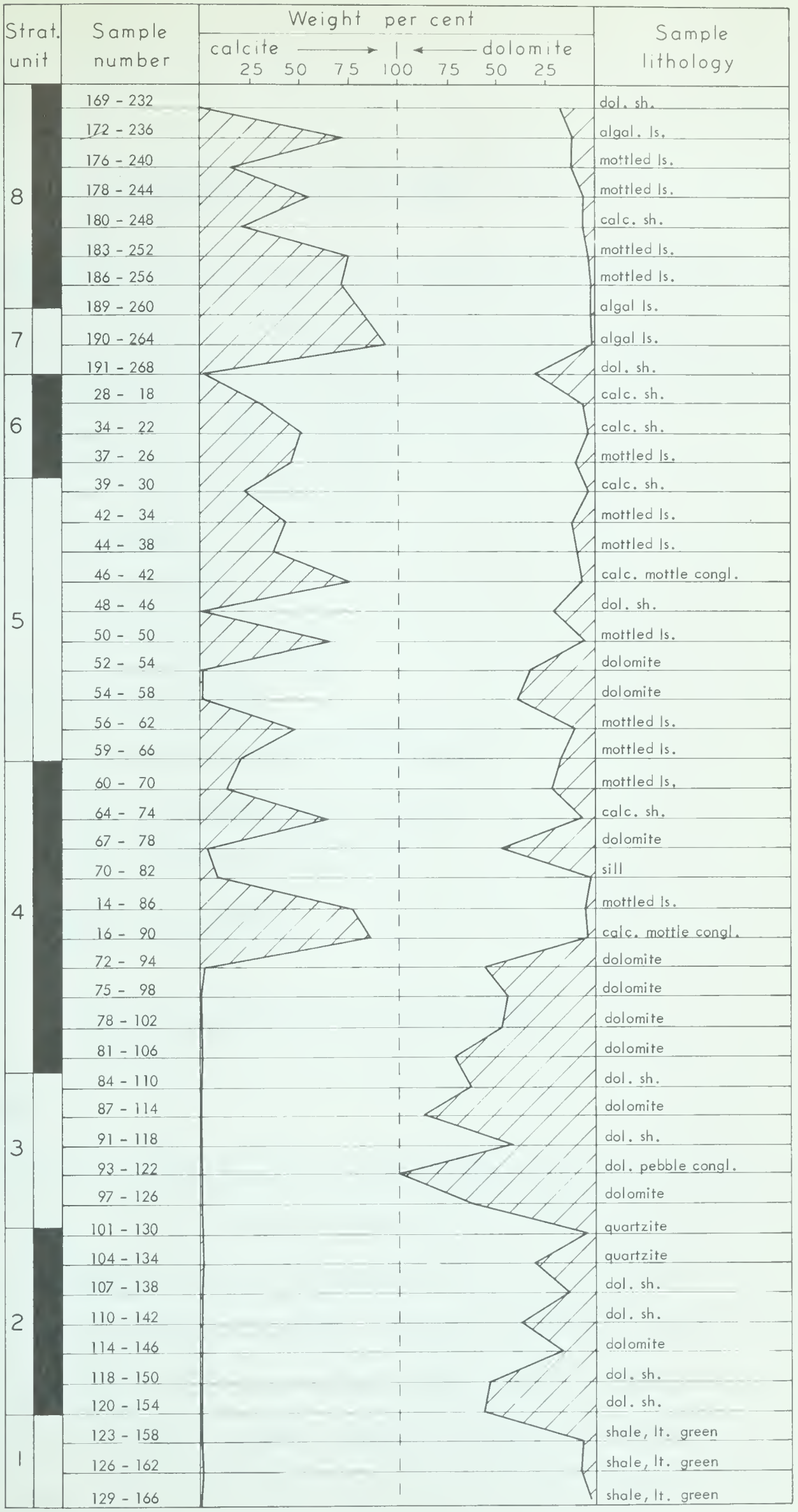

Figure 5. Stratigraphic distribution of calcite and dolomite in the Siyeh formation.

SEDIMENTARY STRUCTURES

Sedimentary structures of the Siyeh formation can be divided into two groups that overlap in time and space, which are distinct from those structural or metamorphic effects that took place during the uplift associated with the formation of the Rocky Mountains in Tertiary time. These two groups are as follows:

(1) primary depositional structures

--crossbedding

--graded bedding

--scour or erosion surfaces

(2) secondary structures

--roiled beds associated with slumping

--calcite-filled shrinkage fractures

--calcite-filled slump fractures

--growth segregations

PRIMARY DEPOSITIONAL STRUCTURES

Crossbedding

All Siyeh carbonate rocks show some evidence of cross-lamination on a microscopic scale, but well-developed crossbeds are confined only to oolite beds. However, crossbedding is common in the upper clastic unit of the Siyeh formation and in the underlying Grinnell formation. Combined inclination values of cross-beds (bedding corrected) from these two units range from 17 to 34 degrees, most being from 15 to 25 degrees. Azimuth readings of direction of inclination of cross-beds in the upper Siyeh and Grinnellformations show a similar direction, though the

units are 1600 feet apart. The resultant direction is to the northwest (Figure 6).

Graded bedding

Graded bedding is well developed in both the mottled limestones and the dolomites. A detailed study of the Siyeh graded bedding was undertaken to determine the magnitude and stratigraphic distribution of such structures throughout the Siyeh formation. In addition, an attempt was made to determine whether characteristic differences in the thickness of graded beds exists between the mottled limestones (most displaying shrinkage fractures) and the dolomites. It was originally thought that if differences between the rock types were found, these would reflect differences in sedimentation, and perhaps throw some light on the genesis of shrinkage fracture segregations.

Most graded beds comprise two components, a lower coarse layer and an upper fine layer of sediment, and are classified as continuous or discontinuous, depending on the nature of the transition from coarse to fine material within individual graded beds.

Discontinuous beds are characterized by an abrupt break in grain size at the top of the lower, coarse component. The coarse sediment is composed of quartz grains and secondary dolomite rhombs of similar size, set in a fine-grained matrix in which grains of calcite are commonly present. In a few instances quartz grains decrease in size towards the top of the coarse component, but in most cases the quartz grain size remains fairly constant. The coarse secondary dolomite rhombs, unlike the quartz grains, generally decrease slightly in size towards the top of the coarse component, and the proportion of matrix to grains increases. The break in grain size at the top of the coarse layer is distinctly erosional in only a few cases. In most beds it appears

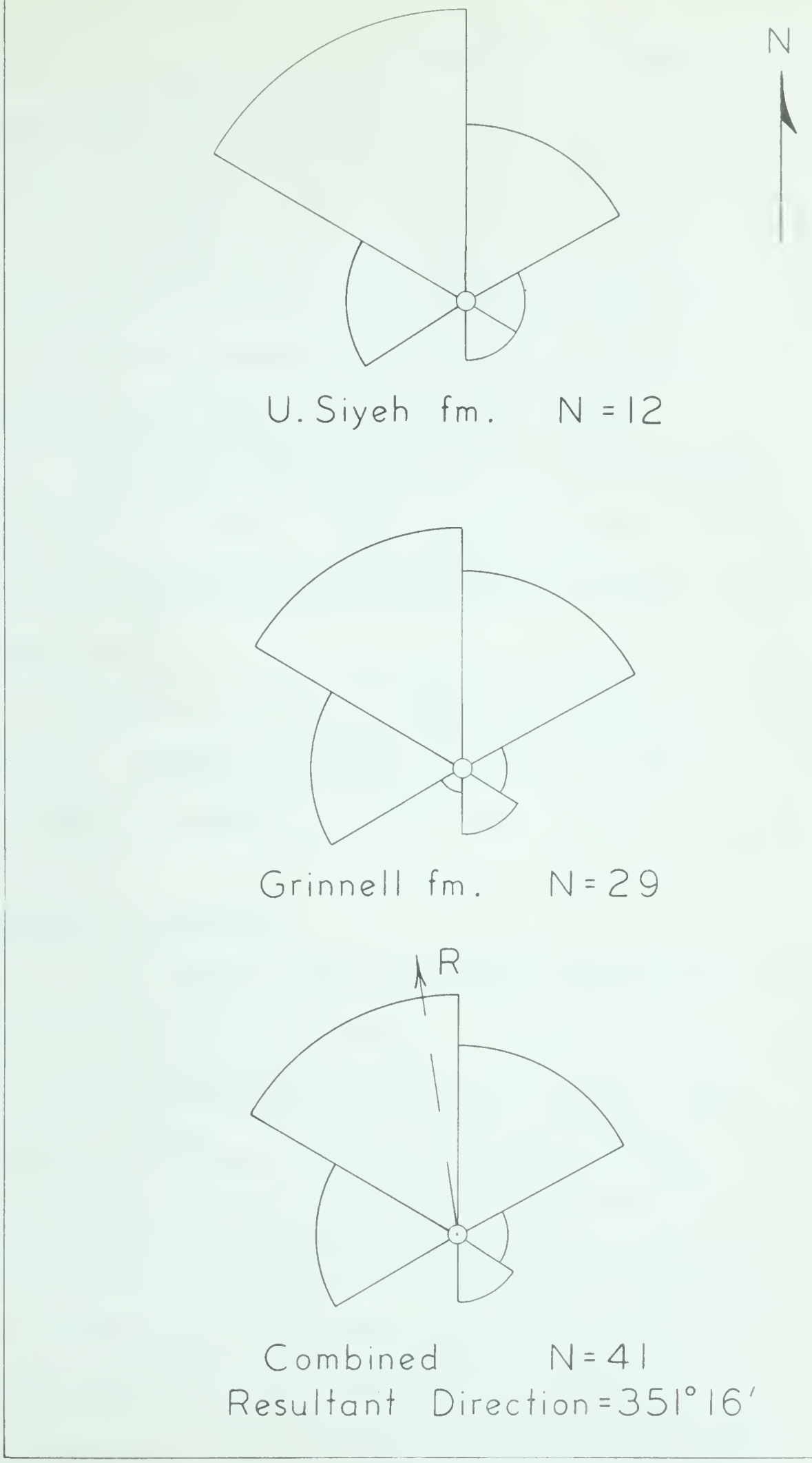

Figure 6. Azimuthal distribution of crossbedding in the Precambrian Siyeh and Grinnell formations, Loaf Mountain ridge locality, southwestern Alberta. N = number of readings

to represent a sudden change in sedimentation. A thin transition zone, also graded, marks the change from coarse to fine material in a few beds. The upper fine component appears uniformly fine-grained, with most constituents less than 10 microns in size.

Three component discontinuous graded beds, composed of three layers, each of a finer grain size than the one below and separated by distinct boundaries, are rare.

Continuous graded beds exhibit no major grain size break but rather grade progressively from coarse at the base to fine at the top.

The majority of beds, both continuous and discontinuous, are separated by distinct surfaces of erosion. Minor channels are present in the upper surfaces of the beds, the depressions being subsequently filled with coarse, laminated sediment of the overlying bed.

Many beds exhibit well-developed cross-lamination in the lower coarse component. Graded beds are generally lenticular in shape with little lateral extent, some beds "pinching out" in the field of the hand specimen.

Sampling and measurement

The parameters chosen for quantitative measurement are bed thickness and the thickness of the coarse component. In the laboratory rock slices were obtained from systematic samples collected at 10-foot intervals throughout the Siyeh section. All samples exhibiting graded bedding were examined under a binocular microscope at two- and four-power magnifications. A single traverse line was drawn at random perpendicular to the bedding across the face of each hand specimen. Measurements were made along this line, except where fracture segregations were found cutting across graded beds, in which case these beds were omitted. In the 230 graded beds measured only one three-component discontinuous bed was observed; it was not included in the data tabulation. The thicknesses of 45 graded beds from 13 mottled limestone samples, and 184 graded beds from 20 dolomite samples were measured.

Figure 7. Stratigraphic distribution of Siyeh systematic samples showing graded bedding.

Results

Graded bedding is observed throughout most of the Siyeh carbonate sequence (Figure 7) and is most prevalent in unit 4. The thicknesses range from 0.2 millimeters to 2.7 centimeters with a mean value of 4.22 millimeters (Figure 8). A chi square test of the observed differences in mean thickness between the dolomites and the mottled limestones gives a probability value of 0.289, indicating that the difference in graded bed thickness between the two rock types can be accounted for by random sampling.

Mean sample thickness values plotted against the stratigraphic position of the samples (Figure 7) appear to be greater in unit 4 than unit 5. However, chi square values obtained from the comparison of graded bed thicknesses in units 3 and 4 with 5, 6, and 8, and units 3 and 4 with units 5 and 6 yield non-significant probability values of 0.422 and 0.151, respectively. It thus appears that there is no significant stratigraphic variation in graded bed thickness.

Thickness of the coarse component is plotted against the total graded bed thickness for 157 discontinuous beds in Figure 9. The scatter of points increases with increase in mean thickness, giving a fan-shaped distribution of points. The average thickness of the coarse component in discontinuous beds was estimated by calculating the regression coefficient (b) for the regression equation $Y = bX$, according to the procedure outlined by Snedecor (1956, p. 155). The mean slope is

$$b = \frac{Y/X}{N} = 0.424$$

That is, the coarse component makes up about 40 per cent of the thickness of the average discontinuous bed.

Graded bedding thicknesses in both the mottled limestones and the dolomites appear to be log-normally distributed. Cumulative thicknesses of Figure 10 plotted

against cycle thicknesses on log probability paper (Figure 10) give an almost straight line, indicating that the marked skewness of the original distribution is largely dissipated on transforming the data to a log scale. Pettijohn (1957) notes that many types of sedimentation units in various parts of the stratigraphic column have thickness distributions which are nearly log-normal.

Fenton and Fenton (1937) considered that the graded bedding in the Belt carbonates represents annual fluctuations in sediment supply and calculated a rate of one foot of sediment per 120 to 420 years in the Altyn formation of the Belt series in Montana. A rate of one foot per 72 years was calculated for the Siyeh carbonates on Loaf Mountain ridge, using the mean graded bed thickness (4.22 millimeters) as equal to one year. However, there is no evidence that the graded beds are annual varves, and, in fact, the lenticular nature of the beds, as well as evidence of minor local unconformities, argues against using such a technique to calculate the rate of sedimentation.

Scour surfaces

Erosion surfaces are common throughout the carbonate sequence but especially well-developed in unit 2.

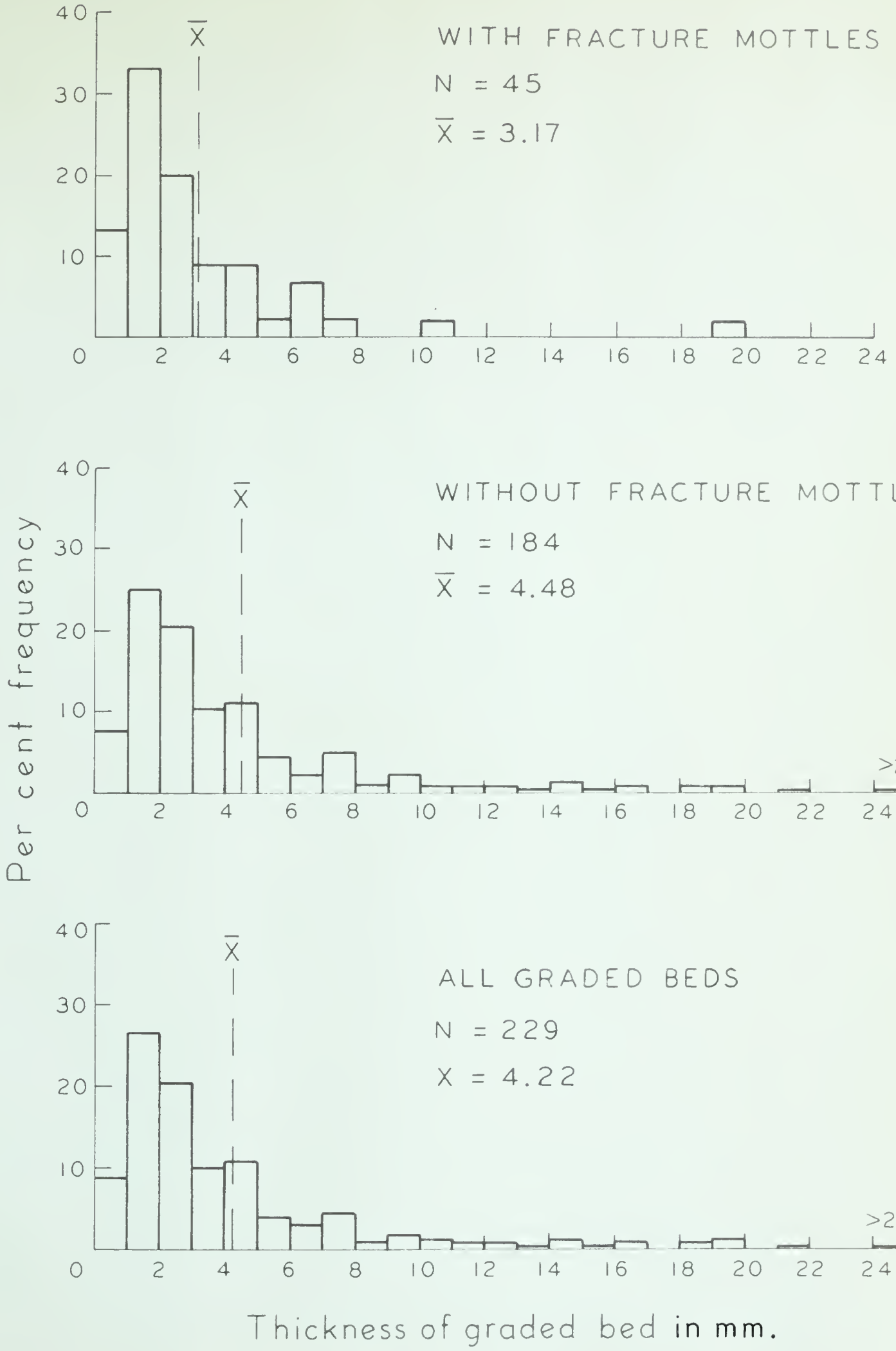

Figure 8. Histograms showing distribution of graded bedding thickness on 33 systematic samples (13 mottled limestones, and 20 dolomites)

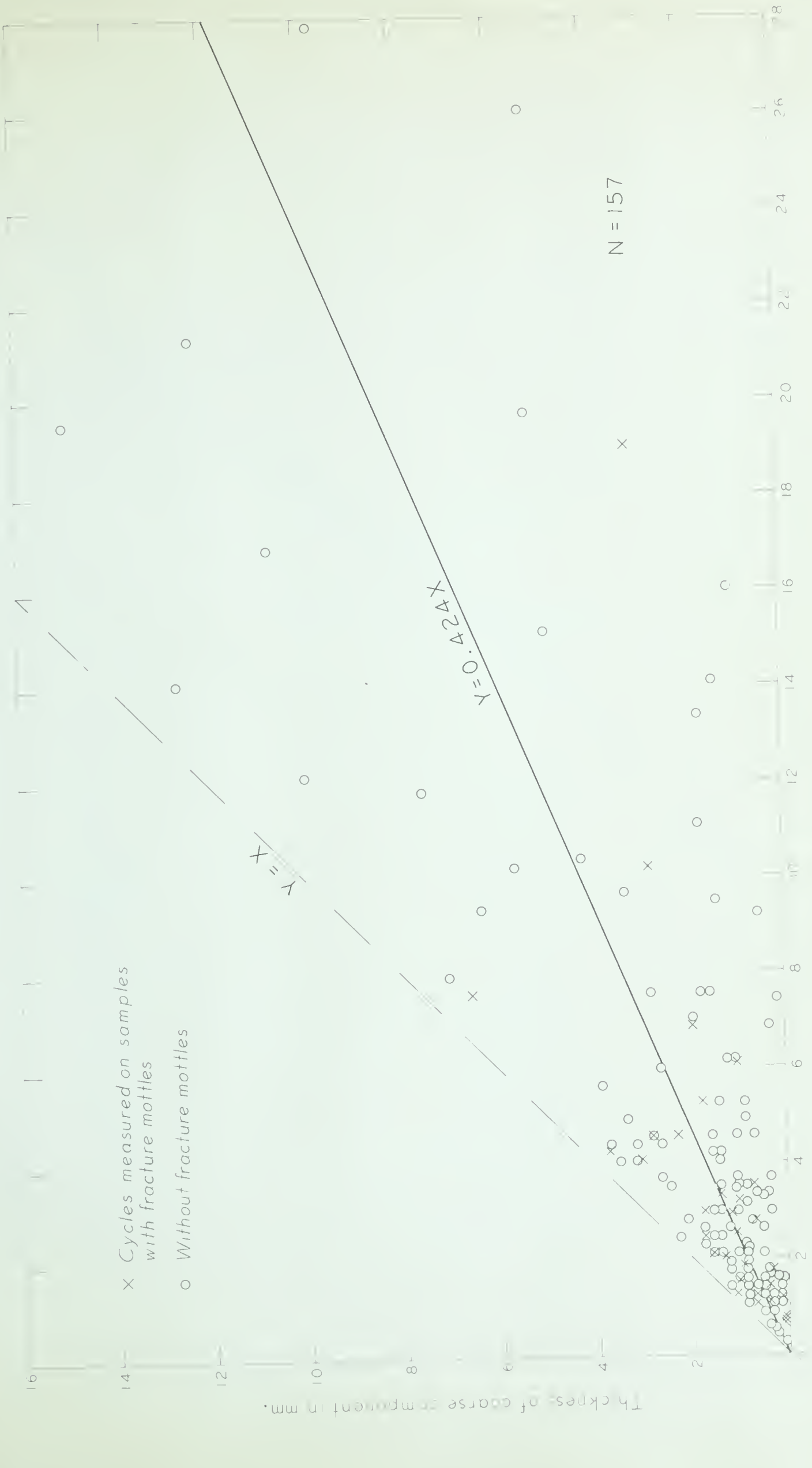

Figure 9. Scatter diagram showing the relationship between graded bed thickness and the thickness of the coarse component in 157 discontinuous graded beds, taken from samples both with and without fracture segregations.

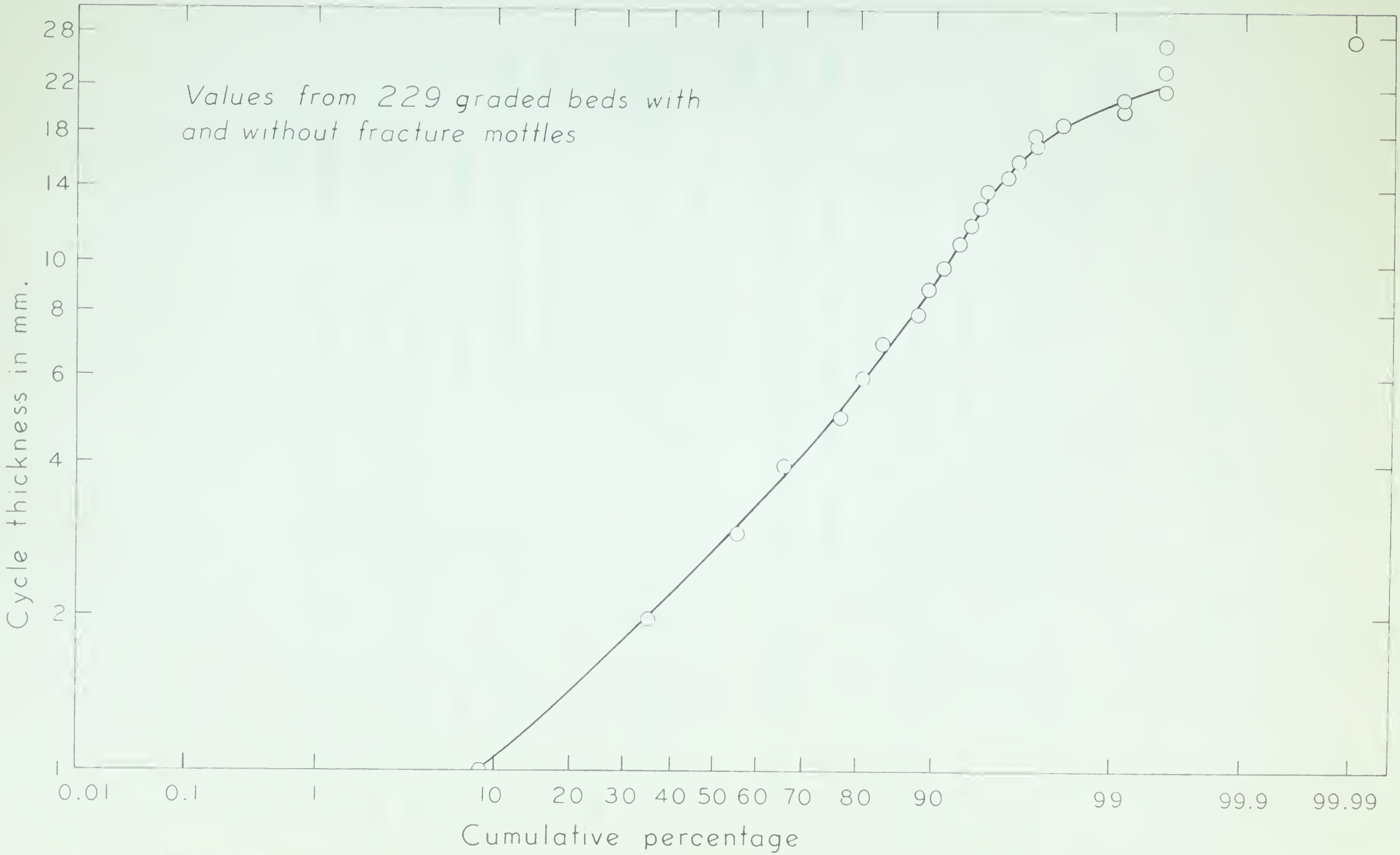

Figure 10. Cumulative frequency curve showing the log-normal distribution of the thickness of graded beds.

SECONDARY STRUCTURES: MOTTLING EFFECTS

Introduction

Mottling in carbonate rocks is usually the result of the presence of two components, one of which, the minor constituent, forms irregular patches in the other, the host. Differences between components may be either predominantly mineralogic or predominantly textural, such as a marked grain size difference between mottles and host. The Siyeh mottled rocks are composed of coarse silt mottles in a host of fine clay or silt-sized detritus (mechanical segregations), or calcite mottles in a dolomitic host containing detritus of all sizes (chemical segregations), as shown in Table 12.

Polished section studies of eighty Siyeh samples, cut perpendicular to the bedding and etched with dilute hydrochloric acid, indicate that the observed mottle effects may be attributed to three processes: soft sediment slumping, *in situ* growth of calcite, and development and cementation of fractures, giving rise to roiled segregations, growth segregations, and fracture segregations respectively. Thus, the term "segregation," as used here, refers to discrete areas differing in composition or texture from the enclosing rock and does not necessarily imply that these areas have formed as a result of a redistribution of material already in the sediment. Some "segregations" have resulted from the precipitation of minerals introduced to the sediment.

Table 12. Genetic classification of the mottled Siyeh rocks.

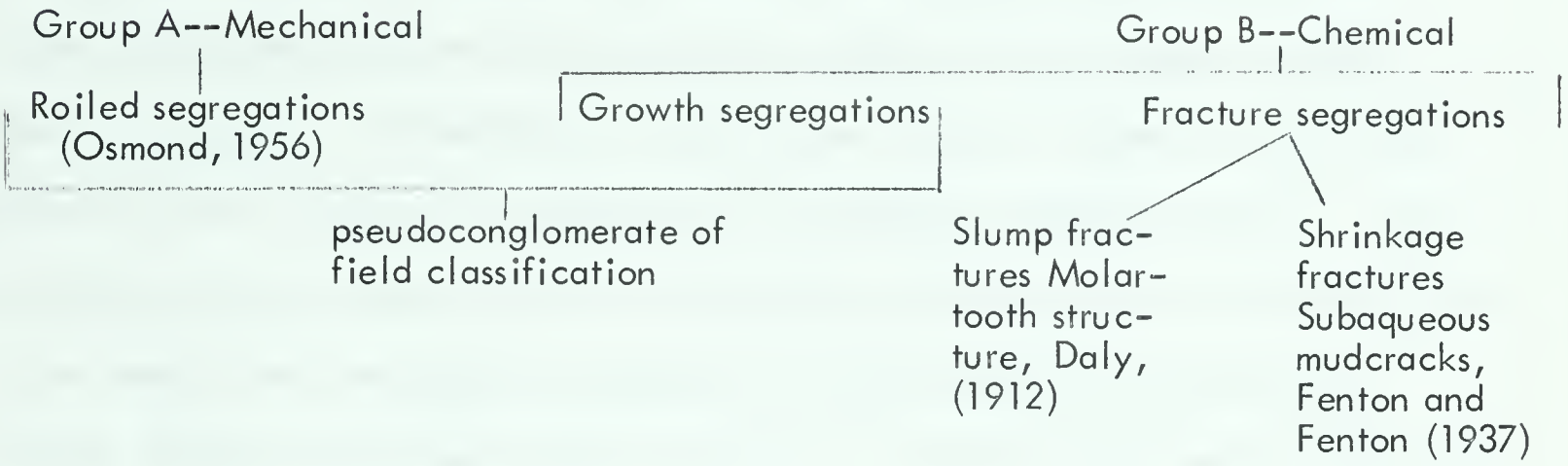

Roiled segregations

Roiled segregations are mechanical structures produced by slumping and flowing of layered sediments during diagenesis. The requirements and mechanism for the formation of such structures were discussed by Osmond (1956), who suggested that mottles produced in this manner are the result of "alternating laminae of two varieties of carbonate sediment with contrasting color and intrastratal soft-rock deformation referred to as roiling."

Most of the Siyeh mottled rocks exhibit fair to well developed primary alternation of coarse and fine material in the form of small scale graded beds (Plate 4, Figure 2). They also contain scattered thin (1/2 inch to 2 inches thick) dark-brown weathering, coarse silt lenses. The coarse silt fraction of the sediment is localized in knots and lumps (Plate 3, Figure 2), which are in some instances connected vertically and horizontally by narrow apophyses of similar material, forming irregular shapes elongate in the bedding direction. The coarse component weathers brown and is resistant in comparison with the more argillaceous light buff to grey weathering groundmass. Slumping generally involves beds about a foot thick, which

can be traced laterally for more than 300 feet along strike and appear to persist over much greater distances. Within beds, slumping is confined to layers two to three inches in thickness which are separated by only slightly deformed primary laminae (Plate 3, Figure 1). The mottles (or "roils") contain angular fragments of laminated sediment (Plate 3, Figure 1) in keeping with the findings of Pettijohn (1957, p. 192), who stated that the coarse material in interbedded argillaceous and sand-silt sediments is more mobile than the clay-mud component and under certain conditions flows, carrying "pieces of the shale along as inclusions." Flowage of the coarse constituents, according to Pettijohn (ibid, p. 190), "produces squeezed out lumps of sand or silt", as is evident in the Siyeh roiled beds.

Segregation bodies may be noncalcareous as shown in Plate 3, Figures 1 and 2, or moderately calcareous, in which case weathered surfaces show mottles of light to medium grey silty calcitic material distributed in irregular fashion through a light brown dolomitic groundmass. The colours on weathered surfaces are thus the reverse of those observed for the noncalcareous roils, and in outcrop the segregations sometime resemble structures formed by quite different means.

Calcite-filled fractures transect silt segregations, having formed after minor soft-sediment slumping. Calcitic roils were probably calcitized at the same time as the later fractures.

Slumping appears to have been intrastratal as no definite erosion surfaces are observed truncating deformed bedding. The only evidence of deformation in the top few inches of the sediment is the presence of minor folds, ranging from two to four millimeters in amplitude, which acted as minor surfaces of relief until buried by overlying detritus. Laminae of the sediment filling troughs on the flanks of such folds wedge out against and eventually drape over the first-order structures. These folds were observed in only a few specimens.

Roiled beds first appear in the lower part of unit 5 (430 feet below the base of unit 7) and become more frequent in the lower part of unit 6, although rarely observed in the upper part of that unit. They were not observed higher than 15 feet above the top of the algal reef (unit 7).

Growth segregations

The second major class of mottles (Group B, Table 1) comprises calcite segregations of various types enclosed in a silty, dolomitic groundmass and is present in beds usually not more than two feet thick.

The first type is termed growth segregations and consists of three main configurations: cylinders, flat-lying sheets, and pinching and swelling sheets composed of loosely connected nodules. Cylinders are generally less than one inch in diameter and lie subparallel in the bedding plane, giving a "washboard" appearance to weathered bedding surfaces; they are rare. Flat-lying sheets generally about one-quarter to one-half inch in thickness are common. However, most of the segregations take the form of nodular bands and pinching and swelling sheets (Plate 2, Figure 1). In two dimensions nodules most commonly appear as ellipsoidal masses, one-half to several inches long, flattened in the bedding plane. Less commonly, the elongation of nodules is at high angles to the bedding, and a pseudoimbricate structure is observed. Examination of serial sections through several specimens shows that in three dimensions individual nodules are commonly joined laterally by thin apophyses to form almost unbroken sheets, so that all gradations exist between sheets and layers of individuals.

Lateral variation in the shape of the mottles is illustrated by the following example. In outcrop, a band composed of individual nodules several inches apart

was traced in a one-foot-thick bed for 200 feet along strike, at which point the nodules were found to coalesce to form thin sheets. Although the shape of segregations may change laterally, the upper and lower limits of the containing strata are remarkably constant; that is, segregation beds appear to persist laterally over great distances.

On etched surfaces relict primary bedding laminae (consisting of authigenic quartz crystals, as well as detrital grains) pass through segregations and continue into the groundmass, following the bedding direction irrespective of the elongation or shape of the segregation (Plate 4, Figure 1).

In contrast, many bedding laminae above and below segregations have been deformed around the margins of the calcitic bodies. It appears that this effect is mainly due to the growth of the segregation rather than to effects of compaction. In one sample (Plate 4, Figure 2), two primary laminae three millimeters apart in the groundmass are separated by ten millimeters where the upper one passes through the middle of a calcitic nodule and the lower one is deformed around the base of the segregation. It is evident that the lower primary lamina has been displaced with respect to the overlying one due to the growth of the nodule, and that the upper lamina has undergone partial replacement. Thus, these segregations have grown in place during diagenesis, both replacing and displacing the still plastic groundmass material.

One such growth segregation shows a one millimeter thick layer of sediment passing over one nodule, down into a depression and up over an adjacent segregation. above this layer, laminae are five millimeters thick over the nodule, about half as thick as the equivalent sediment in the adjacent depression. After the accumulation of five millimeters of sediment over the location of the subsequent nodule, the relief caused by growth was largely compensated for by contemporaneous sedimentation of

nearly flat-lying laminae in the adjacent depression. Thus, the growth of the nodule must have commenced within a few millimeters of the sediment surface, and was completed when the segregation was buried to a depth of only five millimeters. Also, flat-lying erosion surfaces are observed truncating nodule layers, providing further evidence of an early diagenetic origin (Figure 11).

There is no conclusive evidence of the relationship between roiled and growth segregations. The latter are cut by calcite-filled fractures and were formed prior to fracture development.

Growth segregations are sparsely distributed in thin zones throughout units 4, 5, and the lower part of unit 6. In the upper part of unit 6, beds containing these segregations are more common and thicker (up to two feet, Plate 2, Figure 1). They are also common throughout most of unit 8, the last being observed at a horizon 40 feet below the top of that unit.

Fracture segregations

Fractures filled largely with calcite cement constitute the second type of calcitic segregations. Two varieties of fractures are recognized, based largely on the differences between fracture patterns. Fracturing is considered to be caused by shrinking and slumping in a soft sediment.

Shrinkage fractures

Shrinkage fractures show a distinctive polygonal to semipolygonal pattern on weathered bedding surfaces (Plate 5, Figure 1). Calcite filling the fractures appears in outcrop as dark grey, usually contorted veinlets, oriented at high angles to the bedding (usually roughly perpendicular). The veinlets are present in layers one to

Figure 11. a) Showing a calcite-filled shrinkage fracture terminated at the top by a distinct surface of erosion E, as shown by the truncation of graded bedding at A. Calcite phenoclasts of the overlying mottle conglomerate are derived from underlying veinlets, and drape over the veinlet supported "high", showing calcite cementation of fracture preceded deposition of the overlying conglomerate. Natural size, dark areas calcitic.

b) The same as in a)
Natural size, dark areas calcitic.

c) Showing the greater thickness of sediment accumulated in a depression between two growth nodules at B, than over a growth nodule at A.
A. Two surfaces of erosion, the lower forming a channel, pass through the specimen. Note the truncation of growths at the upper surface and the presence of a small "shrinkage" fracture penetrating a lower growth from above.
Natural size, dark areas calcitic.

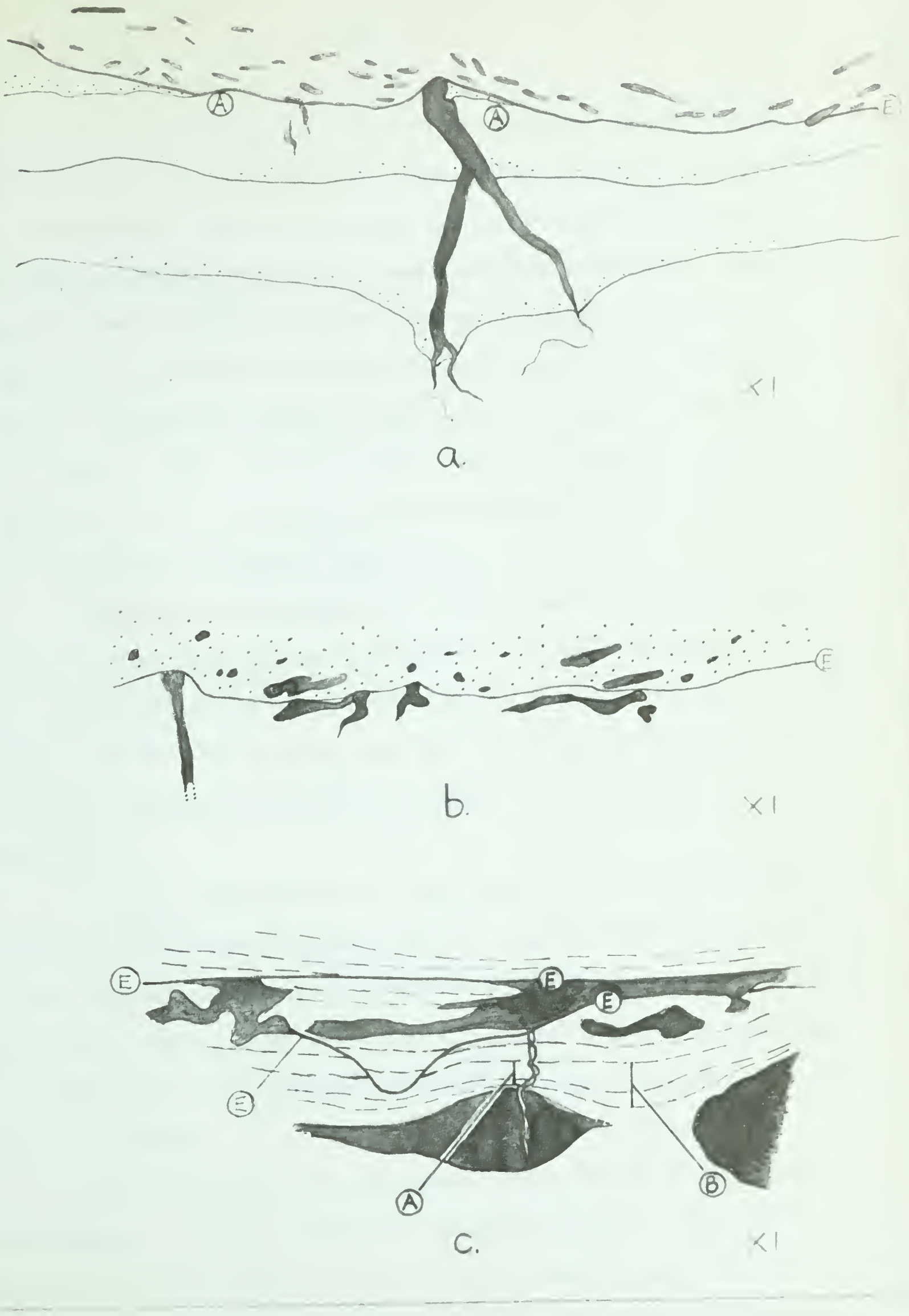

Figure11.

two inches thick. In most cases the layers are closely spaced, giving a banded appearance to the buff weathering, silty, dolomitic host rock (Plate 2, Figure 2). Upper terminations of individual veinlets are usually flat and abut abruptly against the overlying sediment, which in many cases is arched over the veinlets. Veinlets commonly terminate downward in a sharp taper and, where fracture layers are closely spaced, penetrate the sediment of the underlying fracture layer (Plate 2, Figure 2). The veinlets are commonly from two to four millimeters but less than six millimeters in width. A series of parallel slices cut perpendicular to the bedding at one-quarter inch intervals through a typical shrinkage fracture specimen confirms that the segregations are planar in shape rather than tabular.

It is difficult to trace veined layers along strike for more than 20 or 30 feet due to the lack of clearly defined layer boundaries. However, beds comprising several shrinkage fracture layers, generally from one to six feet in thickness, can be traced for more than 300 feet along strike without significant change in the intensity of fracture development or the thickness of the bed, and appear to persist for much greater distances.

Sometimes, spheroidal calcite bodies usually less than three millimeters in diameter are associated with polygonal fractures. Individual "balls" are connected with others by thin irregular calcite sheets located normally along bedding planes. They appear to represent small initial cavities in the sediment, possibly caused by gas pockets, which were subsequently filled with granular calcite cement at the same time as the fractures.

Plastic deformation of primary bedding laminae adjacent to calcite veinlets is common. Usually the bedding laminae are down-curved on either side of veinlets (Plate 4, Figure 3), but in some instances upwarped laminae are observed in contact with shrinkage veinlets. Warping of laminae and the polygonal fracture pattern strongly indicate a shrinkage genesis.

The fractures appear to have formed at the sediment surface as beds of Collenia are invariably found immediately over polygonally fractured surfaces. This confirms Black's (1933) observation that algae of the Collenia type (form genus) grow on mud-cracked surfaces of relief. Additional evidence for a surface or near-surface origin of fractures, cemented very shortly after formation, is the common presence of intraformational mottle conglomerates in association with polygonal fractures. These rocks are found in thin bands (most less than two inches thick) within and above shrinkage fracture beds and rarely persist along strike for more than 50 feet. The majority of phenoclasts, which are commonly subrounded to well rounded and rarely angular, consist of pure calcite. They appear to have been derived from erosion of a sediment containing a polygonal network of calcite veinlets. Fragments derived from veinlets were rounded and redeposited, commonly with imbricate structure, which clearly indicates current deposition. The fact that pebbles are rounded and may attain a length of up to two inches does not suggest strong agitation. Matrix is found adhering to some calcite pebbles, whereas other phenoclasts consisting of dolomitic silt contain calcite veinlets wholly within the pebbles, which represent fragments of veinlet-filled host rocks (Plate 5, Figure 3).

Thin sections of mottle conglomerates and calcite-filled shrinkage fractures reveal that both have an identical fabric of granular calcite cement (Plate 8, Figure 6). Veinlets of granular calcite pass through some dolomitic silty limestone pebbles but terminate abruptly at the rounded margins of the pebbles, clearly indicating cementation of fractures prior to fragmentation (Plate 9, Figure 8).

The arching of sedimentary laminae over the upper flattened terminations of veinlets may now be considered in the light of the foregoing discussion of mottle conglomerates. Shrock (1948, p. 200) reported calcite-filled mud cracks in Silurian

argillaceous limestones of Indiana and Wisconsin, which are similar to those in the Siyeh. Shrock offers the following explanation: "If the mud-cracked surface is buried in such a manner that some of the cracks are not filled, the incoming sediment arching (horizontally) over them instead, the cavity remaining may be filled later with secondary mineral." In the Siyeh, the high angle veinlets in shrinkage layers, overlain by mottle conglomerates in many instances, project three to five millimeters above the erosion surface; they act as minor features of relief, supporting the groundmass for a few millimeters on either side. The depressions between veinlet supported highs are partly filled with rounded calcite phenoclasts, sometimes arranged in an imbricate pattern, and derived from the calcite veinlets (Figure 11). This evidence indicates that in the Siyeh rocks the convex-upward arching of sediment over blunt upper terminations of veinlets was not accomplished prior to cementation of the fractures but, rather, represents a draping of sediment over fracture fillings. Fractures were cemented very soon after their formation, and subsequent minor current action preferentially eroded the enclosing soft groundmass. It would then appear that the intraformational mottle conglomerate did not necessarily form as a result of temporary strong wave action; on the contrary, they could well represent periods of prolonged erosion involving winnowing and sorting of surface sediment by weak bottom currents.

In the majority of occurrences of shrinkage fracture layers, upper terminations of veinlets are overlain by dolomitic silt, rather than mottle conglomerates, and the contact of veinlets with overlying silt is not obviously erosional (as in the case of mottle conglomerates where phenoclasts are derived from underlying veinlets). However, usually some degree of arching of sediment over veinlets is observed. Since this draping is considered an erosional feature in the case of the mottle conglomerates, it is probably also indicative of erosion in the dolomitic silt layers.

A reconstructed picture of the sedimentation of layers within shrinkage fracture beds appears to be as follows:

(1) deposition of less than one inch to several inches of sediment which may comprise one or several graded beds

(2) development of fractures

(3) cementation of fractures

(4) minor erosion (where indicated by arching sediment)

(5) deposition of next layer.

Calcite-filled polygonal fractures are common throughout units 4, 5, 6, and 8, as are the mottle conglomerates, whereas both are conspicuously absent in units 1, 2, and 3, which further emphasizes the relationship between the two phenomena.

A question which now arises is whether the shrinkage took place under subaerial or subaqueous conditions. Fenton and Fenton (1937) favour the latter and term these features "subaqueous mudcracks". If the cracks were formed under subaerial conditions, it is unusual that they should be filled with calcite cement rather than clay, silt, or sand as are the subaerial mud-cracks of the Grinnell red beds and other formations of the Belt series. Early cementation could best be accomplished if the fractured sediment surface was immersed in water from which calcite could be precipitated.

Tanner (1959, p. 329) reports forming subaqueous shrinkage cracks in the laboratory, but does not report the experimental conditions. Various other mechanisms for the formation of subaqueous cracks, such as freezing and thawing of bottom sediments, and substratal drainage (Shrock, 1948), have been suggested but do not give a satisfactory explanation for the Siyeh shrinkage phenomena. Until more is known about the formation of subaqueous mud-cracks, as well as possible calcite filling of cracks in

subaerial beds, it is not feasible to assign with certainty either a subaerial or a subaqueous mode of formation to the Siyeh calcite-filled fractures.

Sand-filled subaerial mud-cracks are rare in the Siyeh carbonate sequence (units 2 to 8), only found associated with one oolite bed in unit 5 and in a few beds near the top of unit 8.

Slump fractures

A pattern of calcite-filled fractures, commonly termed "molar-tooth structure", constitutes a second variety of calcitic fracture segregation. Bauerman (1885) was the first to describe these structures and reported that they strongly resembled the molar tooth of an elephant on favourably weathered surfaces. Daly (1912) adopted Bauerman's term and ascribed to the fractures a post-lithification genesis, suggesting that they were formed during the uplift of the Belt strata. Fenton and Fenton (1937) concurred with Daly's interpretation. Because the term "molar-tooth" is ambiguous and has been used rather freely in later reports to refer to all mottled rocks in the Siyeh formation regardless of their genesis, the term is discarded here in favour of "slump fractures".

On weathered bedding surfaces cemented slump fractures form thin, subparallel calcite veinlets which exhibit a marked linear trend (Plate 6, Figure 2). The veinlets are always less than two millimeters in width, and are generally spaced from two to four millimeters apart. In exposures at right angles to the bedding and perpendicular to the fracture trend (Plate 2, Figure 3) veinlets are observed in distinct layers, which range from two inches to one foot in thickness. The dip of veinlets with respect to bedding generally ranges from 30 to 80 degrees and is usually constant within a layer, although in some layers a complete dip reversal, giving a chevron configuration is present. Fractured layers are commonly separated by thin

argillaceous interlayers and in some instances breccia bands, usually less than one inch in thickness.

Slump fracture beds comprise one or several slump layers and range in thickness from several inches to five feet, most commonly from two to four feet. Beds can be traced for 300 feet along strike with only slight variation in thickness and are thought to persist over much greater distances. Layers within beds were not traced for more than short distances, due to the difficulty in finding favourably weathered, laterally persistent exposures on which individual layers could be distinguished. Upper and lower surfaces of fracture layers generally follow the bedding, and individual layers are thought to persist for considerable distances.

Slump fractures are distributed stratigraphically throughout the upper part of unit 4 (sparse beds), units 5 and 6 (common, becoming rare in the upper part of unit 6), and the lower part of unit 8, where the last slump bed was observed 75 feet above the base of the unit. The subparallel traces of slump fractures on bedding planes show a fairly constant trend from layer to layer within a single bed and also between beds. Bearings (taken in a horizontal plane) of the line of intersection of veinlets with the bedding plane were taken on one layer in each of 15 beds distributed stratigraphically throughout units 4, 5, and 8. The results show that there is little variation in the strike of veinlets throughout about 750 feet of section in which the slump fractures are developed, except for one reading (80-100°).

Table 13. Direction of line of intersection of bedding (strike: 149°; dip: 19°SW) and slump fracture veinlets.

Direction of line of intersection (in degrees)	Number of readings	Direction of line of intersection (in degrees)	Number of readings
80-100	1	180-200	4
100-120	---	200-220	5
120-140	---	220-240	---
140-160	---	240-260	---
160-180	5		

Primary sediment laminae adjacent to slump fractures show signs of having been deformed while still plastic, and the veinlets themselves sometimes consist of segments which are crowded or broken into segments. This may be a reflection of the initial slump fracture configuration, although later minor movement in the slump layer, perhaps due to compaction, could also account for a slight displacement of veinlets and some folding of primary laminae prior to lithification.

The relationship of slump fractures to the groundmass of the rock and growth segregations is well shown in one sample (Plate 4, Figure 2). A growth segregation is displaced along a small slump fracture developed in the growth layer in association with other calcite-filled slump fractures cutting the same growth. On tracing the fracture from the growth segregation into the groundmass below, a lamination composed of coarse silt is encountered, from which coarse material flowed for about five millimeters down the fracture trace. This indicates that the slump fractures formed after growth segregations but while the groundmass was still plastic enough for minor local flow of more mobile material.

Similarly, the relationship between slump fractures and shrinkage fractures is one of slumping following shrinkage, as linear slump fractures are superimposed

upon, and cut across, the polygonal fractures. Fenton and Fenton (1937), in describing the same features, noted this relationship between their "subaqueous mudcracks" and "molar-tooth structure."

The argillaceous and brecciated bands between fracture layers appear to represent zones of slippage along which minor movement in non-lithified sediment took place. Of particular interest are the breccias, which are composed of fragments of pure calcite and associated fragments of laminated dolomitic rock (Plate 7, Figure 2). The calcite fragments appear to have been derived from pre-existing calcite fracture fillings (shrinkage fractures) where slippage occurred through a bed containing cemented polygonal fractures. A sample (Plate 7, Figure 2) was taken from a slump-fracture bed in which fracture layers five inches thick are present immediately above and below the breccia. Examination of the upper surface of the sample shows definite development of a polygonal pattern, although slump fractures have probably been superimposed. Veinlets above and below do not pass into the breccia but instead are sharply terminated against it, indicating brecciation of pre-existing fracture fillings and the lack of penetration of slump fractures which probably were formed in the sediment above and below the breccia at the time of slippage. It is probable that all the slump fracture layers within one bed were formed at the same time, but that differential movement within the bed accounted for the formation of several adjacent slump layers.

In no instances were intraformational mottle conglomerates found overlying the eroded surface of a slump fracture layer. In cases where recognizable conglomeratic bands were observed overlying slump fracture layers, the slump fractures penetrate the conglomerates. As there is no evidence to support slumping in the surface layers, the slumping is assumed to have taken place after burial but before lithification.

Contact Metamorphism

At the Loaf Mountain ridge locality a diabase sill 18 feet thick is present within the Siyeh formation 1,568 feet below the base of the Purcell Lava and 675 feet below the base of unit 7 (Conophyton zone 1, Rezak, 1957). This intrusive body is probably the same one near Logan Pass, Montana, dated by K-Ar techniques at 1,110 million years (Hunt, 1961, p. 116). Ross (1959, p. 56) in discussing the Precambrian intrusive rocks in the "Siyeh limestone" in northwestern Montana comments: "In most places only a single sill is exposed, and this is commonly a short distance below the Conophyton zone 1." All previous writers assign a Precambrian age to the Siyeh intrusives (Ross, ibid).

Above and below the sill contact metamorphic zones four feet thick are present in which various segregation structures are preserved. In the zone above the sill a six inch thick slump fracture layer, which has been metamorphosed to light green and white marble, shows the characteristic chevron configuration, with veinlets dipping at low angles (Plate 7, Figure 1). The same specimen shows lumps of almost pure calcite which may represent growth segregations. Also in the upper contact zone a bed of shrinkage fractures exhibiting several layers of small calcite veinlets is well preserved. The lower contact metamorphic zone contains a bed several inches thick consisting of light grey nodules (identical with growth segregations) embedded in a light green groundmass.

The metamorphism of slump, shrinkage, and growth segregations by a Precambrian sill provides further evidence of the early time of formation of these structures and shows that the slump fractures ("molar tooth" structure) were not formed during the uplift of the Belt rocks in early Tertiary time.

Summary

In summary, the mottled or veined appearance of many of the Siyeh calcareous rocks can be attributed to processes of shrinkage, slumping, and cementation which took place during lithification of the still plastic sediment. These processes gave rise to four main types of mottles or fracture fillings, listed below in the probable order of their formation, although the relationship of roiled segregations to growth segregations and shrinkage fractures is still obscure.

(1) shrinkage fractures = growth segregations

(2) roiled segregations

(3) slump fractures

The relationship between growth nodules and shrinkage fractures is also uncertain, as they are rarely observed together, although one specimen shows shrinkage fractures penetrating nodules (Figure 11). Both appear to form in the upper layers of the sediment. Metamorphism of beds containing all but the roiled segregations by a sill of Precambrian age indicates that the rocks were essentially lithified and in their present state before deposition of the overlying Palaeozoic sediments.

PETROGRAPHY

INTRODUCTION

Forty-three of the 191 systematically collected Siyeh samples were thin sectioned for modal analysis. The 43 samples are from unit 1 and the main carbonate sequence (units 2 to 8) of the formation; their relation to the various rock types and total number of systematic samples is given in Table 14. Every fourth sample was chosen for analysis, but most of the shale samples were excluded because of their fine grain size.

(to p. 63)

Table 14. Systematic sample distribution in Siyeh carbonate sequence (units 2 to 8), and unit 1.

Lithology	Number of thin sections examined	Systematic samples: Number collected	Systematic samples: Percentage distribution of those collected
Dolomite	11	42*	22*
Mottled limestone	15	38	20
Dolomitic shale	1	30	16
Calcareous shale	4	26	14
Shale	2	22	12
Algal limestone	4	17	9
Limestone (not mottled)	--	5	<5
Quartzite	2	4	<5
Oolite	1	2	<5
Shale pebble conglomerate (calcareous)	--	2	<5
Mottle conglomerate	2	2	<5
Shale pebble conglomerate (dolomitic)	1	*	*
Algal dolomite	--	1	<5
TOTAL	43	191	100

* Includes several samples of dolomitic shale pebble conglomerate.

The thin sections were cut perpendicular to the bedding and stained with Alizarin Red-S (Friedman, 1959) to distinguish between calcite and dolomite. Percentages of mineral constituents were estimated from counts of 100 points per slide for the mottled limestones and quartzites and 50 points per slide for the other rock types. Grain size of the various constituents was determined using a micrometer eyepiece. Identification and size measurements were made at a magnification of 562.5.

MOTTLED LIMESTONE

Mottled limestones and the dolomites account for more than 40 per cent of the Siyeh carbonate succession. The depositional fabric of the mottled limestones is well-preserved, having been only partially dolomitized and having undergone no noticeable recrystallization. All samples contain calcitic fracture segregations, but no growth segregations or roiled bedding features were observed in the systematic thin sections.

Grain size measurements were made on grains of quartz, calcite and dolomite. The lower limit of measurement was 3.14 microns. The composition of the mottled limestones, determined from point-counts on 15 slides (100 points per slide) is shown in Table 15. Most of the samples are the same as those for which X-ray determinations of calcite and dolomite have been made.

Mineral constituents

Quartz

Quartz is present as discrete grains, authigenic overgrowths on grains, authigenic euhedral crystals, and composite quartz masses, as well as a con-

Table 15. Percentages of mineral constituents in mottled limestone samples*

SAMPLE NUMBER (in stratigraphic order)	MINERAL CONSTITUENTS										
	SILICATES (>10μ)				CARBONATES					SILICATES (<10μ) = MATRIX	OTHERS (mainly sphene, authigenic quartz and hematite)
					CALCITE			DOLOMITE			
	QUARTZ	FELDSPAR	ROCK FRAGMENTS	MICA	IN SEGREGATIONS	IN GROUNDMASS	TOTAL	MINIMUM	MAXIMUM		
176-240	5.5			1.0	57.0		57.0	6.0 - 17.0		17.5	2.0
178-244	6.5	1.0	5.5	2.0	40.0		40.0	8.0 - 20.5		24.5	
183-252	7.5		1.5	1.0	16.0	38.5	54.5	10.0 - 10.0		19.5	6.0
185-255	7.5		8.0	2.5	4.0	18.5	22.5	27.5 - 37.0		22.5	
186-256	21.0	3.0	9.5	2.0	5.0	17.0	22.5	18.5 - 18.5		19.5	4.0
37-26	24.0	1.0	1.0	2.0	23.0	24.0	48.0	5.0 - 11.0		9.0	4.0
42-34	4.0				12.0	22.5	34.5	11.0 - 33.5		27.0	1.0
44-38	10.0		1.0		26.0	9.5	35.5	8.0 - 21.0		29.5	3.0
50-50					21.5	48.5	70.0	5.5 - 19.5		9.5	1.0
56-62	13.0	1.0	3.0	2.0	6.0	22.5	28.5	11.5 - 26.5		24.0	2.0
59-66	1.5			1.0	8.0	12.0	20.0	10.5 - 33.5		43.0	1.0
60-70	12.5	3.0	4.0	2.0	5.0	5.5	10.5	37.5 - 53.5		13.5	1.0
61-71	1.0		1.0	1.0	9.0	4.5	13.5	37.0 - 71.0		12.5	
14-86	5.5			1.0	25.0	39.5	65.5	9.0 - 16.0		11.0	1.0
74-97	4.0			3.0	56.0	3.0	59.0	11.5 - 15.5		17.5	1.0
AVERAGE	8	1	2	1	17**	20**	39	14	- 27	20	2

Dolomite minimum = euhedral - subhedral crystals.
maximum = euhedral, subhedral, and anhedral grains, some of which may be fine-grained mica.
* 100 points per thin section.
** average of 13 slides, excluding 172 - 240 and 178 - 244.

stituent of rock fragments. Quartz grains greater than 10 microns (maximum diameter) were included in the quartz point-count class; particles less than 10 microns were included with matrix but distinguished as quartz when possible. Quartz grains account for 8 per cent of the rock, authigenic quartz for less than 8 per cent, recognizable quartz particles (lessthan 10 microns) for 1 to 2 per cent, and quartz in rock fragments for not more than 1 per cent. This is only one-half the amount of quartz present by normative calculation; the remainder is presumed to be in the form of finely divided quartz particles in the matrix.

Detrital quartz grains greater than the lower limit of measurement (3.14 microns) have a modal grain size of 15 to 27 microns (Figure 12). All grains show straight extinction and are generally subangular to subrounded. Corrosion of grain boundaries by secondary dolomite, and to a lesser extent by micaceous matrix, is common. Calcite is rarely found replacing detrital quartz grains or intruding grain boundaries. Inclusions are common, consisting of trains of vacuoles, scattered rutile needles, and rare zircon microlites.

In the more coarse-grained orthoquartzites (fine sand grain size) of the Siyeh, elongate quartz is found as a straight-edged component of schistose rock fragments, which also contain coarse muscovite shreds, both quartz and muscovite aligned in the direction of elongation of the fragment (Plate 9, Figure 7). Although these fragments are rarely observed in the mottled limestones, quartz grains may have been derived from similar rocks.

Authigenic quartz occurs most commonly as euhedral rhombs and anhedral masses within and along the margins of calcitic fracture segregations (Plate 8, Figure 8), although it is also sparsely distributed as overgrowths on quartz grains in the groundmass. The rhombs show straight extinction and coalesce in some cases to

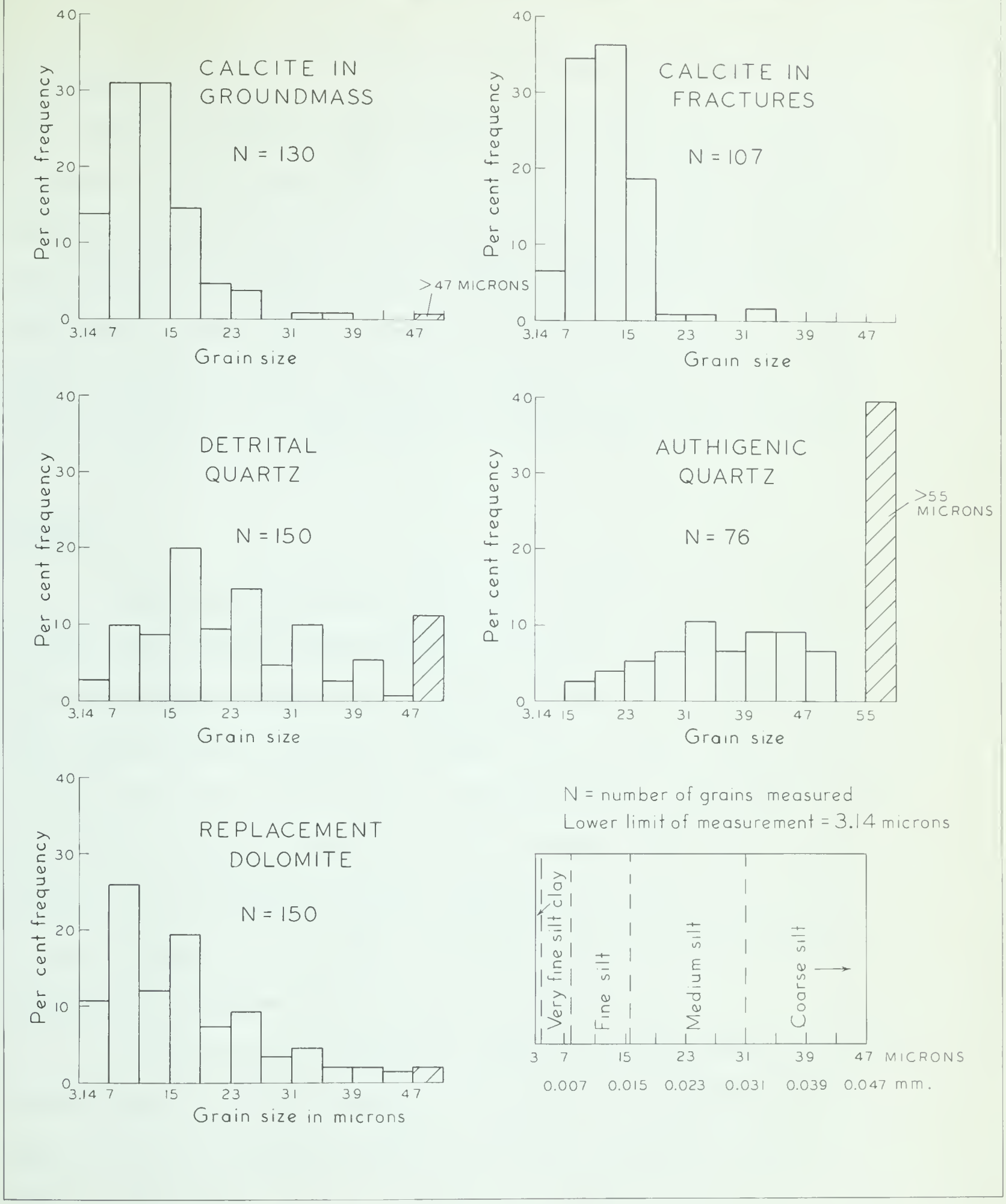

Figure 12. Histograms showing grain size frequency distributions of calcite, quartz, and dolomite in 15 samples of Siyeh mottled (fracture segregations) limestone.

form composite quartz masses of similar size. Grain size measurements on grouped single crystals and composite masses indicate a usual range of from 27 to 51 microns, with some much larger patches (Figure 12). Both individual rhombs and masses contain abundant spherical calcite inclusions smaller than the polygonal grains of calcite surrounding the authigenic quartz. Euhedral crystals and composite masses usually show no signs of growth initiated by detrital quartz grains, but in a few cases an inclusion-free grain is observed surrounded by a mass of inclusion-filled authigenic quartz, having been seeded by the detrital grain (Plate 8, Figure 5).

Feldspar

The mottled limestones generally contain less than 1 per cent feldspar as grains with a maximum diameter greater than 10 microns (Table 15). Microcline and twinned sodic plagioclase ($An_{10}Ab_{90}$) predominate; untwinned feldspar, some of which is orthoclase, is present in trace amounts. Twinned plagioclase is twice as abundant as microcline plus untwinned feldspar. These observations are supported by the results of chemical and X-ray analyses. Orthoclase is rarely detected on X-ray diffraction patterns, whereas distinct albite and less intense microcline reflections are recorded. Chemical analyses show minor amounts of Na_2O, which yields about 2 per cent normative plagioclase.

The grains are well-rounded to rounded and usually subequant to elongate. Twinned plagioclase shows all degrees of alteration to fine-grained muscovite. Microcline grains showing characteristic cross-hatch twinning are noticeably fresh (Plate 8, Figure 7).*

---

* Photograph of microcline grain taken from quartzite sample; similar grains found in mottled limestones.

Rock fragments

Recognizable rock fragments account for about 2 per cent of the composition of the mottled limestones. Several types are present: phyllitic fragments, two schistose varieties, and fragments composed largely of chlorite. All grains are well-rounded and similar to associated detrital quartz in size.

The phyllite fragments contain finely divided quartz and mica, as well as spots of opaque, dark-brown ferruginous material (Plate 9, Figure 1). One type of schist fragment is composed mainly of quartz and feldspar (twinned plagioclase in some instances) in subequant crystals about five microns in size, with scattered muscovite flakes. Quartz-muscovite schistose fragments containing elongate quartz individuals up to 30 microns in length constitute the other variety and have been dealt with in the discussion of quartz. The chloritic fragments may result from the complete alteration in place of ferromagnesian minerals such as biotite, which is usually found highly altered to chlorite, and hornblende (rarely observed).

Disaggregation of rock fragments may account for an additional several per cent of the rock in the form of finely divided quartz and mica (chlorite and muscovite) matrix.

Matrix

Matrix comprises fine-grained siliceous material less than 10 microns in size and constitutes about 20 per cent of the mottled limestones. It is composed of finely divided chlorite, illite, and quartz.

Most of the chlorite in the groundmass is light green and in some instances clearly authigenic, as minute fibers are found oriented perpendicular to the walls

of extremely small cavities. However, some of the light green chlorite may be detrital in origin, transported as grains to the site of deposition. Matrix chlorite may also have been derived from disaggregation of chlorite rock fragments (either detrital or completely altered ferromagnesian minerals). In addition to the light green variety, a minor amount of a later authigenic yellow-green chlorite, which appears almost isotropic under crossed nicols, is observed filling cavities and replacing detritus and carbonates in both the groundmass and calcitic segregations. This chlorite may have formed during a phase of low-grade metamorphism suggested by an illite age of 740 million years (K-Ar), and 780 million years (Rb-Sr), determined by Goldich et al (1959) on a shale sample collected near the top of the Siyeh formation. If the late chlorite is metamorphic its sparse distribution in thin sections indicates that the effects on Siyeh clays were slight. Goldich et al (ibid) reached a similar conclusion with respect to other shale samples analysed from different stratigraphic horizons of the Siyeh formation.

The illite is likely detrital in origin, although some may be derived from the disintegration of schistose rock fragments on compaction or have formed in the sediment during diagenesis.

Fine-grained quartz included with matrix forms about 2 per cent of the rocks. Normative calculations show that as 26 per cent of the rock is quartz, only 12 per cent of which is accounted for by modal analyses, much of the remaining quartz in the matrix must be of clay size and hence not detectable in thin sections.

Authigenic opaque minerals

Crystals of pyrite are rare in the mottled limestones; none were recorded in point-counts. Euhedral hematite crystals, blood-red in colour and displaying sharp rhombic outlines, were observed in trace amounts in all thin sections, and are scattered as stringers and crystal aggregates throughout the groundmass and within calcite-filled fractures. Hematite crystals are usually under 10 microns in size, and when present with pyrite, appear to have formed from the latter, as clusters of small euhedral hematite crystals transgress pyrite margins and are concentrated within and around larger pyrite crystals. Also, hematite is associated with the yellow-green authigenic chlorite cement, both minerals having formed after calcitization of the diagenetic fractures (Plate 9, Figure 6).

Non-opaque heavy minerals

Sphene is the only non-opaque heavy mineral found in appreciable amount in the Siyeh limestones. It is observed in almost all thin sections and is recorded in a few of the point-counts. Grains are well-rounded, amber, and usually range in size from 10 to 20 microns. Other heavy minerals present are zircon, tourmaline, and hornblende, all of which are extremely rare.

Carbonate minerals

Calcite and dolomite are the most abundant minerals in the Siyeh mottled rocks. The results of point-counts indicate the rocks are composed of 39 per cent calcite and 14 to 27 per cent dolomite. The calcite is, on the average, equally distributed among groundmass and fracture segregations (Table 15), whereas dolomite is found only in the groundmass.

(i) Calcite

Calcite is present in the groundmass in several forms: equant single crystals (very common; Plate 8, Figure 1); small, irregular patches--probably cement (rare); irregular replacement patches in host rock adjacent to calcite-cemented fractures (uncommon; Plate 8, Figure 2); and as a late cement filling cavities and post-lithification fractures (rare; Plate 9, Figure 6). Equant crystals are by far the most abundant. They are largely anhedral to subhedral (one or two plane edges) and sometimes are found as sharp euhedral rhombs (Plate 8, Figure 1). Where grains are in contact, boundaries between them are generally curved, although scattered plane intergranular boundaries are present. The size of groundmass grains larger than the lower limit of measurement (3.14 microns) ranges from this limit to 23 microns with most falling within the interval 7 to 15 microns (fine silt size). They are present as isolated individuals or are scattered through the groundmass in stringers composed of irregular clusters of crystals. In many instances stringers approximate the bedding direction but are linked vertically with other stringers, irregular patches of connected grains and individuals.

Microscopic examination of graded bedding contacts shows that the calcite is graded in the same manner as quartz and other detrital constituents. In some cases, the graded calcite is in the form of euhedral rhombs (Plate 9, Figure 4), which gradually decrease in size towards the top of the graded bed.

Authigenic calcite filling fracture segregations is composed of equant polygonal crystals, which form an even-grained, granoblastic mosaic with plane grain-to-grain contacts (Plate 8, Figure 6). Grain size ranges from slightly below the lower limit of 3.14 microns to 19 microns, with scattered larger grains.

Grains less than the lower limit of measurement are rare as this limit corresponds closely with the lower grain size limit of crystals in the fracture segregations. The majority of grains range from 7 to 15 microns, almost identical with the groundmass calcite size-distribution (Figure 12), the major difference being that the groundmass calcite contains a larger number of clay-size grains.

Margins of calcite-filled veinlets are usually sharp (Plate 8, Figure 8), although they may also be gradational over a distance of one-half millimeter. Patchy variation in grain size and irregular intergranular contacts characterize the transition zone calcite, which usually has replaced most of the original groundmass. Large authigenic quartz patches are commonly associated with the replacement calcite. In some instances elongate drusy calcite crystals line the walls of segregations, indicating that cementation began at the original boundaries of the fractures, progressing inwards towards the center of the veinlet.

Detrital quartz grains, relicts of rock fragments, and mica shreds incorporated within the fracture filling are rare, possibly indicating that only minor amoun ts of detrital constituents entered the fractures prior to cementation.

Microscopic examination of shrinkage and slump fracture segregations confirms minor displacement of veinlets. The presence of V-shaped openings in the walls of veinlets, as well as minor displacement along fractures within veinlets, is indicative of movement after the cementation of fractures. The movement appears to have taken place when the surrounding groundmass was still plastic, as micro-fracture traces, along which very minor movement in segregations occurred, disappear into the groundmass on emergence from the veinlets. If movement had occurred after lithification, the fracture trace would

be expected to carry through into the micaceous groundmass. In addition, euhedral crystals of authigenic quartz are concentrated along fracture zones within veinlets, indicating minor movement in the sediment shortly after cementation of veinlets, and prior to the development of authigenic quartz and dolomitization.

Calcite found in growth segregations has replaced most of the pre-existing fabric. Grains are not uniform in size, and boundaries are irregular. The fabric is similar to that of the transition zones along some calcite fracture segregations. Growths were formed prior to dolomitization as euhedral dolomite rhombs are found replacing calcite cement within segregations (Plate 8, Figure 3).

Calcite also is present in post-lithification veinlets as granular cement or spar calcite. These veins are not irregular in shape as are the diagenetic types; they are usually straight, cutting through the middle of individual quartz grains, across dolomite containing inclusions of slump fracture calcite, and through fracture segregations.

Spar calcite, probably related to the same late phase of mineralization, is observed as a pore cement in small vugs in fracture segregations and groundmass. In one instance, a pore in the granular calcite mosaic of a fracture segregation (Plate 9, Figure 6) is lined with nearly isotropic light yellow-green chlorite with associated stringers of hematite crystals; the core is filled with spar calcite extending in an elongate arm out through the segregation into the surrounding groundmass.

(ii) Dolomite

Dolomite is present mainly as discrete secondary euhedral to subhedral rhombs, diffused evenly throughout the groundmass, replacing pre-existing fabric,

including authigenic quartz crystals and composite masses, and calcite in both the groundmass and in fracture segregations. In many instances, dolomitization appears to have affected individual calcite grains, as numerous dolomite rhombs with sharp euhedral crystal outlines, but containing cores of calcite were observed. Almost all of the dolomite greater than 10 microns in size shows rhombic habit, whereas material less than 10 microns is equally divided between anhedral and euhedral crystals. Where dolomitization was intense crystal boundaries are distorted with the resulting development of anhedral forms.

Measurements of grain size were made on euhedral and subhedral dolomite crystals (lower size limit of slightly over 3 microns). Most crystals range from this limit to 19 microns (Figure 12). Anhedral crystals, constituting one-half of the dolomite under 10 microns in size, were not measured due to the difficulty in distinguishing many of the clay to fine silt-sized dolomite crystals from finely divided groundmass illite. Thus, the grain size distribution is unduly weighted to the coarser grain sizes (greater than 10 microns), although dolomite, in contrast to the groundmass calcite, shows a much greater range of sizes, some crystals far exceeding 47 microns.

Direct evidence of dolomite rhombs replacing slump and shrinkage fracture material is found in only a few of the thin sections as dolomite is present rarely within calcite fracture segregations, being largely confined to the groundmass. However, some examples of dolomite replacement were found, one of which is shown in Plate 9, Figure 3. Other textural features suggest that dolomite was emplaced after the development of authigenic quartz, which in turn contains numerous inclusions of veinlet calcite, so that dolomite is the last-formed major constituent of the rock; forming after the cementation of calcite-filled slump and shrinkage fractures.

Grain size measurement

Five traverses were made across each of the 15 slides, and two "grains" of detrital quartz, authigenic quartz, dolomite (rhombs), groundmass calcite, and calcite in segregations, were measured for each traverse. Results are shown in Figure 12.

CALCAREOUS SHALE

Calcareous shales are composed essentially of carbonates (about 55 per cent) and micaceous matrix (about 35 per cent), with scattered detrital material greater than 10 microns (Table 16).

Calcite is in excess of dolomite and is uniformly distributed through the fabric. Calcite grains range from 1.5 to 15 microns, most being from 3 to 6 microns in size. Grain boundaries are irregular, and shape is usually equant to subequant. Secondary dolomite rhombs are uniformly distributed and range in size from 3 to 15 microns although most are less than 4 microns.

The matrix is composed of fine-grained micas (illite and chlorite) oriented parallel to the bedding and contains scattered angular quartz grains up to 30 microns in size.

Straingers of authigenic hematite crystals, 3 to 4 microns in size, are common and are found forming from pyrite.

INTRAFORMATIONAL MOTTLE CONGLOMERATE

Mottle conglomerates are composed about equally of phenoclasts and groundmass (Table 17). Phenoclasts are generally well rounded, but may also be angular, and range from 2 to 5 millimeters in length. They are of two types:

Table 16. Percentages of mineral constituents in calcareous shale samples*

SAMPLE NUMBER (in stratigraphic order)	MINERAL CONSTITUENTS															
	SILICATES					CARBONATES									SILICATES	OTHERS
	QUARTZ	>10μ FELDSPAR	>10μ ROCK FRAGMENTS	>10μ MICA		CALCITE >10μ	CALCITE <10μ	TOTAL CALCITE	DOLOMITE >10μ E-S	DOLOMITE >10μ A	DOLOMITE <10μ E-S	DOLOMITE <10μ A	TOTAL DOLOMITE		(<10 microns) = MATRIX	(pyrite and authigenic quartz)
180 - 248	4			4		8	11	19	4		6	4	14		59	
28 - 18	7			2		4	30	34		2	12	12	26		31	
31 - 30 (Silt lens)	28	8	12			9		9	2	6	2	2	12		29	2
64 - 74	6					25	22	47	8	2	2	14	26		19	2
AVERAGE (excluding silt lens 31-30)	6			2		12	21	33	4	1	7	10	22		36	1

* 50 points per thin section

E - S = Euhedral-subhedral A = Anhedral

Table 17. Percentages of mineral constituents in intraformational mottle conglomerate samples*

SAMPLE NUMBER	MINERAL CONSTITUENTS																			
	PHENOCLASTS						GROUNDMASS													
	COMPOSED OF SEGREGATION MATERIAL			COMPOSED OF HOST ROCK MATERIAL			SILICATES (<10 microns)				CARBONATE						SILICATES	OTHERS
	CALCITE >10μ <10μ		SILICATES >10μ (Quartz)	CALCITE >10μ <10μ		SILICATES <10μ	QUARTZ	FELDSPAR	ROCK FRAG-MENTS	MICA	CALCITE >10μ	CALCITE <10μ	DOLOMITE >10μ E-S	DOLOMITE >10μ A	DOLOMITE <10μ E-S	DOLOMITE <10μ A	<10μ (MATRIX)	(pyrite)
46 - 42	26	8	2	2	6		4		4		10	8	4	6	2	12	6	
16 - 90	47	16									6	6	4		2	4	14	1
AVERAGE	37	12	1	1	3		2		2		8	7	4	3	2	8	10	1

SAMPLE NUMBER	COMPONENTS				MINERALS		
	SEGREGATION PHENOCLASTS	HOST ROCK PHENOCLASTS	TOTAL PHENOCLASTS	TOTAL GROUNDMASS	TOTAL QUARTZ	TOTAL CALCITE	TOTAL DOLOMITE
46 - 42	36	8	44	56	6	60	24
16 - 90	63		63	37		75	10
AVERAGE	50	4	54	46	3	68	17

E - S = Euhedral--subhedral A = Anhedral * 50 points per thin section

those consisting of almost pure granular calcite (about 50 per cent of the rock), and those composed mainly of grains of calcite plus detrital silicates and secondary dolomite (about 4 per cent of the rock). The first type is derived from pre-existing calcite veinlets, whereas the other represent fragments of the host rock containing veinlets (mottled limestones).

Authigenic quartz, commonly found replacing granular calcite in the fracture fillings of the mottled limestones, is present also in phenoclasts of the derived mottle conglomerate. Striking evidence of the early genesis of the authigenic quartz may be found in some phenoclasts where the quartz is present as a rim, for example, along one side of a granular calcite phenoclast. Euhedral quartz crystals penetrate and form a saw-tooth contact with the granular calcite within the pebble, but the surface between the quartz and the surrounding groundmass at the margins of phenoclasts is smooth and curved, conforming to the rounded shape of the pebble. It thus appears that the authigenic quartz replaced veinlet calcite prior to fragmentation and that fragments of veinlets bearing authigenic quartz were subsequently rounded by current action and redeposited.

Groundmass quartz is generally more coarse-grained than in the mottled limestones, ranging in size from 15 to 90 microns. Other detrital constituents, although larger in size, are identical with those in the mottled limestones.

Calcite grains range mainly from 6 to 15 microns, slightly more coarse than the mottled limestone calcite. Dolomite rhombs ranging from 10 to 45 microns are spread evenly through the groundmass but rarely indent the margins of granular calcite phenoclasts.

Table 18. Percentages of mineral constituents in algal limestone and dolomite samples*

SAMPLE NUMBER (in stratigraphic order)	MINERAL CONSTITUENTS														
	CEMENT (GRANULAR TO SPAR CALCITE)		ALGAL SEDIMENT									REPLACEMENT DOLOMITE			
			DETRITAL >10 microns				CALCITE (Includes original fine-grained calcilutite in addition to coarse recrystallized patches)								
	>10μ	<10μ	QUARTZ	FELDSPAR	ROCK FRAGMENTS	MICA	>10μ	<10μ	Total	SILICATES <10μ (MATRIX)	OTHERS	>10μ	<10μ	TOTAL DOLOMITE	TOTAL CALCITE
172 - 236 (ls.)	4	12	2	1	2		10	17	27	25		16	11	27	43
189 - 260 (ls.)	2		2				46	44	90	2	4				92
190 - 264 (ls.)	16		2				54	28	82						
191 - 268 (dol.)			12		2							63	23	86	
AVERAGE COMPOSITION OF ALGAL LIMESTONE (sample 191-268 excluded)	7	7	2	1	1		37	30	67	9	4	5	4	9	78

* 50 points per thin section

ALGAL LIMESTONE AND DOLOMITE

Algal limestones are composed of 85 to 90 per cent calcitic algal sediment and 5 to 15 per cent granular calcite cement which filled voids between successive algal layers probably soon after deposition of the sediment. The bulk of the algal sediment is in layers less than 1 millimeter thick composed of very fine-grained calcite (2 to 6 microns) which has undergone varying degrees of recrystallization, giving rise to patchy crystal mosaics containing individual crystals up to 65 microns in size (Plate 8, Figure 4). The relict sediment (most grains less than 5 microns) is considerably finer-grained than the calcite of other rock types and probably was formed by the algae. Detrital quartz is found associated with the algal calcite, but authigenic quartz is confined to the granular calcite cement.

Dolomite is distributed uniformly through the algal sediment in small secondary rhombs ranging from 3 to 15 microns in size. It is present also as a cement, filling vugs and fractures which opened after the initial calcite cementation. Dolomite cement and the replacement rhombs in the groundmass may represent the same phase of dolomitization.

DOLOMITE

Siyeh dolomites are composed predominantly of replacement dolomite with fine-grained siliceous matrix material constituting about one-quarter of the composition of the rocks. The majority of the fine-grained crystals (less than 10 microns) are anhedral, whereas the larger crystals are usually euhedral or subhedral. Dolomite crystals are evenly distributed throughout the rock. Most crystals are less than 6 microns in size but range up to 40 microns.

Table 19. Percentages of mineral constituents in dolomite, dolomitic shale, and dolomitic shale pebble conglomerate*

SAMPLE NUMBER (in stratigraphic order)	MINERAL CONSTITUENTS												
	SILICATES					CARBONATE						SILICATES	OTHERS
		>10μ					DOLOMITE						
	QUARTZ	FELDSPAR	ROCK FRAGMENTS	MICA		CALCITE	>10μ E-S	>10μ A	<10μ E-S	<10μ A		(<10μ) = MATRIX	(mainly authigenic quartz and hematite)
169 - 232 (dol.)	20	6	10				18	2	5	8	33	31	
52 - 54 (dol.)						2	24	6	35	30	95	3	
54 - 58 (dol.)							14		20	49	83	17	
65 - 75 (dol.)	2		4				18	4	20	27	69	25	
67 - 78 (dol.)	2					2	23	8	13	26	70	23	3
72 - 94 (dol.)							33	4	15	27	79	21	
75 - 98 (dol.)	2						28	4	26	19	77	21	
78 - 102 (dol.)				1				2	22	47	31	28	
81 - 106 (dol.)	4		2				28	2	14	40	84	8	2
87 - 114 (dol.)	24						11	2	6	26	45	29	2
97 - 126 (dol.)							10		38	19	67	31	2
AVERAGE DOLOMITE	5	1	1	1		1	19	3	19	29	67	22	1
84 - 110 (dol.sh.)	2		5				44	4	21	15	84	9	
93 - 122 (dol.sh. pebble conglomerate)							8 4(P)	4	6	57 10(P)	89	3	8 (largely pyrite)

P = constituents in pebbles (percentage of pebbles)
E - S = Euhedral-subhedral A = Anhedral
* 50 points per thin section

Dolomitization was selective, as in parts of unit 4, beds of dolomite in the order of one foot thick alternate with beds of mottled (fracture) limestone of similar thickness. Transition zones, less than several inches thick, separate the beds. Dolomite beds invariably show neither slump nor shrinkage fractures, and the groundmass of beds with fracture segregations is usually only partially dolomitized.

Dolomitic shale varies little from the dolomites except that crystals have a maximum size of about 20 microns. Dolomitic shale pebble conglomerate is similar in texture and composition to the dolomites.

QUARTZITE

Detrital constituents greater than 10 microns constitute about 65 per cent of the quartzites. Most of the grains are quartz, which accounts for 50 per cent of the composition of the rock (Table 20). The grains are subrounded to subangular and range from 70 to 280 microns, most being from 140 to 210 microns (fine sand size).

Feldspar grains consist of microcline (fresh) and plagioclase altered to varying degrees. They are similar in size to quartz.

Rock fragments are composed largely of fine-grained quartz-mica schist (Plate 9, Figure 7). Some chert and metaquartzite fragments are also present.

Cement constitutes about 30 per cent of the rocks. Spar dolomite accounts for two-thirds of the cement and occurs as single spar crystals filling pore spaces. Authigenic quartz is also present, cementing pore spaces and occurring as overgrowths on most grains.

CALCAREOUS OOLITE

Oolitic rocks are composed of accretionary, concentrically laminated forms (oolites), rock fragments (pseudoolites), and quartz. Pseudoolites predominate. All

Table 20. Percentages of mineral constituents of quartzite samples*

SAMPLE NUMBER	MINERAL CONSTITUENTS														
	SILICATES >10 microns									CEMENT				SILICATES	
	QUARTZ	QUARTZITE	CHERT	FELDSPAR: PLAGIOCLASE	FELDSPAR: MICROCLINE	FELDSPAR: UNTWINNED	ROCK FRAGMENTS	MICA	OTHERS (sphene)	CALCITE	DOLOMITE	MICROCRYSTALLINE QUARTZ (chert)	QUARTZ	(<10μ) MATRIX	
101 - 130	55	5	1	5	2	4	3					5	17	3	
104 - 134	41.5			1	2	2	4	1	1		39		0.5	8	
AVERAGE	48	2.5	0.5	3	2	3	3.5	0.5	0.5		19.5	2.5	9	5.5	

SAMPLE NUMBER	GRAINS	CEMENT	MATRIX
101 - 130	75	22	3
104 - 134	52.5	39.5	8
AVERAGE	64	30.5	5.5

* 100 points per thin section

Table 21. Percentages of mineral constituents in calcareous oolite*

SAMPLE NUMBER	MINERAL CONSTITUENTS																	
	GRAINS												CEMENT			QUARTZ REPLACING		
	PSEUDOOLITES									OOLITES (CALCITE)						PSEUDOOLITES		
	GRANULAR CALCITE >10μ <10μ	DOLOMITE >10μ E-S	DOLOMITE >10μ A	DOLOMITE <10μ E-S	DOLOMITE <10μ A	FINE-GRAINED SILTY LIMESTONE QUARTZ	FELDSPAR	CALCITE >10μ	CALCITE <10μ	SILICATES <10μ (MATRIX)	>10μ <10μ	COMPOSITE FRAGMENTS + QUARTZ	CALCITE	DOLOMITE	QUARTZ	GRANULAR CALCITE	DOLOMITE	FINE-GRAINED SILTY LS.	OOLITES
49 - 47	6	6	2			2		39			12	2	20	2	2			3	4

* 50 points per thin section

E - S = Euhedral-subhedral A = Anhedral

MINERAL CONSTITUENTS			ROCK COMPONENTS			
CALCITE	DOLOMITE	QUARTZ	PSEUDOOLITE	OOLITE	COMPOSITE GRAINS	CEMENT
87	4	9	58	16	2	24

grains are well-rounded, ovoid to spherical in shape, and range in size from 0.25 to 0.80 millimeters, most being about 0.50 millimeters (medium to coarse sand size).

Three types of pseudoolites were identified: fine-grained silty limestone, granular calcite, and dolomitic grains. The fine-grained limestones, similar in fabric to the groundmass of mottled limestones, constitutes most of the pseudoolites. Pseudoolites composed of pure granular calcite which is identical with cement in fracture segregations and calcite-cemented void-spaces in algae are less abundant. Dolomitic types are rare.

True oolites show characteristic concentric structure as well as radial recrystallized fabric. However, the radial pattern is in many instances interrupted by small patches or inclusions of very fine-grained (less than 4 microns) calcite. Rounded fragments of original oolites are more abundant than whole grains. Where present, oolite cores consist of both fine-grained silty limestone and granular calcite.

Some oolitic grains may be algal in origin. In the Siyeh, oolite beds are usually closely associated with algal beds, and one sample of brecciated algae from a pebble-filled depression between algal "heads" at the top of an algal bed, showed an abundance of ovoid accretionary forms. Similar features have been described by Carozzi (1960) as algal pellets.

Calcite cement is common, and quartz is found replacing detrital grains.

SHALE

Examination of thin sections of light green shales shows that they are composed predominantly of siliceous detritus consisting of muscovite shreds and angular to subangular quartz grains set in a fine-grained siliceous matrix. Feldspar is extremely rare and only plagioclase was detected. Rock fragments, if present, could

not be distinguished from matrix. Only traces of calcite are observed, although dolomite is common, often showing irregular boundaries, possibly due to penetration by late diagenetic fibrous chlorite.

Table 22. Showing the sequence of diagenetic events in rocks of the Siyeh formation

MECHANICAL ACTIVITY	CHEMICAL ACTIVITY			
	Chlorite replacing pre-existing fabric and filling pore spaces, associated with authigenic hematite			
	Dolomitization			LATE
Veinlets (slump and shrinkage) broken, and primary laminae deformed(?), due to minor movement in sediment (intrastratal)	Development of authigenic quartz along minor fractures in slump and shrinkage veinlets, and along the margins and within the veinlets; authigenic quartz rarely found in the groundmass surrounding the slump and shrinkage veinlets. Some authigenic quartz along the margins of calcite shrinkage fracture veinlets appears to have formed at an earlier stage (p. 78).			
Formation of slump fractures and deformation of primary laminae (intrastratal)				
	Cementation of slump fractures			
Intrastratal soft-sediment deformation (roiling)				
Deformation of primary laminae around growths (near sediment surface)	Formation of shrinkage fractures and deformation of primary laminae (at sediment surface	Calcite cementation in groundmass ? = ?	Development of growth ? = ? segregations	Cementation of shrinkage fractures EARLY

GENESIS OF THE CARBONATE ROCKS

SOURCE OF SEDIMENTS

The composition and relative amounts of the Siyeh mechanically deposited detrital constituents provide an idea of the composition of the source rocks.

Feldspar content is low in comparison with quartz and fine-grained clastics, indicating a metamorphic source. This is substantiated by the rock fragment assemblage of quartz-mica schists, quartz-feldspar schist, phyllite fragments, and rare metaquartzite and chert. The generally fine-grained nature of the detrital constituents probably reflects fine-grained source rocks (low-grade metamorphic types) and a low-lying rather than a distant source area, as shoreline red beds are in gradational contact with the base and top of the carbonate sequence.

Crossbed data indicate a source area to the southeast of the site of Siyeh deposition. (Reesor (1957) concluded an eastern source for Purcell sediments best fitted the available evidence.

ORIGIN OF THE SIYEH CARBONATES

Calcite

The granular calcite in calcareous shales and the groundmass of the mottled limestone may owe its origin to mechanical deposition as discrete grains, or, it may represent a cement, precipitated within the detrital framework of the Siyeh sediment shortly after deposition.

Mechanical deposition is favored by (i) the common presence of calcite as discrete grains, surrounded in two and probably three dimensions by detrital quartz;

(ii) the slight variation in grain size; and (iii) the grading of calcite grain size with quartz and other detrital constituents in small-scale graded beds.

Mechanically deposited calcite may be derived from the erosion of pre-existing carbonate rock, or through inorganic or biochemical precipitation. Derivation from carbonate rocks is unlikely; algal rock has provided some thin breccia layers, but it is improbable that the large amounts of uniformly fine calcite silt observed in the mottled limestones could have been supplied by this source.

If it is assumed that the grain size of the Siyeh calcite (7 to 15 microns) is essentially the same today as during deposition, which Bathurst (1961) has indicated is the case for mechanically deposited Mississippian calcilutites and calcite siltstones,* an inorganic, mechanically deposited origin is doubtful, as recent deposits forming in this manner show a grain size range of 0.5 to 4 microns.

Similarly, an algal source is doubtful. Bathurst (1961), in discussing the origin of grains in the calcite siltstones, stated: "Algal origin is less likely, because algal deposits have the grain size range of calcite mudstone 0.5 to 4 microns". In thin sections of algal sediment from the Siyeh, relict patches of preserved initial fabric consist of even-textured calcilutite (most grains less than 4 microns). Thus there appears to be no readily available source of mechanically deposited carbonate grains of silt size in the Siyeh limestones.

A cementation origin is supported by the following petrographic data: (i) the distinctive rhombic shape of many calcite crystals, even in cases where the calcite is graded with quartz and other detrital constituents (Plate 9, Figure 4);

---

* Precipitation of calcite rim cement derived from solution of super-soluble clay-sized carbonate particles serves only to sharpen grain margins, not increase detrital grain size.

(ii) the marked similarity in grains size of calcite in the groundmass and granular calcite cement in the fracture segregations; (iii) calcite-cemented shrinkage and slump fractures, as well as growth segregations which grade into the surrounding groundmass; and (iv) the presence of grain-growth (recrystallized) mosaic in thin sections of algal sediment only, not in the mottled limestones or other calcareous rocks. Bathurst (1959) noted that "Pure cement appears to be stable," and observed no evidence for recrystallization of granular cement in Mississippian calcilutites.

It is concluded that most, if not all, of the granular silt-size calcite in the Siyeh rocks is of authigenic rather than clastic origin, having resulted from early cementation of the still-wet detrital framework during diagenesis.

Dolomite

It has been shown that diffuse dolomitization followed all phases of calcite cementation, and probably occurred at some depth (unknown) below the surface of the sediment. The original calcite content of the dolomites (unknown) has been almost completely replaced by dolomite (65 per cent of the rock), whereas the carbonate portion of the groundmass of the mottled limestones is composed of equal amounts of calcite and dolomite. As dolomitization was generally moderate in beds with calcite-cemented fractures, which were themselves rarely dolomitized, and intense in those without fractures (some exceptions), something associated with the calcitic fractures appears to have inhibited dolomitization. Perhaps the presence of calcite-filled veinlets prevented lateral movement of dolomitizing solutions. Present evidence is inadequate to provide an explanation for this phenomenon.

SEDIMENTARY ENVIRONMENT

The depositional environment of the Siyeh formation is thought to be similar to that now observed in the modern Shark Bay marine lagoon (inland sea) of Western Australia (Logan, 1961). The floor of the lagoon has an area of about 5,000 square miles, five times the area underlain by Beltian strata in the Lewis thrust sheet of Canada and the United States. The maximum depth of water in Shark Bay is only 60 feet, so that slight changes in sea level can inundate or drain large areas. Logan (ibid) describes two types of algae, the flat-lying algal mat deposits, and distinctive algal "heads" (stromatolites). Both are found only in the intertidal zone, in which hypersaline conditions exist. The flat-lying algae are found in protected mudflats, whereas the algal "heads" occur along headlands exposed to wave action. Logan concluded that the shape or form of algae is a reflection of the environment in which the algae grow.

Siyeh strata preserve the record of a series of minor transgressive and regressive phases (units 1 to 6) of late Precambrian seas, culminating in a major transgression (unit 7) followed by a final regressive phase (unit 8).

The Grinnell quartzites and shales underlying the Siyeh appear to grade into the lower Siyeh beds. The basal Siyeh is composed of light green shales (unit 1), commonly containing pyrite, with scattered thin quartzite lenses usually under one foot in thickness. These sediments appear to have been deposited in a sheltered environment largely isolated from the rest of the sea and may represent a fairly rapid transgression (probably a large marine lagoon) toward the source area.*

---

* South-southeast of depositional site, according to meagre crossbed data.

Above the basal beds coarse clastics interbedded with carbonates (dolomite and dolomitic shale, unit 2) may be indicative of a near-shore environment, also suggested by the abundance of scour surfaces and channels up to a foot across. Towards the top of unit 2 and through the lower half of unit 3 large bioherms (discrete algal "heads") are found (Plate 1, Figure 3). Such high relief structures, according to Logan (1961), are indicative of intertidal deposition in agitated water. Near the middle of unit 3 graded bedding is first observed, although only in scattered beds.

At the base of unit 4 shrinkage fractures are first observed and are common through to unit 9 (excluding unit 7). Algae are present in unit 4 as thin (usually less than one foot thick) biostromes regularly spaced at stratigraphic intervals of 2 to 20 feet apart throughout the unit. Logan has shown that similar thin biostromes in Shark Bay develop in protected mudflats at the head of embayments in the larger marine lagoon (inland sea). That this mode of occurrence may also have been the environment of the Siyeh algae is indicated by the development of small-scale graded bedding in many of the samples of unit 4. These finely laminated sediments suggest relatively quiet sedimentation, although sediment must be continually introduced and transported by weak bottom currents. Graded bedding of this nature would probably be destroyed periodically by storm waves.

Unit 5 is distinguished by the presence of oolites, particularly in the middle portion. Most of the algae in unit 5 are less than one foot thick and are similar to the biostromes in unit 4. However, a few thick layers composed of discrete biohermal "heads" were also observed; these were found closely associated with oolite beds (commonly 1 foot thick). The oolites and high-relief algae probably formed during periods of agitation, alternating with periods of more sheltered deposition, as shown by the presence of scattered graded beds.

In unit 6, oolites are absent and algae are present only near the top. Scattered graded bedding was noted, indicating a return to sheltered sedimentation.

Rezak (1957) examined in detail the Conophyton zone 1 (unit 7) and concluded that the lower one-third of the algal reef represents an intertidal mudflat environment. The middle part, composed of Conophyton, was thought by Rezak to indicate a depth of water below low tide, as no evidence of an intertidal mode of formation was indicated. Conophyton is not found in Recent environments. The upper part of the reef represents a return to the intertidal mudflat environment (Rezak, ibid). The reef is of considerable lateral extent, being mapped for more than 50 miles south into Montana and present throughout the Clark Range in Canada.

Unit 8 contains numerous algal "heads" in a zone about 75 feet above the reef, as well as more bioherms near the top. The lithology changes from limestones and calcareous shales to dolomites at the top, finally grading into the upper clastic unit of dolomitic-argillaceous rocks and red beds.

REFERENCES

Arkin, H., and Colton, R.R. (1959): Statistical methods, fourth edition, revised; Barnes and Noble, Inc., New York, 226 pages.

Bathurst, R.G.C. (1959): Diagenesis in Mississippian calcilutites and pseudobreccias; J. Sed. Petrology, vol. 29, pp. 365-376.

Bauerman, H. (1885): Report on the geology of the country near the forty-ninth parallel of north latitude west of the Rocky Mountains, from observations made in 1859-61; Geol. Surv., Canada, Rept. Prog. 1882-84, pt. B.

Black, M. (1933): The algal sediments of Andros Island, Bahamas; Trans. Roy. Soc. London Philos., Ser. B, vol. 122, pp. 165-192.

Carozzi, A.V. (1960): Microscopic sedimentary petrography; John Wiley and Sons, Inc., New York, 485 pages.

Clark, L.M. (1954): Cross-section through the Clarke Range of the Rocky Mountains of southern Alberta and southern British Columbia; Guide book, Alta. Soc. Petrol. Geol., Fourth Annual Field Conference, pp. 105-109.

Daly, R.A. (1912): Geology of the North American Cordillera at the forty-ninth parallel; Geol. Surv., Canada, Memoir No. 38.

Fenton, C.L., and Fenton, M.A. (1937): Belt series of the north: stratigraphy sedimentation, paleontology; Bull. Geol. Soc. Amer., vol. 48, pp. 1873-1970.

Folk, R.L. (1959): Petrology of sedimentary rocks; Hemphill's, Austin, Texas, 154 pages.

Friedman, G.M. (1959): Identification of carbonate minerals by staining methods; J. Sed. Petrology, vol. 29, pp. 87-97.

Ginsburg, R.N. (1957): Early diagenesis and lithification of shallow-water carbonate sediments in South Florida, in: Regional aspects of carbonate deposition, S.E.P.M., Special Publ. 5, pp. 80-100.

Goldich, S.S., Baadsgaard, H., Edwards, G., and Weaver, C.E. (1959): Investigations in radioactivity-dating of sediments; Bull. Am. Assoc. Pet. Geol., vol. 43, pp. 654-662.

Hunt, G.H. (1961): The Purcell eruptive rocks; Unpublished Ph.D. thesis, University of Alberta, 139 pages.

Illing, L.V. (1954): Bahaman calcareous sands; Bull. Am. Assoc. Pet. Geol., vol. 38, pp. 1-95.

Kerr, P.F. (1959): Optical mineralogy, third edition; McGraw-Hill Book Company, Inc., New York, 442 pages.

Logan, B.W. (1961): Cryptozoon and associate stromatolites from the Recent, Shark Bay, Western Australia; J. Geol., vol. 69, pp. 517-533.

MacEwen, D.M.C. (1950): Some notes on the recording and interpretation of X-ray diagrams of soil clays; J. Soil Sci., vol. 1.

Mellon, G.B. (1961): Sedimentary magnetite deposits of the Crowsnest Pass Region, southwestern Alberta; Research Council, Alberta, Bulletin 9, 98 pages.

Osmond, J.C. (1956): Mottled carbonate rocks in the Middle Devonian of eastern Nevada; J. Sed. Petrology, vol. 26, pp. 32-41.

Pettijohn, F.J. (1957): Sedimentary rocks, second edition; Harper and Brothers, New York, 718 pages.

Reesor, J.E. (1957): The Proterozoic of the Cordillera in southeastern British Columbia and southwestern Alberta; The Proterozoic in Canada, pp. 150-177; Roy. Soc. Can., Spec. Pub. No. 2, J.E. Gill, ed.; Univ. of Toronto Press, 191 pages.

Rezak, R. (1957): Stromatolites of the Belt Series in Glacier National Park and vicinity, Montana; U.S. Geol. Surv., Prof. Paper 294-D, 154 pages.

Ross, C.P. (1959): Geology of Glacier National Park and the Flathead region, northwestern Montana; U.S. Geol., Surv., Prof. Paper 296, 125 pages.

Shirozu, Haruo (1958): X-ray powder patterns and cell dimensions of some chlorites in Japan, with a note on their interference colors; Mineralogical J., vol. 2, pp. 209-223.

Shrock, R.R. (1948): Sequence in layered rocks; McGraw-Hill Book Company, Inc., New York, 507 pages.

Snedecor, G.W. (1961): Statistical methods, fifth edition; Iowa State University Press, Iowa, 534 pages.

Tanner, W.F. (1959): Permo-Pennsylvanian paleogeography of part of Oklahoma; J. Sed. Petrology, vol. 29, pp. 326-335.

Tennant, G.B., and Berger, R.W. (1957): X-ray determination of dolomite-calcite ratio of a carbonate rock; Am. Mineralogist, vol. 42, pp. 23-29.

Walcott, C.D. (1899): Pre-cambrian fossiliferous formations; Bull. Geol. Soc. Amer., vol. 10, pp. 199-244.

Warshaw, C.M., and Roy, R. (1961): Classification and a scheme for the identification of layer silicates; Bull. Geol. Soc. Amer., vol. 72, pp. 1455-1492.

Willis, B. (1902): Stratigraphy and structure, Lewis and Livingston Ranges, Montana; Bull., Geol. Soc. Amer., vol. 13, pp. 305-352.

APPENDIX A

X-ray diffraction data for percentages of calcite and dolomite in Siyeh formation (units 1 to 8 inclusive).

Stratigraphic unit	Sample number	Slide	Intensity (counts/sec)				Percentages derived from mean intensity values	
			Calcite		Dolomite			
			Corrected value*	Mean	Corrected value*	Mean	Calcite	Dolomite
8	169-232	a	2.72		166.46			
		b	2.47	2.60	215.84	191.15	1.5	17.7
"	172-236	a	462.03		133.23			
		b	441.48	451.76	135.18	134.21	71.6	11.2
"	176-240	a	96.11		140.22			
		b	94.64	95.38	145.32	142.77	16.0	12.1
"	178-244	a	356.03		60.99			
		b	345.36	350.70	61.46	61.23	55.8	5.1
"	180-248	a	138.47		72.52			
		b	134.71	136.59	72.56	72.54	22.4	5.9
"	183-252	a	458.09		18.58			
		b	510.68	484.39	20.46	19.52	76.7	2.7
"	186-256	a	451.28		2.06			
		b	455.60	453.44	2.83	2.45	71.9	2.0
7	189-260	a	515.65		7.51			
		b	537.03	526.34	7.36	7.43	83.2	2.2
"	190-264	a	623.64		-3.49			
		b	572.64	598.14	-2.44	-2.97	94.4	1.8
"	191-268	a	9.37		296.67			
		b	8.06	8.72	253.86	275.27	2.4	30.2
6	28-18	a	193.80		59.48			
		b	192.76	193.28	64.76	62.12	31.2	5.1
"	34-22	a	353.73		16.66			
		b	300.72	327.23	15.54	16.10	52.2	2.6
"	37.26	a	300.14		113.80			
		b	285.95	293.05	111.03	112.42	46.8	9.1
5	39.30	a	144.05		20.19			
		b	137.71	140.88	19.36	19.78	23.1	2.7

* Background intensity for each slide subtracted from recorded calcite and dolomite readings to give corrected values.

Stratigraphic unit	Sample number	Slide	Intensity (counts/sec.)				Percentages derived from mean intensity values	
			Calcite		Dolomite			
			Corrected value*	Mean	Corected value*	Mean	Calcite	Dolomit
5	42-34	a	289.80		133.96			
		b	268.52	279.16	134.17	134.07	44.7	11.2
"	44-38	a	226.95		93.91			
		b	236.30	231.63	199.36	97.14	37.2	7.8
"	46-42	a	477.59		67.74			
		b	486.21	481.90	65.49	66.62	76.3	5.4
"	48-46	a	1.53		204.47			
		b	1.90	1.72	215.34	209.91	1.3	20.2
"	50-50	a	499.83		52.35			
		b	341.53	420.68	56.00	54.18	66.7	4.6
"	52-54	a	4.49		296.55			
		b	5.16	4.83	272.03	284.29	1.8	31.8
"	54-58	a	5.27		320.51			
		b	5.57	5.42	332.30	326.41	1.9	39.4
"	56-62	a	291.74		106.47			
		b	317.01	304.38	109.95	108.21	48.6	8.7
"	59-66	a	127.50		173.71			
		b	129.79	128.65	171.64	172.68	21.2	15.4
4	60-70	a	76.66		212.19			
		b	78.01	77.34	208.15	210.17	13.2	20.3
"	64-74	a	414.19		82.72			
		b	407.50	410.85	71.70	77.21	65.2	6.2
"	67-78	a	18.26		332.74			
		b	22.00	20.13	380.79	356.77	4.2	45.5
"	70-82	a	52.62		-1.35			
		b	52.50	52.56	-1.20	-1.28	9.3	1.8
"	14-86	a	481.40		55.56			
		b	486.48	483.94	56.95	56.26	76.6	4.7
"	16-90	a	541.50		21.81			
		b	552.52	547.01	22.06	21.94	86.5	2.8
"	72-94	a	12.99		440.61			
		b	10.52	11.76	370.96	405.79	2.9	56.2
4	75-98	a	4.83		344.01			
		b	4.53	4.68	356.70	350.36	1.8	44.2

Stratigraphic unit	Sample number	Slide	Intensity (counts/sec.)				Percentages derived from mean intensity values	
			Calcite		Dolomite			
			Corrected value	Mean	Corrected value	Mean	Calcite	Dolomite
4	78-102	a	2.24		361.84			
		b	2.64	2.44	354.36	358.10	1.5	45.8
"	81-106	a	3.43		472.61			
		b	4.74	4.09	496.43	484.52	1.7	69.3
3	84-110	a	2.48		468.72			
		b	2.28	2.38	391.19	429.96	1.5	61.9
"	87-114	a	1.31		560.51			
		b	1.31	1.31	484.98	522.74	1.3	86.4
"	91-118	a	1.03		325.50			
		b	0.04	0.54	346.32	335.91	1.2	41.3
"	93-122	a	-0.82		587.44			
		b	0.00	-0.41	538.22	562.83	1.0	98.3
"	97-126	a	0.43		439.28			
		b	0.72	0.58	421.38	430.33	1.2	62.0
2	101-130	a	3.50		10.69			
		b	3.27	3.39	10.82	10.76	1.6	2.3
"	104-134	a	6.85		310.45			
		b	4.66	5.76	241.97	276.21	2.0	30.4
"	107-138	a	0.79		165.60			
		b	2.22	1.51	136.67	151.14	1.3	13.0
"	110-142	a	0.89		296.55			
		b	2.18	1.54	330.31	313.43	1.3	37.0
"	114-146	a	0.56		171.04			
		b	3.29	1.93	177.66	174.35	1.4	15.6
"	118-150	a	0.77		342.36			
		b	-0.23	0.27	443.77	393.07	1.1	53.3
"	120-154	a	1.73		402.92			
		b	1.18	1.46	403.70	403.31	1.3	55.7
1	124-158	a	1.14		68.50			
		b	1.93	1.54	58.96	63.73	1.3	5.2
"	126-162	a	4.47		92.50			
		b	0.94	2.71	80.89	86.70	1.5	6.9
"	129-166	a	1.08		3.40			
		b	2.42	1.75	5.00	4.20	1.4	2.0

PLATE 1

FIELD PHOTOGRAPHS

1. Drywood Mountain, southwestern Alberta, showing Purcell lava at upper left underlain by Siyeh formation with the upper quartzites of the underlying Grinnell formation in the lower right. View to the north from Loaf Mountain ridge.

2. Intraformational conglomerate (at level of hammer) underlain by silty mottled limestone grading to calcareous shale at base.

3. Algal dolomite, unit 3.

PLATE I

1

2

3

PLATE 2

FIELD PHOTOGRAPHS

1. Growth segregations, unit 6, height of exposure 2 feet.

2. Shrinkage fractures.

3. Slump fractures = "molar-tooth structure".

PLATE 2

1

2

3

PLATE 3

PHOTOGRAPHS OF ROCK SLABS ETCHED WITH DILUTE HCL

Note: scale in inches

1. Roiled segregations; intrastratal soft-sediment slumping confined to layers 3 inches thick. Dark grey areas are silty and noncalcareous, light grey rock is more argillaceous. Note angular fragment incorporated in silty "roil".

2. Roiled segregations; lumps of sand, noncalcareous, surrounded by fine-grained argillaceous material. Sand knots are cut by calcite-filled slump fractures.

PLATE 3

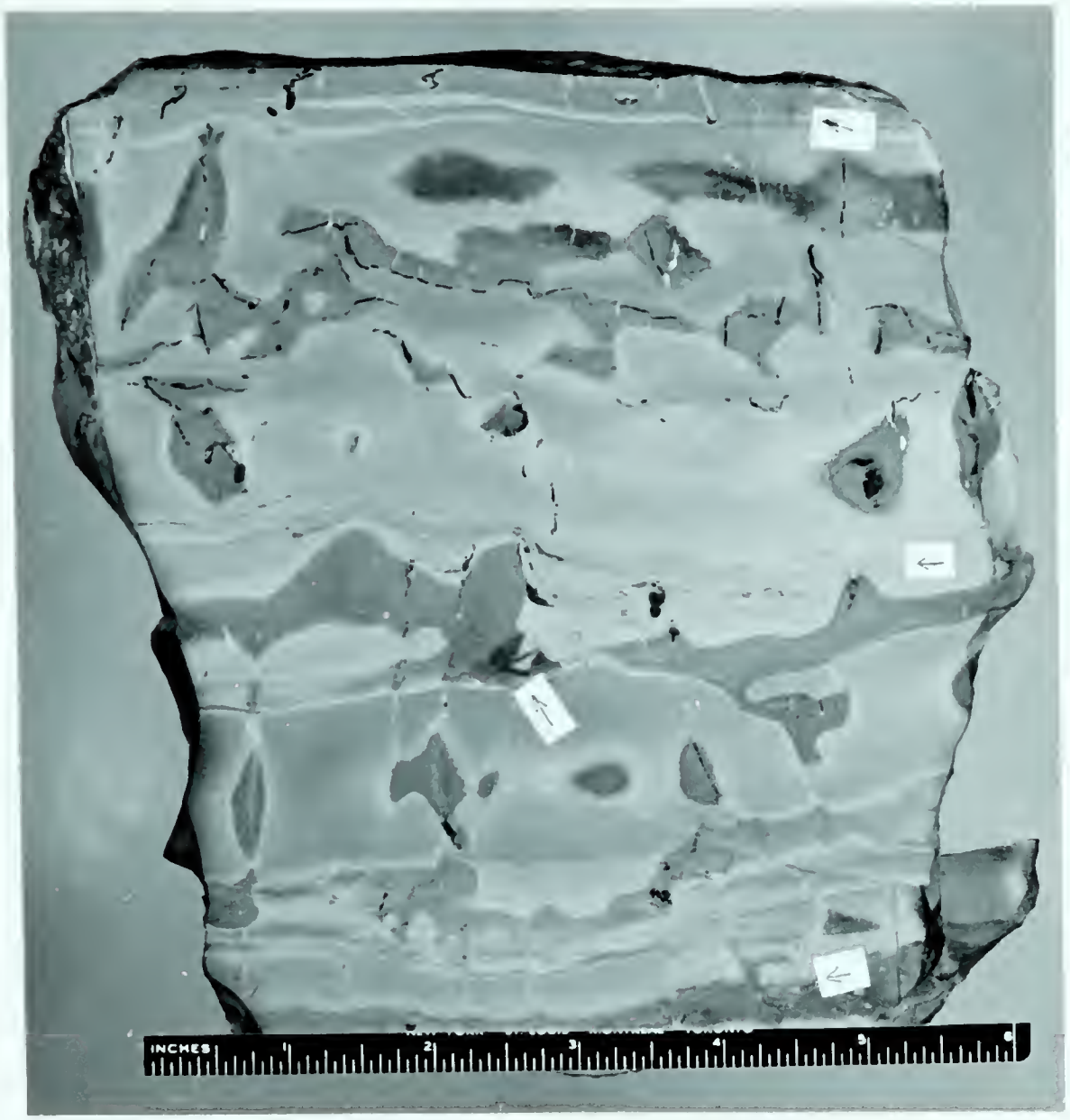

1

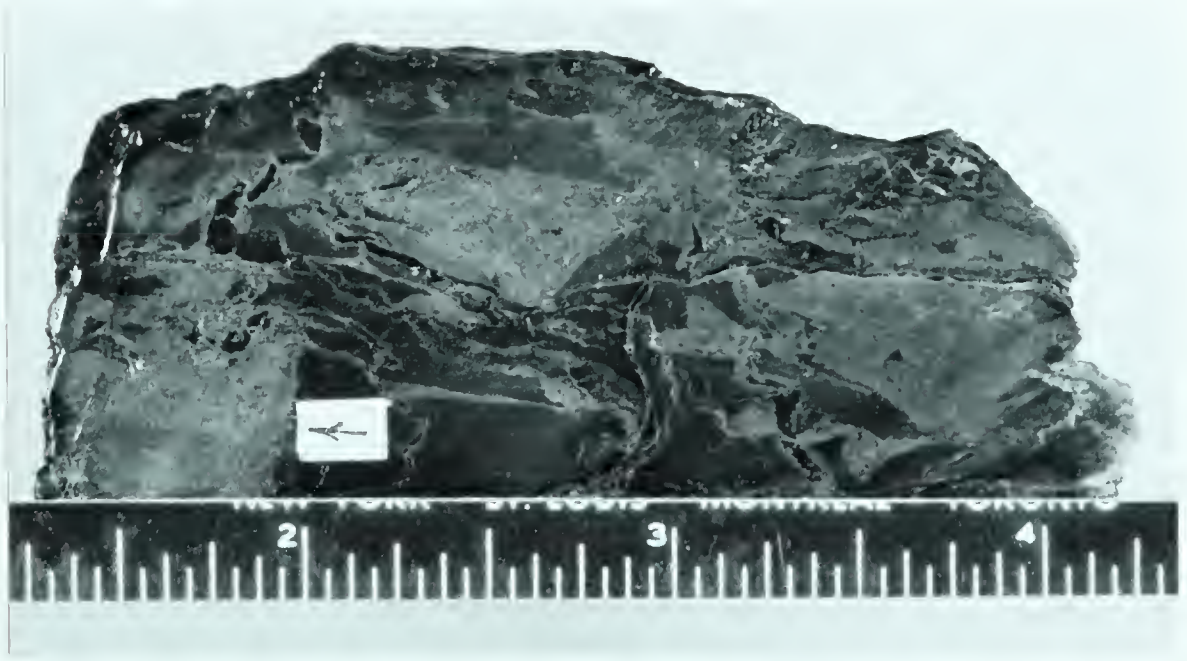

2

PLATE 4

PHOTOGRAPHS OF ROCK SLABS ETCHED WITH DILUTE HCL

Note: scale in inches

1. Growth segregations; areas of authigenic calcitization, showing relict primary laminae passing through segregations.

2. Growth segregations cut by slump fractures. Arrow on right indicates primary laminae passing through growth. Arrow on left indicates a slump fracture on either side of which there has been displacement in the overlying growth, but when traced down into the containing rock a coarse silt layer is encountered from which material has flowed down several millimeters along the fracture trace.

PLATE 4

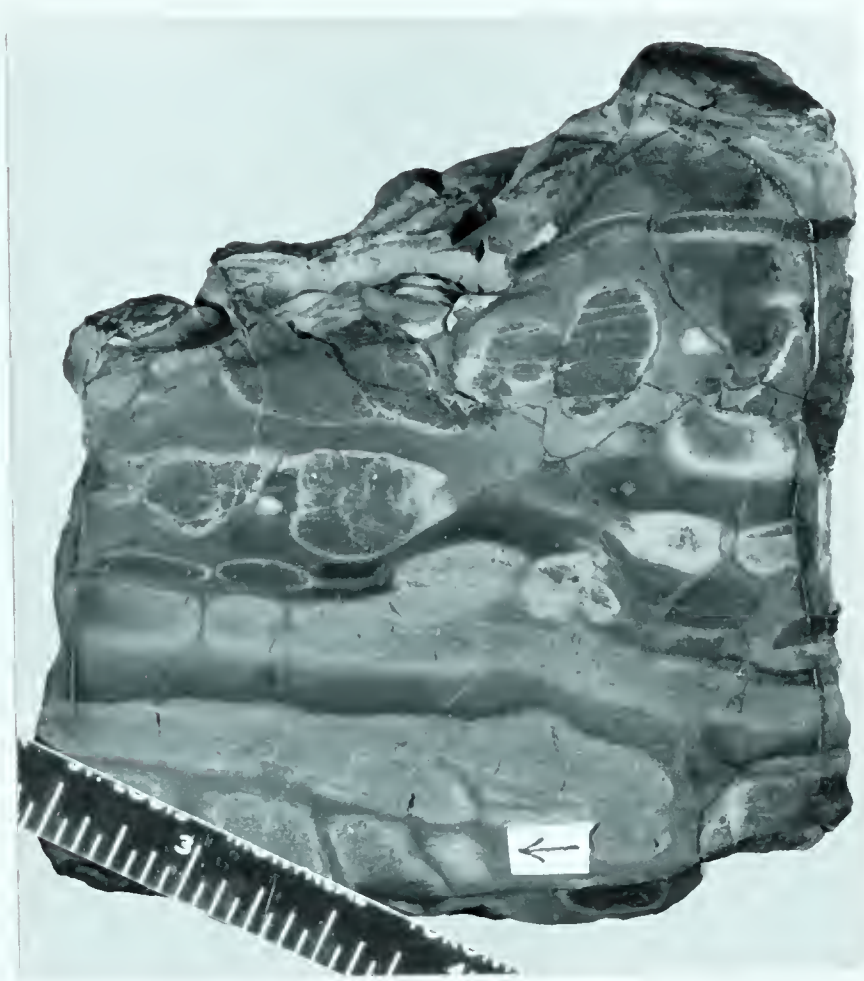

1

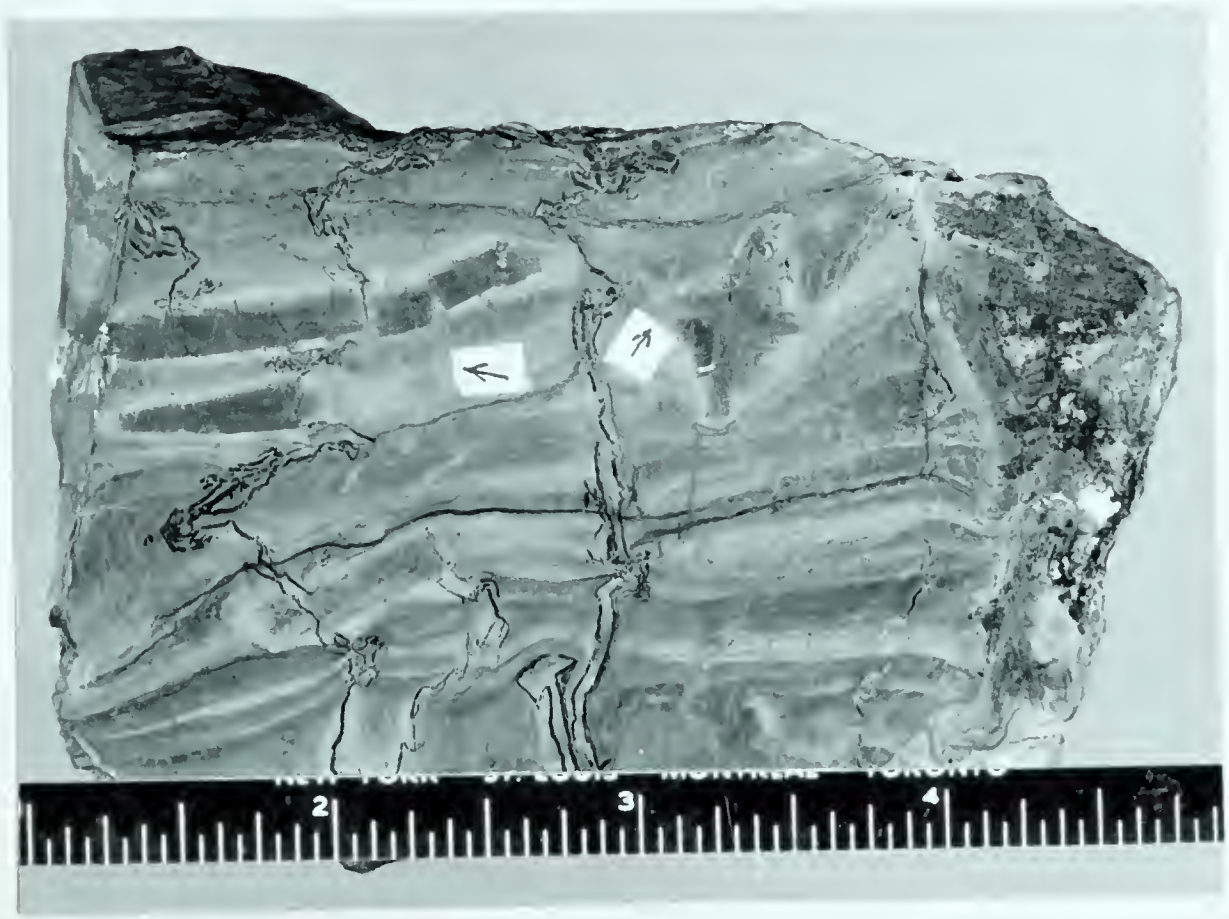

2

PLATE 5

PHOTOGRAPHS OF ROCK SAMPLES

Note: scale in inches

1. Shrinkage fractures in plan view on a weathered bedding surface. Black is pure calcite, light grey is dolomitic silty host rock.

2. Graded bedding; the thick lower couplet represents a continuous graded bed, most of the other thin couplets are discontinuous graded beds.

3. Etched surface of rock slice of a shrinkage fracture layer (lower half) overlain with erosion by a mottle conglomerate in which phenoclasts are composed of pure calcite (black) derived from underlying fracture layer which was cemented prior to deposition of overlying conglomerate. Upper arrow indicates fragment of a calcite veinlet (cemented shrinkage fracture) with adhering groundmass. Middle arrow shows a phenoclast of silty groundmass (similar to that of underlying shrinkage fracture layer) containing calcite cemented veinlet wholly within the pebble. Also note on the margin of the same pebble small calcite veinlet fragments penetrating the "less rigid" groundmass material. Lower arrow indicates deformation of primary laminae near shrinkage fracture veinlet.

PLATE 5

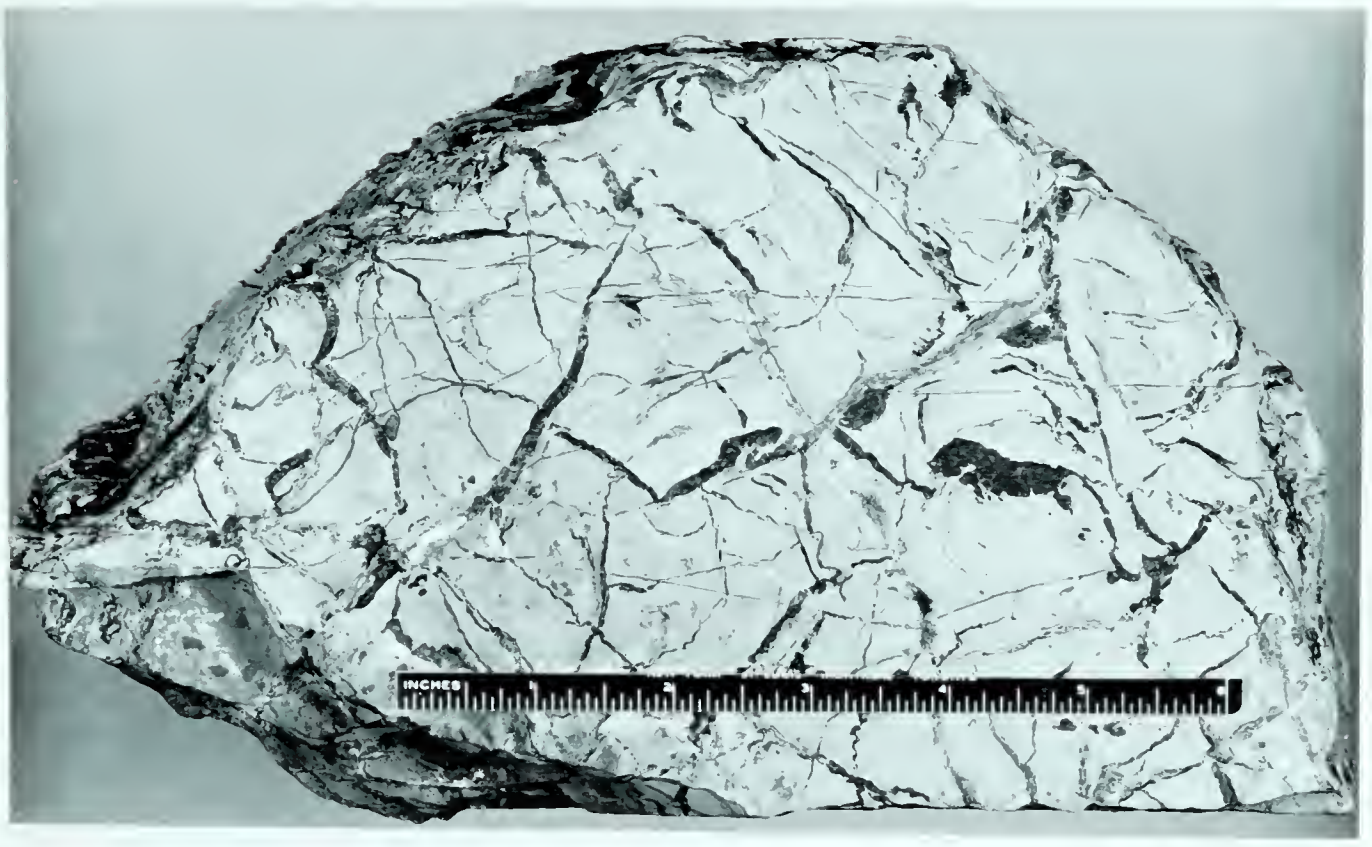

1

2

3

PLATE 6

PHOTOGRAPHS OF ROCK SAMPLES

Note: scale in inches

1. Slump fractures, filled with calcite (black on etched surfaces); sample cut perpendicular to bedding and trend of veinlets, shows plastic deformation of primary laminae near fractures. Also note evidence of movement in the sediment after cementation of slump fractures as shown by broken and segmented veinlets.

2. Slump fractures, as observed in plan view on weathered bedding surface. Note subparallel trend.

PLATE 6

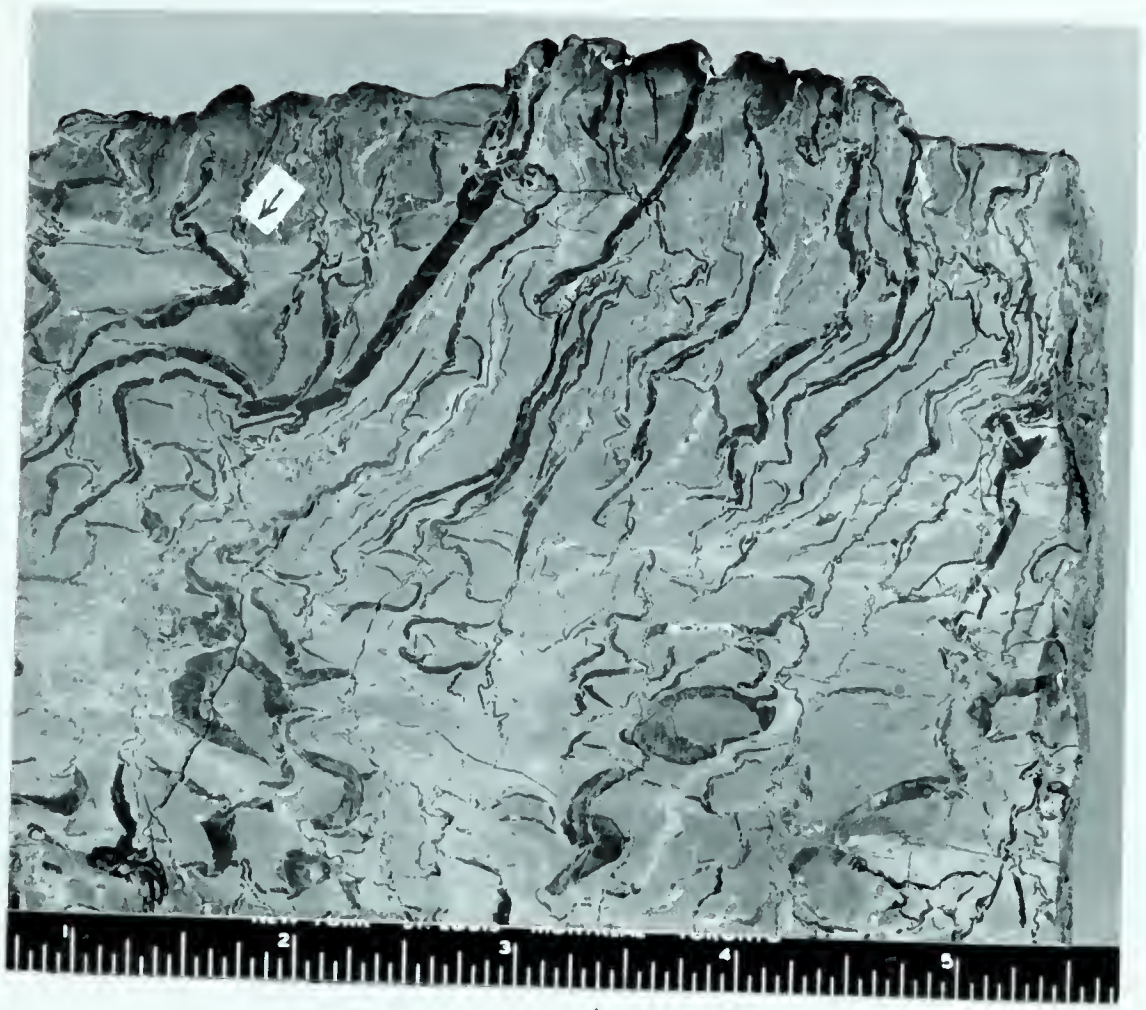

1

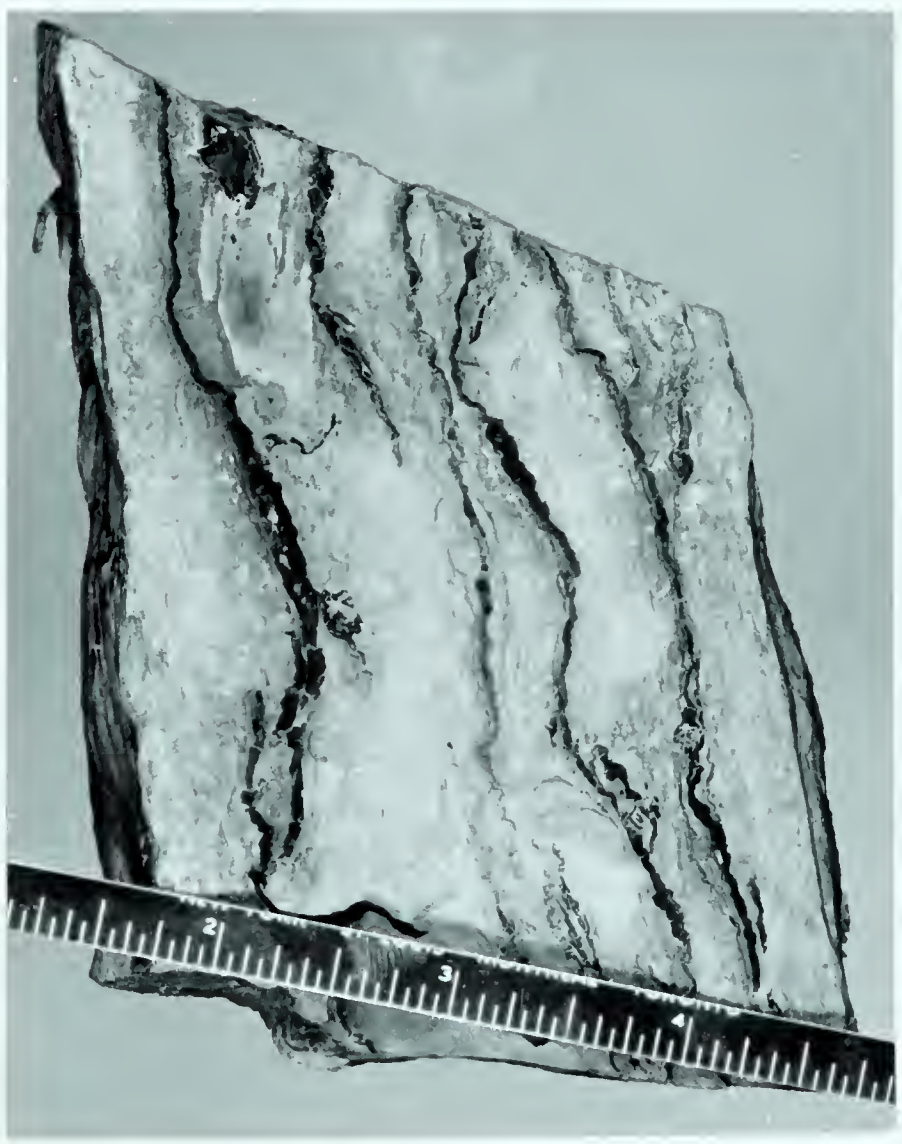

2

PLATE 7

PHOTOGRAPHS OF ROCK SLICES

Note: scale in inches

1. Light green-white marble, formed by the intrusion of a Precambrian sill into mottled limestone sediment, shows well-preserved slump fractures as well as white calcite lumps which may have been growth segregations.

2. Slump breccia band, found occurring between layers of slump fractures (2 inches to 1 foot thick); c.f. Plate 2, Figure 5.

PLATE 7

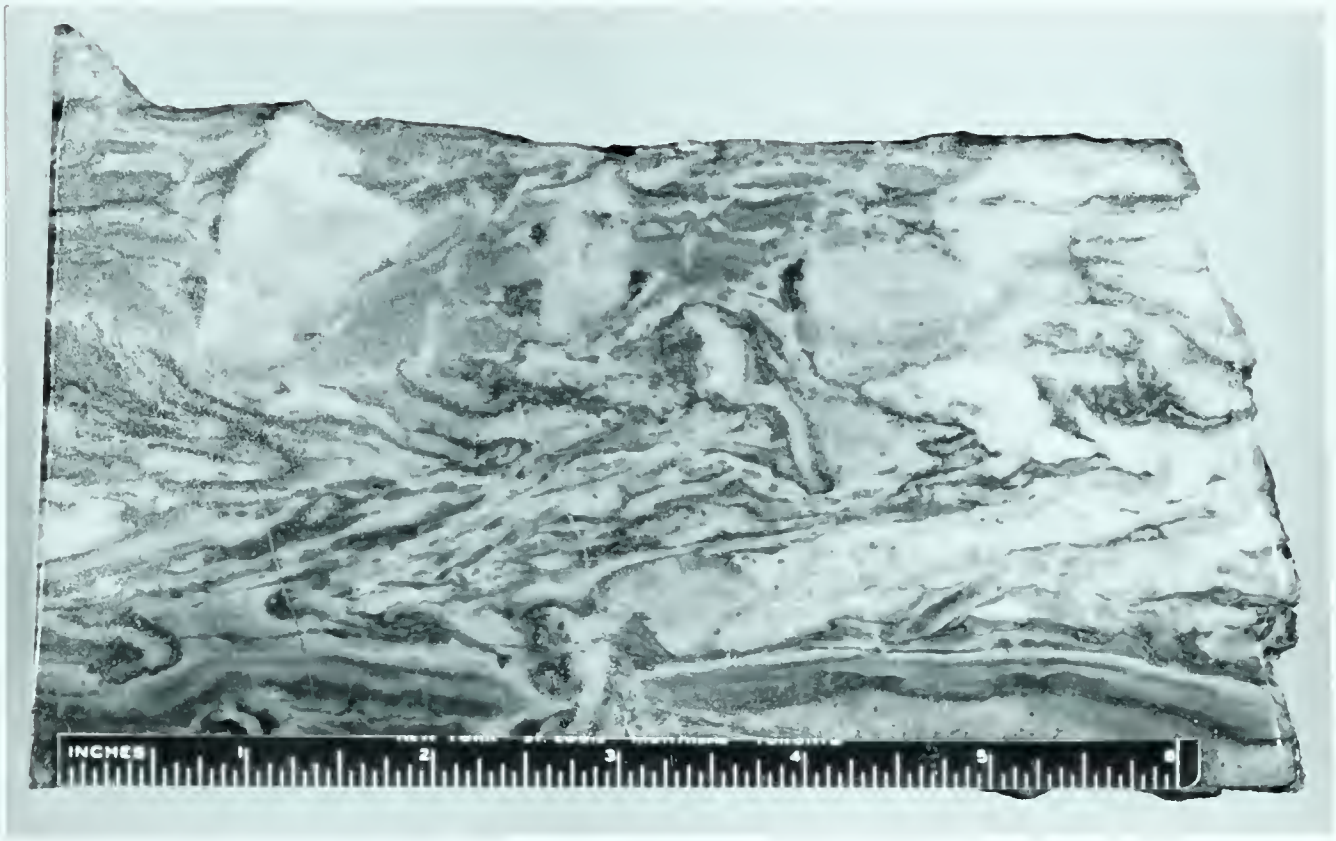

1

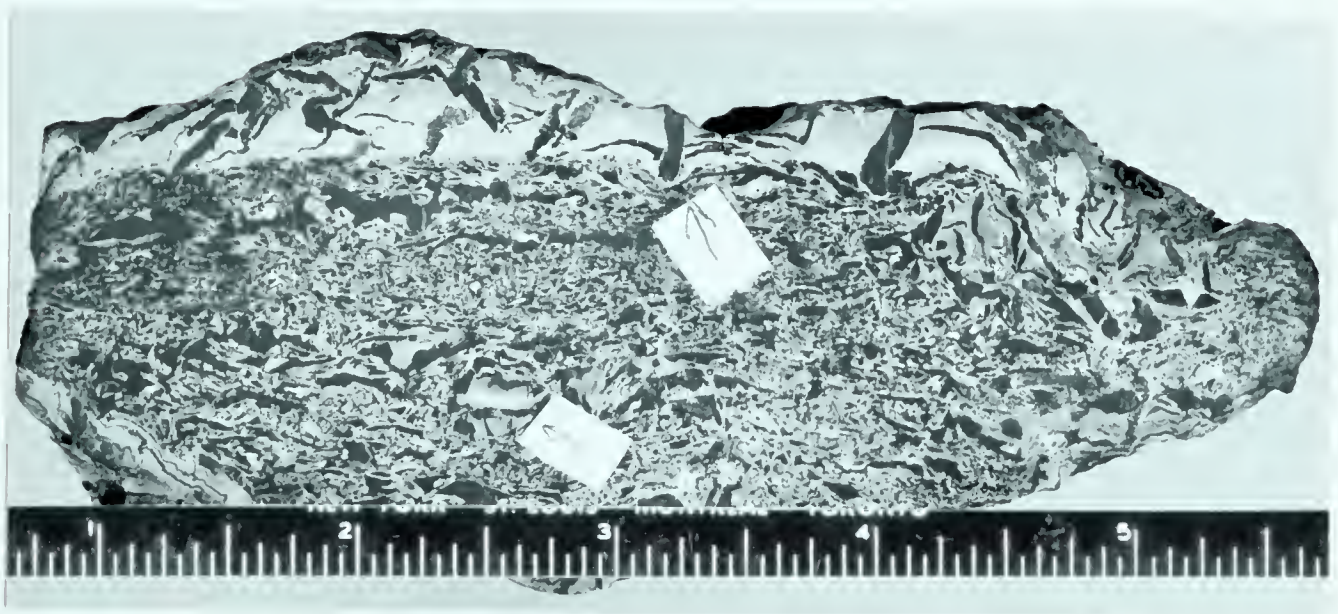

2

PLATE 8

PHOTOMICROGRAPHS

1. Mottled limestone, showing typical granular calcite (A), (crystals to the left of labels), and dolomite (B). Sample 42-34. Ordinary light. Magnification 625x.

2. Mottled limestone, showing zone of intensive calcitization adjacent to a calcite-filled fracture. Sample 37-26. Ordinary light. Magnification 625x.

3. Mottled limestone, interior of a growth segregation showing authigenic quartz in middle replacing calcite cement, in turn intruded by a dolomite rhomb. Sample 51-52A. Crossed nicols. Magnification 625x.

4. Algal limestone, showing grain growth or recrystallized mosaic of almost pure calcite. Relict patches of initial fine-grained algal sediment are found scattered throughout the recrystallized fabric. Sample 190-264. Crossed nicols. Magnification 100x.

5. Mottled limestone, showing a granular calcite-cemented veinlet containing a patch of (dark) authigenic quartz, seeded by an initial detrital quartz grain (without inclusions) in central part of patch. Sample 14-86. Crossed nicols. Magnification 255x.

6. Mottled limestone, showing granular calcite cement in a fracture segregation. Sample 74-97. Ordinary light. Magnification 500x.

7. Quartzite, showing well rounded, fresh, microcline grain. Sample 104-134. Crossed nicols. Magnification 255x.

8. Mottled limestone, showing calcite-cemented fracture containing an euhedral authigenic quartz rhomb. Boundaries of the fracture segregation (veinlet) are sharp. Sample 14-86. Crossed nicols. Magnification 255x.

PLATE 8

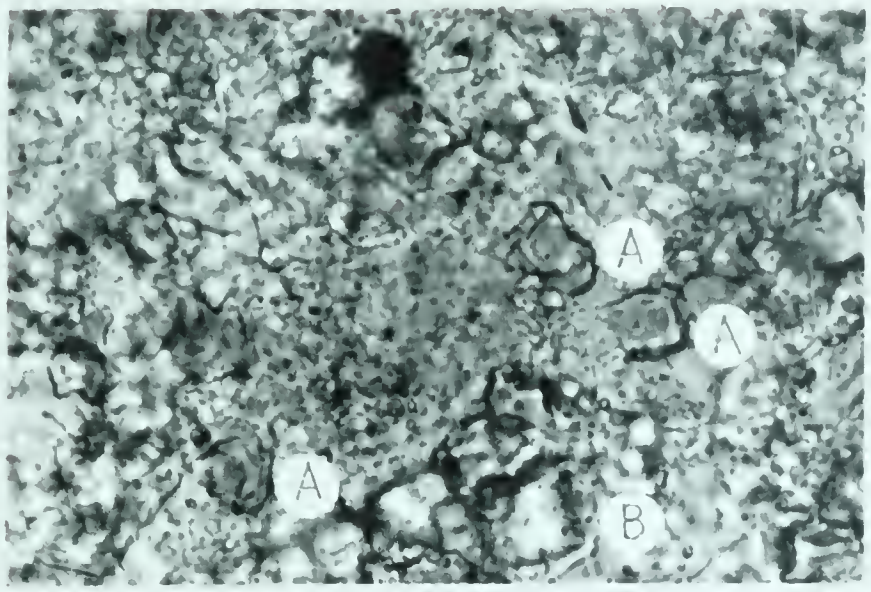

1

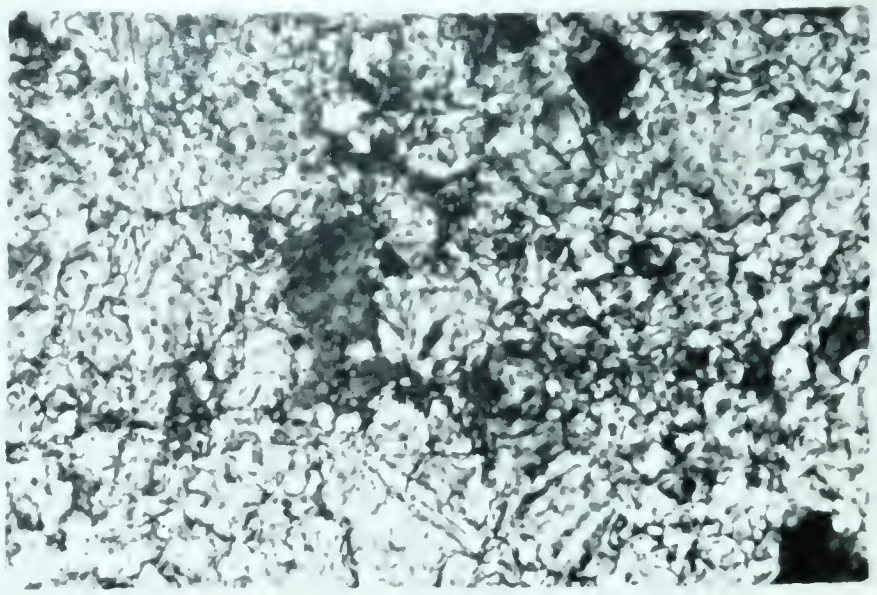

2

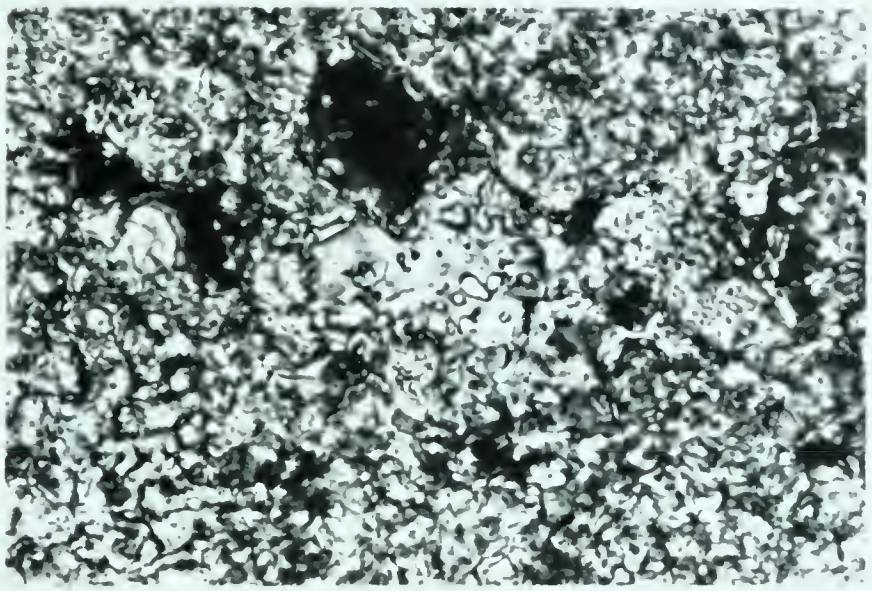

3

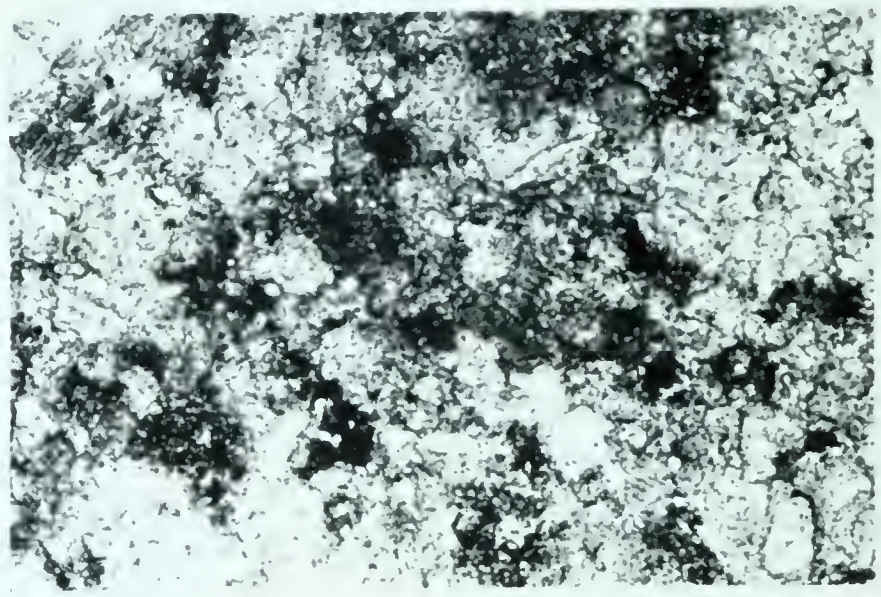

4

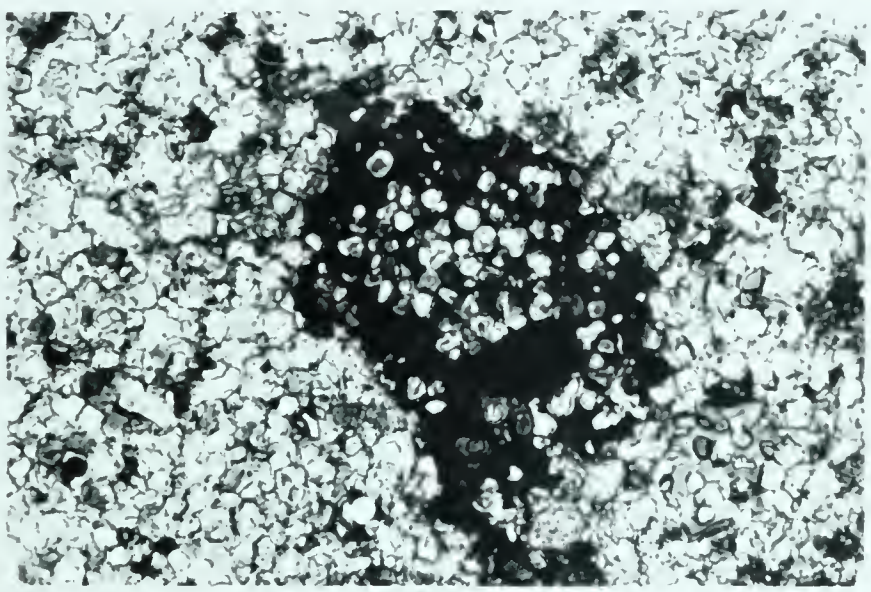

5

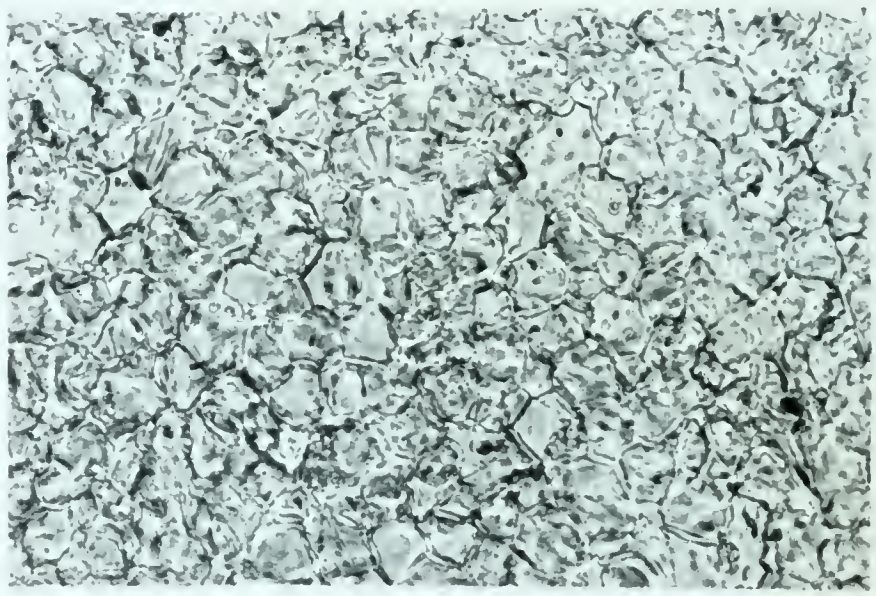

6

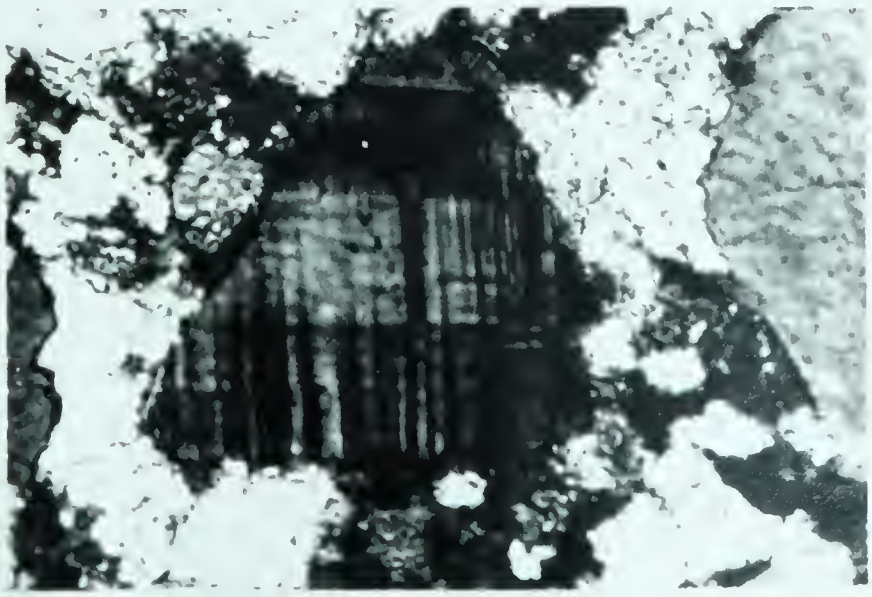

7

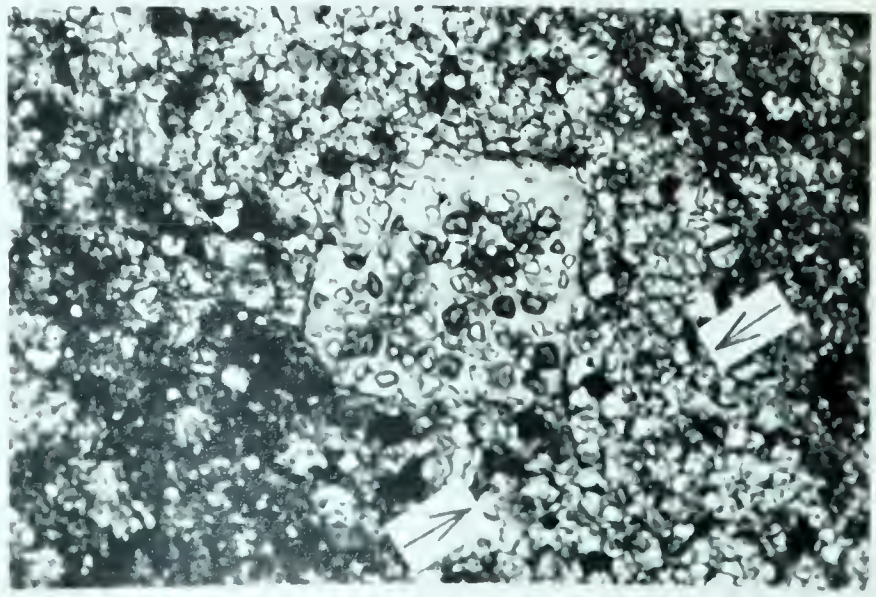

8

PLATE 9

PHOTOMICROGRAPHS

1. Mottled limestone, showing typical detrital fabric (groundmass), (A) quartz, (B) phyllite. Letters are placed to the right of grains. Sample 39-30. Crossed nicols. Magnification 255x.

2. Mottled limestone, showing subangular to angular quartz grains. Sample 37-26. Crossed nicols. Magnification 255x.

3. Mottled limestone, showing patch of dolomite replacing granular calcite of slump fracture origin. Sample 183-252. Crossed nicols. Magnification 40x.

4. Mottled limestone, showing contact between coarse (above arrow) and fine-grained sediment. Note abundance of calcite rhombs both above and below contact, although differing in size. Sample 74-97. Ordinary light. Magnification 255x.

5. Oolite, showing: (A) granular calcite pseudoolite, (B) oolite, and (C) rounded oolite fragment. Other pseudoolites consist of fine-grained silty limestone. Sample 49-47. Crossed nicols. Magnification 25x.

6. Mottled limestone, showing paragenesis of four elements: (1) groundmass, (2) granular calcite cement in a fracture segregation, (3) late diagenetic coating of walls of pore with chlorite-hematite, and (4) spar calcite deposited in center of pore and in an arm extending out into groundmass. Sample 37-26. Crossed nicols. Magnification 62.5x.

7. Quartzite, showing quartz-muscovite schist fragment. Sample 104-134. Crossed nicols. Magnification 400x.

8. Mottle conglomerate, showing pebble (B) containing a fracture filled with granular calcite cement. Pebble (A) is composed entirely of granular calcite. Sample 175-239. Crossed nicols. Magnification 25x.

PLATE 6

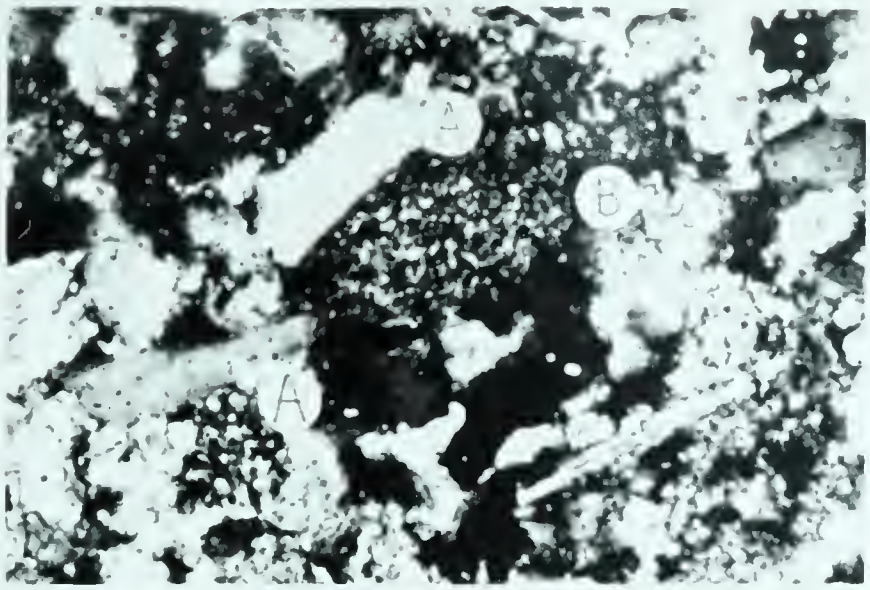

1

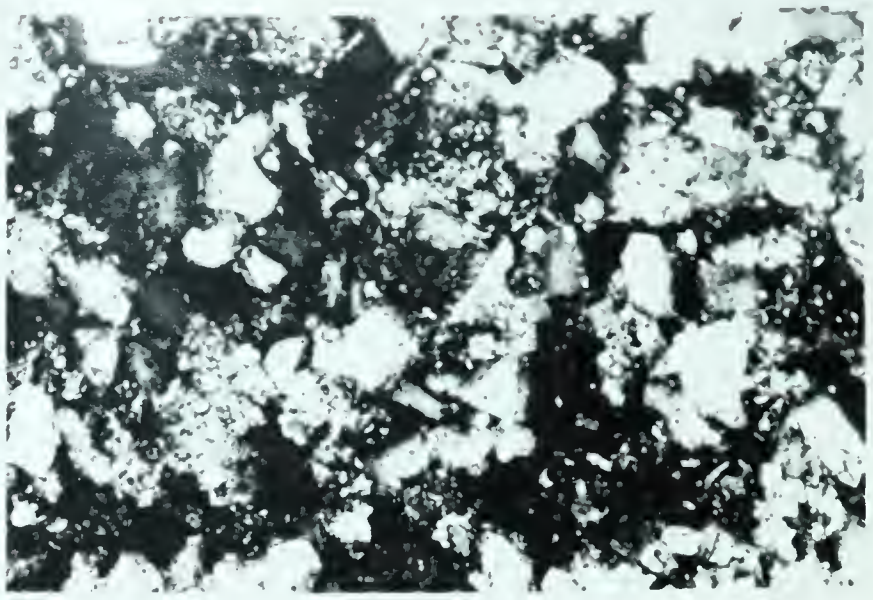

2

3

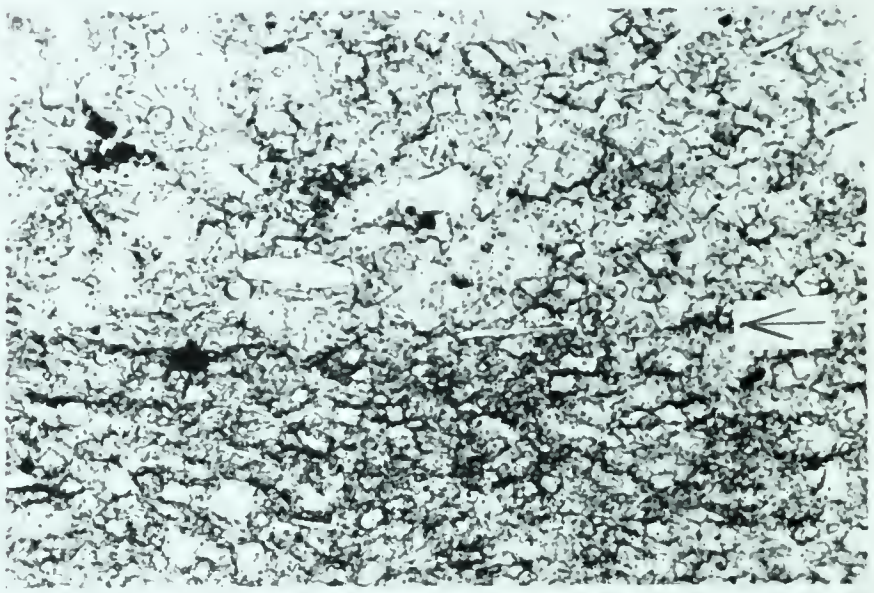

4

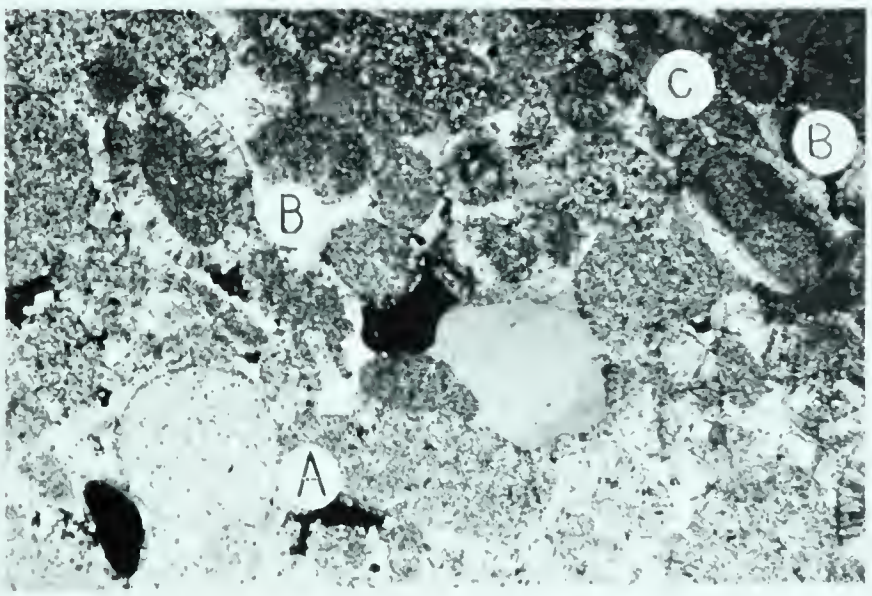

5

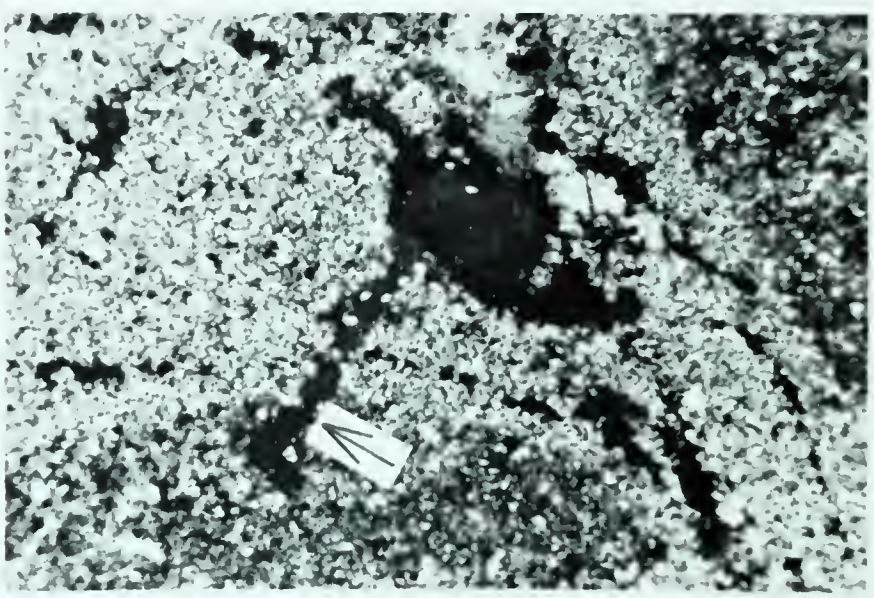

6

7

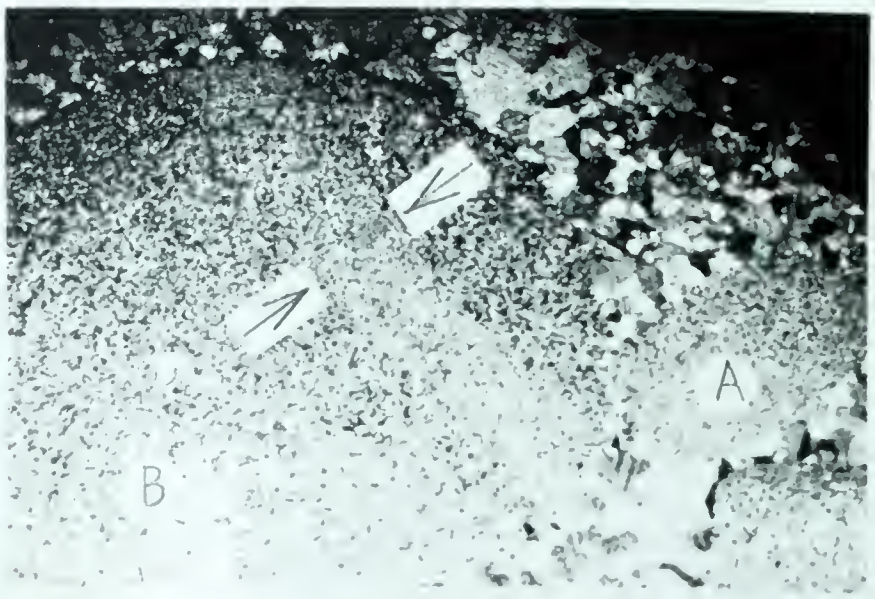

8